water deprivation test and their renal tubules showed poor response to DDAVP. No defect of the regeneration of HCO₃ was detected by chronic acid loading and furosemide test. These indicated abnormalities were confined to the proximal tubules and the medulla.

The concentrating ability defect found in β-thal/Hb E resembled the condition reported in sickle cell and Cooley's anemia [9, 24–26]. There are several hypotheses concerning the pathogenesis of tubular defects such as the theory of increased blood flow through the vasa recta which will disturb the effectiveness of countercurrent multiplication, or increased renal circulation causing a lower maximal concentrating capacity in the counter current system described in sickle cell anemia [24–26]. The blood overflow in the vasa recta could cause a 'washout' of medullary hyperosmolality with hypotonic urine [9]. However, the increased amount of medullary fibrosis which was also observed in some renal biopsies of Cooley's anemia could be an explanation for the poor urine concentrating ability [9, 27].

Another reason for the defect in concentrating ability in thalassemic patients could be due to organic lesions of the nephron segments which regulate the countercurrent mechanism as shown in autopsies of hemosiderin deposition at the proximal and distal convoluted tubules [18, 28-32]. It has been shown that excess of tissue iron, which is the common finding in most thalassemic patients, might be responsible for the increase in lipid peroxidation [33, 34] as demonstrated by the increase in plasma and urine malondialdehyde (MDA), highly significant in our patients. The plasma MDA also correlated with the levels of serum ferritin (fig. 1). Our data support previous studies of increased oxidative stress in β-thal/Hb E [35] which showed increased MDA from iron overload. It could be speculated that excess MDA further damaged the kidney cell [36] resulting in tubular defects seen by increased lowmolecular-weight protein, β₂-microglobulin, enzymuria, aminoaciduria, proteinuria and hyposthenuria.

The degree of tubular dysfunction was more marked in splenectomized patients than in the nonsplenectomized group (fig. 2). The splenectomized β -thal/Hb E patients are known to have higher iron overload than patients with intact spleen [37].

Urine NAG and β_2 -microglobulin excretion have been proven to be sensitive markers in diagnosing proximal tubular dyfunctions [38–40]. In the proximal tubules, iron deposition was seen in the straight or distal nephron and the proximal portion was relatively spared. There was an increase of urinary β_2 -microglobulin statistically different from controls, but no correlations between degree of

anemia, serum ferritin and tubular dysfunctions were found. We confirmed that thalassemic patients have tubular defects both from elevated NAG and β_2 -microglobulin levels. The increase in oxidative stress from iron overload and both anatomical and physiological abnormalities could contribute to the pathogenesis of tubular dysfunction seen in this study.

Our data do not support the previous impression that glomerular diseases appeared to have higher incidence in thalassemia. We failed to demonstrate heavy proteinuria or any characteristics of glomerular disease. The fact that small-molecular-weight proteinuria was found in most of the patients is another set of data against the glomerular involvement. Glomerular diseases have been found in autopsy of patients with thalassemia and have been reported to lead to end-stage renal disease in some [7, 11]. Etiologies such as repeated infection, inability to clear the immune complexes caused by infection and repeated use of desferroxamine have been postulated [7, 9, 30]. Proteinuria of less than 2 g/day was apparent in over 95% of the cases together with abnormal tubular marker, all suggesting that proteinuria originated mainly from tubules.

In conclusion, we describe renal abnormalities in a group of adult patients with β -thal/HbE disease. The data indicated that the patients have high prevalence of proximal tubular and medullary defects. We also demonstrated that the defects correlate with the disease severity, particularly in the splenectomized group and those with high levels of serum ferritin. Significant increases in serum and urine MDA were also found suggesting that oxidative stress might play a major role in the pathogenesis.

Acknowledgements

This study was supported by research grant from Mahidol University. The authors would like to thank Miss Duangporn Chuavattana, Miss Rattiya Charoensakdi, Mr. Surin Kanyok, Mr. Supong Boonsaner and Mr. Sompong Liemmongkolkul for their excellent laboratory assistance. P. Malasit was supported by a Senior Research Scholar Grant (No. RTA/04/2539) from the Thailand Research Fund.

References

- Walker BR, Alexander F, Birdsall R, Warren RL: Glomerular lesions in sickle cell nephropathy. JAMA 1971;215:437-440.
- 2 Buckalew VM, Someren A: Renal manifestations of sickle cell disease. Arch Intern Med 1974;133:660-669.
- 3 Elfenbein JB, Patchesfsky A, Schwartz W, Weinstein AG: Pathology of the glomerulus in sickle cell anemia with and without the nephrotic syndrome. Am J Pathol 1974;77:357– 376
- 4 Alleyne GAO, Statius Van Eps LW, Addae SK, Nickolson GD, Schouten H: The kidney in sickle cell anemia. Kidney Int 1975;7:371– 379.
- 5 De Jong PE, De Jong-van den Berg LTW, Statius van Eps LW: The tubular reabsorption of phosphate in sickle cell nephropathy. Clin Sci Mol Med 1978;55:429-434.
- 6 De Fronzo R.A., Taufield PA, Black H, Mc Phedram P, Cooke CR: Impaired renal tubular potassium secretion in sickle cell disease. Ann Intern Med 1970:90:310-316.
- 7 Tejani A, Phadke K, Adamson O, Nicastri A. Chen CK, Sen D: Renal lesions in sickle cell nephropathy in children. Nephron 1985;39: 352-356.
- 8 Strauss J, Zilleruelo G, Abithol C: The kidney and hemoglobin S. Nephron 1986;43:241– 245
- 9 Mastrangelolo F, Lopez T, Rizzelli S, Manisco G, Corliano C. Alfonso L: Function of the kidney in adult patients with Cooley's disease: A preliminary report. Nephron 1975;14:229– 236
- 10 Shehab M, Barakat AY: Thalassemia b with distal renal tubular acidosis: A previously undescribed association. Int J Pediatr Nephrol 1985;6:143.
- 11 Wasi P, Na-Nakorn S, Pootrakul S, Sukenek M, Disthasongchan PM, Panich V: Alpha- and beta-thalassemia in Thailand. Ann NY Acad Sci 1969;165:60–82.
- 12 Wasi P, Na-Nakorn S, Pootrakul S, Panocj P: Incidence of hemoglobin Thai: A reexamination of the genetics of a-thalassemic diseases. Ann Hum Gen 1972;35:467-470.
- 13 Hemoniugsen L, Skaarup P: β₂-microglobulin in urine and serum determined by ELISA technique. Scand J Clin Invest 1985;45:367-371.
- 14 Lustgasten JA, Wenk RE: Simple rapid kinetic method for serum creatinine measurement. Clin Chem 1972;18:1419-1422.

- 15 Moore JC, Moris JE: A simple automated colorimetric method for determination of N-acetyl-b-D-glucosaminidase. Ann Clin Biochem 1982:19:157-159.
- 16 Toftegaard Nielson TA: A method for enzymatic determination of citrate in serum and urine. Scand J Clin Lab Invest 1976;36:513-519
- 17 Knight JA, Smith SE, Kinder VE, Pieper RK: Urinary lipoperoxides quantified by liquid chromatography and determination of reference values for adults. Clin Chem 1988;34: 1107-1110.
- 18 Efran ML, Young O, Moser HW, MacCready RA: A simple chromatography screening test for the detection of disorder of amino acid metabolism. N Engl J Med 1964;270:1378– 1380.
- 19 Lim CW, Chisnall WN, Stokes YM, Debnam PM, Crooke MJ: Effects of low and high relative molecular protein mass on four methods for total protein determination in urine. Pathology 1990;22:89-92.
- 20 Morrissey JH: Silver stain for proteins in polyacrylamide gel: A modified procedure with enhanced uniform sensitivity. Anal Biochem 1981;117:307-310.
- 21 Miles LEM. Lipschitz DA, Bieber CP, Cook ID: The measurment of serum ferritin by a 2site immunoradiometric assay. Anal Biochem 1974:61:209-224.
- 22 Yagi K: Short communications: A simple method for lipoperoxide in blood plasma. Biochem Med 1976;15:212-216.
- 23 Vasuvattakul S. Gougous A, Halperin ML: A method to evaluate renal amniogenesis in vivo. Clin Invest Med 1993;16:265–273.
- 24 Keitel HG, Thompson D, Itano HA: Hyposthenuria in sickle cell anemia: A reversible renal defect. J Clin Invest 1956;35:998-1003.
- 25 Schmidt JD, Flocks RH: Urologic aspects of sickle cell hemoglobin. J Urol 1971;106:740– 744
- 26 Statius van Eps LW, Schouten H, La Porte-Wusman LW. Struyker-Boudier AM: The influence of red blood cell transfusions on the hyposthenuria and renal hemodymamics of sickle cell anemia. Clin Chim Acta 1967;17: 119-121.
- 27 Lever AF: The vasa recta and countercurrent multiplication. Acta Med Scand 1965; 434(suppl):178.
- 28 Landing BH, Gonick GC, Nadorra RL, Hyman CB, Wells TR, Villarreal-Engelhardt G, Mersch J, Agness CL: Renal lesions and clinical findings in thalassemia major and other chronic anemias with hemosiderosis. Pediatr Pathol 1989;9:479-500.

- 29 Grossman H, Dische R. Winchesier PH, Canale V: Renal enlargement in thalassemia major. Radiology 1971;100:645-648.
- 30 Hyman CB, Gonick HC, Agness MT, Nadorra R, Landing B: Effects of deferoxamine on renal function in thalassemia. Birth Defects Orig Article Ser 1988;23:135–140.
- 31 Bhamarapravati N, Na-Nakorn S, Wasi P, Tuchinda S: Pathology of abnormal hemoglobin diseases seen in Thailand. I. Pathology of bthalassemia hemoglobin-E disease. Am J Clin Pathol 1967;47:745-758.
- 32 Sonakul D, Pacharee P, Thakernpol K: Pathologic findings in 76 autopsy cases of thalassemia. Birth Defects Orig Article Ser 1988;23: 157-176.
- 33 Zager RA, Burkhart KM, Lonrad DS, Gmur DJ: Iron, heme oxygenase, and glutathione: Effects on myohemoglobinuric proximal tubular injary. Kidney Int 1995;48:1624–1634.
- 34 Shuler TR, Pootrakul P, Yarnsukon P, Nielsen FH: Effect of thalassemia/HbE disease on macro, trace, and ultratrace element concentrations in human tissue. Trace Elements Exp Med 1990;3:31-43.
- 35 Ong-ajyooth S, Suthipak K, Shumnumsirivath D, Likidlilid A, Fucharoen S, Pootrakul P: Oxidative stress and antioxidants in b-thalassemia/hemoglobin E. J Med Assoc Thailand 1987;70:270-275.
- 36 Bird RP, Droper HH: Uptake and oxidation of malonaldehyde by cultured mammalian cells. Lipids 1982:17:519-523.
- 37 Pootrakul P, Vongsmasa V, La-ongpanich P, Wasi P: Serum ferritin levels in thalassemias and the effect of splenectomy. Acta Haematol 1981;66:244-250.
- 38 Sherman RL, Drayer DE, Leyland-Joms MC, Reidenberg MM: N-acetyl-b-glucosaminidase and b2-microglobulin. Their urinary excretion in patients with renal parenchymal disease. Arch Intern Med 1983;143:1183-1185.
- 39 Sohardun GHC, Statius van Eps LW: b2microglobulin: Its significance in the evaluation of renal function. Kidney Int 1987;32: 635-641.
- 40 Portman RJ, Kissane JM, Robson AM, Peterson LJ, Richardson A: Use of b2-microglobulin to diagnose tubulointerstitial renal lesions in children. Kidney Int 1980;30:91–98.

Dengue Virus Infection of Human Endothelial Cells Leads to Chemokine Production, Complement Activation, and Apoptosis¹

Panisadee Avirutnan,** Prida Malasit,* Barbara Seliger,* Sucharit Bhakdi,* and Matthias Husmann*

Dengue hemorrhagic fever and dengue shock syndrome (DHF/DSS) are severe complications of secondary dengue virus (DV) infection. Vascular leakage, hemorrhagic diathesis and complement activation are the hallmarks of the disease. The short-lived nature of the plasma leakage syndrome has led to the conclusion that altered permeability is most likely effected by a soluble mediator. In the present study, we show that infection of human endothelial cells with DV induces the transcriptional upregulation and secretion of RANTES and IL-8 and, in the presence of anti-dengue Abs, the formation of nonlytic complement complexes. Extremely high levels of IL-8 were detected in plasma and pleural fluid samples from patients with DSS. Furthermore, DV infection of endothelial cells in vitro caused apoptosis. Complement activation, chemokine induction, and apoptotic cell death may act in concert to cause the fulminant but short-lived vascular leakage that is characteristic of DHF/DSS. The Journal of Immunology, 1998, 161: 6338-6346.

engue hemorrhagic fever and dengue shock syndrome (DHF/DSS) are serious clinical conditions that occurs almost exclusively in response to secondary infection by dengue virus (DV) (1, 2). It remains a major health problem in South East Asia, Central America, and the Pacific region, representing one of the major causes of child death in several countries (3). Cardinal signs of DHF/DSS include hemorrhage, abrupt onset of vascular leakage, and shock, accompanied by severe thrombocytopenia and massive complement activation (4, 5). Typically, survivors of DHF/DSS show rapid recovery with minimal sequelae (4). The pathogenesis of shock and leakage is poorly understood. Vascular endothelia in serosal tissues appear to be preferentially affected by some critical pathogenetic mechanism, since ascites and pleural effusion clearly account for most of the plasma leakage in DSS (6). As recently proposed by Innis, "the lack of structural damage, the short lived nature of the plasma leakage syndrome, and the remarkably rapid recovery of children with DSS all suggest that altered permeability is effected by a soluble mediator" (6). Deregulated cytokine responses (7-9) and complement activation by non-neutralizing Abs (10) have been implicated in the vascular leakage syndrome. Animal models of DSS do not exist, and biopsies cannot be taken from the pleura and peritoneum of patients because of the unacceptable accompanying risk. As a consequence, tissue samples relevant to studies of dengue shock are rarely available. In the face of this difficulty, all evolving concepts for the pathogenesis of DHF/DSS have been based on experimental in vitro observations. This pertains also to the question regarding the identity of the primary target cells, and their response to infection. The majority of earlier studies concentrated on monocyte/macrophages as possible targets, because uptake of virus-Ab complexes via Fc Rs could most easily explain the well-established phenomenon of Ab-dependent enhancement that was originally described by Halstead and O'Rourke (9). However, even under optimal conditions, DV infection of monocytes is rather inefficient in vitro, and the cytokine responses in infected cells cannot readily explain the leakage syndrome. Endothelial cells have also been considered as targets, and productive in vitro infection of these cells has been reported (11, 12). In the present study, we sought to characterize the infection of endothelial cells (EC) by DV in more detail, to investigate the response of the cells to infection, and to uncover a possible link between EC infection and complement activation. We report that DV infection of human EC provokes production of RANTES and IL-8, in the virtual absence of production of several other proinflammatory cytokines. A directed search revealed that plasma and pleural fluids (PF) of patients suffering from DHF/DSS had remarkably high levels of IL-8. Furthermore, we report that cross-seroreactive Abs to DV activate complement on infected EC. Independent of this activation, DV-infected cells die within a few days via programmed cell death. Together, these findings lead to the formulation of a hypothesis on the pathogenesis of DSS that envisages a selective permeability increase in the serosal vasculature due to the selective binding of cationic chemokines acting in concert with complement anaphylatoxins possibly produced locally on DV-infected cells. Vascular permeability increases culminate with the apoptotic

*Institute of Medical Microbiology and Hygiene and 'IIIrd Department of Internal Medicine, Johannes Gutenberg University, Mainz, Germany; and 'Medical Molecular Biology Unit, Office of Research and Development, Faculty of Medicine, Siriraj Hospital, Mahidol University, Bangkok, Thailand

Received for publication March 25, 1998. Accepted for publication August 11, 1998.

The costs of publication of this article were defrayed in part by the payment of page charges. This article must therefore be hereby marked *advertisement* in accordance with 18 U.S.C. Section 1734 solely to indicate this fact.

¹ P.M. is supported by the Senior Research Scholar Grant (no. RTA/04/2539) from the Thailand Research Fund. P.A. is a Ph.D/M.D fellow under the Medical Scholar program, supported by Mahidol University and the China Medical Board (New York). This work is a contribution from the Thai Network for Biomolecular Research (TNBR) and the Deutsche Forschungsgemeinschaft (SFB "Immunopathogenesis," project D10).

² Address correspondence and reprint requests to Dr. Matthias Husmann, Institute of Medical Microbiology and Hygiene, University of Mainz, Augustuspiatz, D-55101 Mainz, Germany, E-mail address; makowiec@goofy.zdv.uni-mainz.de.

³ Abbreviations used in this paper: DHF/DSS, dengue hemorrhagic fever and dengue shock syndrome: DTAF, dichlorotriazinyl amino fluorescein: DV, dengue virus; EC, endothelial cells: EMSA, electrophoretic mobility shift assay: GAPDH, glyceralde-hyde-3-phosphate dehydrogenase; MCP-1, monocyte chemotactic protein-1; MOI, multiplicity of infection: PF, pleural fluid: RT, room temperature: TPB, tryptose phosphate broth; TUNEL, TdT-mediated dUTP nick-end labeling.

breakdown of the endothelial barrier, leading to the fulminant but transient leakage syndrome that is the hallmark of DHF/DSS.

Materials and Methods

Cell culture

The human umbilical cord vein endothelial cell line (ECV304), obtained from American Type Culture Collection (ATCC CRL-1998), Manassas, VA, was grown in medium 199 (Life Technologies, Paisley, Scotland) supplemented with 10% FCS (Life Technologies), 2 mM L-glutamine (Life Technologies), 100 U/ml penicillin, and 100 µg/ml streptomycine (Life Technologies) at 37°C in humidified air containing 5% CO₂. C6/36, a cell line from Aedes albopictus, and PscloneD, a swine fibroblast cell line, were cultured at 28°C and 37°C, respectively, in L-15 medium (Life Technologies) containing 10% tryptose phosphate broth (TPB) (Sigma, St. Louis, MO), 10% FCS, 100 U/ml penicillin, and 100 µg/ml streptomycin. Untransformed human umbilical vein endothelial cells and human dermal microvascular endothelial cells were purchased from Promocell (Heidelberg, Germany) and were cultured in endothelial cell culture medium with growth supplement and 2% FCS, provided by the supplier. Only cells from passages 2 to 5 were used for experiments.

Preparation of virus stock and virus titration

Dengue-2 virus strain 16681 was propagated in C6/36 cells. Monolayer of cells in 75 cm2-tissue culture flasks (Greiner, Frickenhausen, Germany) received L-15 medium containing 1% FCS and 10% TPB prior to DV infection. The virus culture medium was first harvested after 5 days of incubation and fresh medium was then added. Later, virus culture fluid was harvested every second day until infected cells fully expressed the cytopathic effect. After removal of cell debris by centrifugation at 900 × g, the virus supernatant was aliquoted and stored at -70°C until used. Virus was titrated in plaque formation assays on PscloneD cells. Monolayers of cells were trypsinized and resuspended in L-15 medium containing 3% FCS and 10% TPB and plated at 1×10^5 cells/well in a volume of 0.5 ml in 24-well plates (Nunc, Roskilde, Denmark). Subsequently, dilutions of virus supernatant were added and the mixtures were incubated at 37°C for about 2-3 h; then 0.5 ml of L-15 medium containing 3% FCS, 10% TPB, and 2% (w/v) carboxymethylcellulose (Sigma) was added to each well. After 5 days of incubation at 37°C, the plaques were visualized by staining with a dye solution composed of 0.1% (w/v) napthalene black 10B (Serva, Entwicklungslabor, Heidelberg, Germany), 1.36% (w/v) sodium acetate (Carl Roth, Karlsruhe, Germany), and 6% (v/v) glacial acetic acid (Roth). Virus concentrations are given as plaque-forming units/milliliter.

Infection of endothelial cells

Monolayers of EC were trypsinized and resuspended in growth medium. About $2\text{-}3 \times 10^5$ or 8×10^4 ECV304 cells were seeded into each well of 24-well tissue-culture plates or 8-well glass chamber slide (Nunc), respectively. Primary cells were seeded at a density of $1\text{--}2 \times 10^4$ /well in 96-well tissue-culture plates. After overnight incubation, virus culture fluid or heatinactivated virus suspension (80°C, 20 min) was added to confluent monolayers of cells at the multiplicity of infection (MOI) of 0.1 and incubated at 37°C for 2 h. The virus supernatant was then removed and fresh growth medium was added to each well. Culture media and infected cells were harvested at various times after infection for further experiments.

Flow cytometry analysis

At 24, 48, and 72 h after infection, DV-infected and control cells were harvested from 24-well plates. Flow-cytometric assessment of percentage of dead cells was done after pooling populations of cells in suspension and trypsinized adherent cells of a given sample. Propidium iodide (Sigma) was added to give a final concentration of 0.2 µg/ml and samples were analyzed in a FACScan (Becton Dickinson Immunocytometry Systems, San Jose, CA). For flow-cytometric determination of DV infection, the harvested cells were washed twice with medium 199 and then fixed with 2% formaldehyde (Roth) in PBS for 1 h at room temperature (RT). After two washing steps with PBS, the fixed cells were permeabilized with 0.1% Triton X-100 in PBS. Permeabilized cells were incubated with dengue hyperimmune mouse ascitic fluid, generously provided by Dr. A. Nisalak (Armed Forces Research Institute of Medical Sciences, Bangkok, Thailand), at a final dilution of 1:400 for 1 h at RT. The cells were then washed twice with permeabilization solution and incubated with dichlorotriazinyl amino fluorescein (DTAF)-conjugated F(ab')2 fragment of goat anti-mouse IgG (Dianova, Hamburg, Germany) at a final concentration of 3.75 µg/ml for 30 min at RT in the dark. The cells were washed once with an excess volume of permeabilization solution and analyzed by flow cytometry.

Chemokine and cytokine quantitation

Supernatants from DV-infected, mock-infected, and heat-inactivated virustreated EC were quantitated for cytokine and chemokine production. RANTES and monocyte chemotactic protein-1 (MCP-1) were measured using ELISA kits from Biosource International, Camarillo, CA. ELISA kits for IL-8 were obtained from Innogenetics, Zwijndrecht, The Netherlands; for IL-1β from Immunotech/Coulter, Hamburg, Germany; for IL-1α from Endogen, Biozol Diagnostica Vertrieb, Eching, Germany; for IL-7, and granulocyte-macrophage-CSF (GM-CSF) from R&D Systems, Wiesbaden, Germany; for IL-15 from Cytoscreen, Laboserv Diagnostica, Giessen, Germany; and for TNF-α from Medgenix Diagnostic SA, Fleurus, Belgium.

Plasma and pleural fluid samples from DSS patients

EDTA plasma and PF samples obtained from six children dying of DSS were also assayed in ELISA for the chemokines MCP-1, RANTES, and IL-8. Diagnosis of DSS was based on the clinical criteria established by the World Health Organization (13); all patients were suffering from grade IV DSS. Bacteria were not found in smears and routine cultures of these samples. Albumin ratios for all plasma/PF pairs were above 0.5, indicating that these PF represented exudates. IL-8, MCP-1, and RANTES were determined using the same ELISA kits as described above. Albumin was quantitated at our clinical chemistry department.

RNA extraction and RT-PCR

Total RNA preparations from untreated cells or cells treated with inactivated or active virus were obtained by the method described by Chomezynski and Sacchi with minor modifications (14), RNA was quantitated by spectrophotometry (Pharmacia, LKB Biochrome, Little Chalfont, U.K.) at 260 nm. Approximately 1 µg of total RNA was used for the first-strand synthesis with oligo(dT) primer, AMV-RT, and reaction buffers as described by the manufacturer (reverse transcription system, Promega, Madison, WI). Subsequently, the newly synthesized first-strand cDNA was subjected to 20 rounds of PCR amplification of 95°C for 40 s, 62°C for 1 min, and 72°C for 3 min. Reaction mixtures contained primers at 1.5 µM each, MgCl₂ (1.5 mM), dNTP (0.2 mM each), and 1 U of Tao polymerase (Life Technologies) in a total reaction volume of 50 µl. The amplification primers were 5'-ATGACTTCCTTCTGGCCGTGGC-3' (forward) and 5'-TCTCAGCCCTCTTCAAAAACTTCTC-3'(reverse)forIL-8;5'-TGCCTC CCCATATTCCTCGG-3' (forward) and 5'-TCATGTTTGCCAGTAA GC-3' (reverse) for RANTES; 5'-CAAACTGAAGCTCGCACTCT CGCC-3' (forward) and 5'-ATTCTTGGGTTGTGGAGTGAGTGTTCA-3' (reverse) for MCP-1; 5'-CGGAGTCAACGGATTTGGTCGTAT-3' (forward) and 5'-AGCCTTCTCCATGGTGGTGAAGAC-3' (reverse) for glyceraldehyde-3-phosphate dehydrogenase (GAPDH). GAPDH served as a control to exclude variations between samples. Under these conditions, linear amplification of a cloned MCP-1 template was achieved as described elsewhere (15). RT-PCR products were electrophoresed in 1.8% agarose (FMC BioProducts, Rockland, ME) and stained with ethidium bromide. Results were documented with a Biometra imaging system (BioDocII, Göttingen, Germany).

Transient transfection and luciferase assay

Reporter plasmids plL8(-420/+102)LUC and pRANTES(-935/ +73)LUC were constructed by standard procedures. Fragments of the human IL-8 promoter region comprising position -420 to +102 and of the human RANTES promoter region between -935 and +73 were generated from human genomic DNA by PCR amplification with primers 5'-GGATCCATTGGCTGGCTTATCTTCACC-3' (IL-8, forward) and 5'-GGATCCTTTACACACAGTGAGAATGGT-3' (IL-8, reverse) or 5'-TGAAGCTTTCATATTCTGTAA-3' (RANTES, forward) 5'-CTAAGCTTGGTACCTGTGGGAGAGGCT-3' (RANTES, reverse). The PCR products were cloned into pCR3.1 (Invitrogen, De Schelp, The Netherlands) and the insert was subcloned via restriction sites incorporated into the primers. The IL-8 promoter fragment was cloned into the BamHI site of the multiple cloning site in the promoterless pGL2 basic plasmid, carrying the firefly luciferase gene (Promega Deutschland, Mannheim, Germany). The RANTES promoter fragment was excised from pCR3.1 with HindIII and subcloned into pGL2 basic via the unique HindIII site contained in this plasmid. Final constructs were verified by Taq dye terminator cycle sequencing using an Applied Biosystems 373A automated sequencer. Plasmids for transfections were prepared by two rounds of cesium chloride density centrifugation. Transient transfection of ECV304 cells was achieved with Lipofectin (Life Technologies) according to the manufacturer's protocol. Approximately 3 × 105 cells were seeded per well of 6-well tissue-culture plates (Nunc) and transfected 16 h later with $2 \mu g$ of supercoiled reporter-plasmid. Cells were washed 16-24 h later and treated with virus at a MOI of 0.1 or with an equal amount of inactivated virus. Luciferase assays with cellular lysates were performed 48 h after treatment using assay reagents from Promega and a Biolumat LB9500 instrument from Berthold (Wildbad, Germany). Calculations of the degree of reporter gene induction were based on the relative numbers of viable cells in the samples, as assessed by ATP determinations.

Bioluminescence assay for determination of cellular ATP

DV and mock-infected cells cultured in 24-well plates for various times after infection were harvested for the determination of intracellular ATP by chemiluminescence measurements with luciferase (Boehringer Mannheim, Mannheim, Germany) as described previously (16). Intracellular ATP of virus-infected cells is given as percentage of luminescence relative to that of control cells.

Determination of DNA strand breaks by TdT-mediated dUTP nick-end labeling (TUNEL)

TUNEL assays were performed on DV-infected and control cultures in 8-well glass chamber slides. At 24, 48, and 72 h after infection, cells were fixed with 2% paraformaldehyde (Merck) in PBS for 30 min at RT. The fixed cells were processed for the detection of free 3'OH termini due to DNA strand breaks using the TUNEL kit (Boehringer Mannheim) according to the manufacturer's protocol. In some experiments, mouse antihuman TNF- α neutralizing Ab (R & D Systems, Wiesbaden, Germany) at a concentration of 5 or 10 μ g/ml was added 2 h after virus infection and the cells were processed for the determination of apoptosis as described above.

Detection of nuclear translocation of nuclear factor-κβ (NF-κB)

Confluent ECV304 cells in eight-well glass chamber slides were fixed after dengue or mock infection with cold 70% ethanol for 20 min on ice, washed twice with PBS, and double stained with undiluted culture fluid of mAbs specific for dengue nonstructural protein-1 (NS1) and rabbit Abs against NF- $\kappa\beta$ p65 (Santa Cruz Biotechnology) at the final concentration of 5 μ g/ml for 1 h at RT. Cells were washed three times with PBS and then incubated with a mixture of DTAF-conjugated F(ab')₂ fragment of goat anti-mouse IgG plus Cyt3-conjugated donkey anti-rabbit IgG (Dianova) at a concentration of 3.75 μ g/ml each for 30 min at RT. After three final washes, the cells were covered with mounting fluid and visualized under a fluorescence microscope (Axiophot, Zeiss, Oberkochen, Germany).

Electrophoretic mobility shift assays (EMSA)

Whole cell lysates of untreated or virus-infected ECV304 cells were prepared by four cycles of freezing and thawing in a lysate buffer composed of glycerol, 20% (v/v) KCl, 0.4 M Tris-HCl buffer, 20 mM DTT, 2 mM PMSF, 10µg/ml aprotinin. Complementary synthetic oligonucleotides (5'-GATCCAGAGGGGACTTTCCGAGA-3', 5'-GATCTCTCGGA AAGTCCCCTCTG-3') comprising the NF-kB site (bold letters) of the murine Ig κ-chain gene were annealed, and overhangs (italics) were radioactively labeled with [32P]\adATP using Klenow polymerase. Labeled, double-stranded oligonucleotides were purified by nondenaturing PAGE. Binding reactions containing whole cell lysate (10 µg of protein/reaction) were done as described previously (17). After preincubation of lysates with 2 µg of dIdC, 30,000 cpm of labeled probe were added per reaction mix. After an additional incubation for 15 min at RT, samples were loaded onto 4% nondenaturing PAGE. Complexes were revealed by autoradiography of the vacuum-dried gel for 6-16 h using a reflection screen. In competition experiments, a 200-fold excess of unlabeled double-stranded oligonucleotide was added to the binding reaction. Polyclonal Abs directed to either the 750 or the p65 subunit of NF-kB were obtained from Santa Cruz Biotechnology. For supershift experiments lysates were preincubated with 0.2 μg of Ab/sample at 4°C for 1 h.

Indirect immunofluorescence for cell-bound C3dg

Experiments were performed in 8-well glass chamber slides. Human AB dengue nonimmune serum and heat-inactivated pooled dengue hyperimmune sera (hemagglutinin inhibition titer ≥1/25,600) were used as sources for complement and anti-dengue Abs, respectively. DV-infected cell monolayers at 24 or 48 h were treated with 0.1 ml medium 199 containing complement (at a dilution of 1:5), or anti-dengue Abs (at a dilution of 1:100), or both, for 1 h at 37°C. Heat-inactivated normal human serum (56°C, 30 min) was used as control. The cells were washed three times and were incubated for 1 h on ice with a 1:200 dilution of mAb specific for C3dg (clone 9), provided by Dr. P. J. Lachmann (Centre of Veterenary Sciences, University of Cambridge, Cambridge, U.K.). Then, they were washed three times and incubated with DTAF-conjugated F(ab')₂ fragment

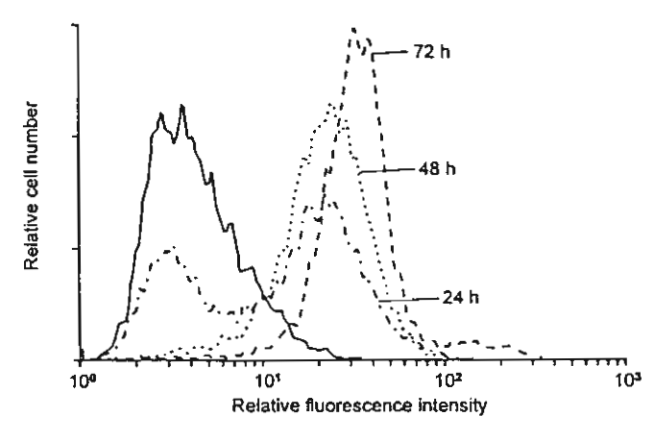


FIGURE 1. Kinetics of infection of ECV304 cells by DV. DV-infected or control cells were harvested at 24, 48, and 72 h after infection. The cells were fixed, permeabilized and treated with dengue hyperimmune mouse ascitic fluid. After staining with fluorescent secondary Abs, the cells were analyzed by flow cytometry. A set of histograms derived from one representative out of three experiments is shown. The solid line indicates the result with uninfected cells. Similarly, controls with nonimmune ascitic fluid yielded negative results with both infected and uninfected cells (not shown).

of goat anti-mouse IgG at a final concentration of 3.75 μ g/ml in the dark for 30 min on ice. The cells were washed twice, covered with mounting fluid, and analyzed by fluorescence microscopy (Axiophot, Zeiss). Medium 199 containing 10 mM NaN₃ (Merck) was used as a diluent and washing solution during the experiment.

Detection of C5b-9 complex formation

Cells grown in 24-well plates were used for complement-activation experiments at 24 or 48 h postinfection. Infected cells were washed twice with medium 199, and 0.2 ml of medium 199 containing complement (1:5) or anti-dengue Ab (1:100) or both was added and incubated for 1 h at 37°C. In some experiments, 10 mM EGTA and 10 mM MgCl₂ (Sigma) were used for inhibition of the classical pathway of complement activation. Heatinactivated serum was used as control. Thereafter, cells were washed twice with PBS. In pilot experiments we used an indirect immunofluorescence assay to detect C5b-9 complexes on cell surfaces and propidium iodide exclusion to assess membrane integrity of the treated cells. Upon microscopic inspection, C5b-9, formed on intact membranes, could be detected by this technique but gave very low fluorescence signals. Therefore, we used a sensitive capture ELISA technique for determination of C5b-9 formation. In this assay, cells were again first treated with Ab and complement. After deposition of C5b-9 complexes on the cell surface, cells were lysed by applying 0.2 ml of lysing buffer (1% Triton X-100 (Roth) in PBS) for a few minutes. Lysates were clarified by centrifugation at 10,000 × g for 5 min to remove cell debris and frozen at -20°C until used. The actual assay for the detection of C5b-9 complexes was performed according to the protocol of Hugo et al. (18) except that swine anti-rabbit IgG conjugated with horseradish peroxidase (Dako, Glostrup, Denmark) at a final concentration of 0.24 µg/ml was used instead of the biotinylated anti-rabbit IgG in the last step and tetramethylbenzidine (Medgenix Diagnostics, Fleurus, Belgium) was used as a chromogen. The absorbency was read at 450 nm in an ELISA reader (EAR 400, SLT Labinstruments, Salzburg, Austria).

Results

Infection of human endothelial cells by dengue virus

DV-infected cells express viral Ags in their cytoplasm (19–21). Hyperimmune mouse ascitic fluid was used to detect dengue viral proteins, and the number of infected ECV304 cells was quantitated using flow cytometry. The analysis of green fluorescence-positive cells was performed with 5000 events from each sample. About 63.5% of the cells at 24 h after infection at MOI of 0.1 expressed DV Ags and almost all cells were infected after 48 and 72 h of incubation (94 and 98.5%, respectively) (Fig. 1). Approximately 25% of untransformed EC were infected at 72 h as assessed by

The Journal of Immunology 6341

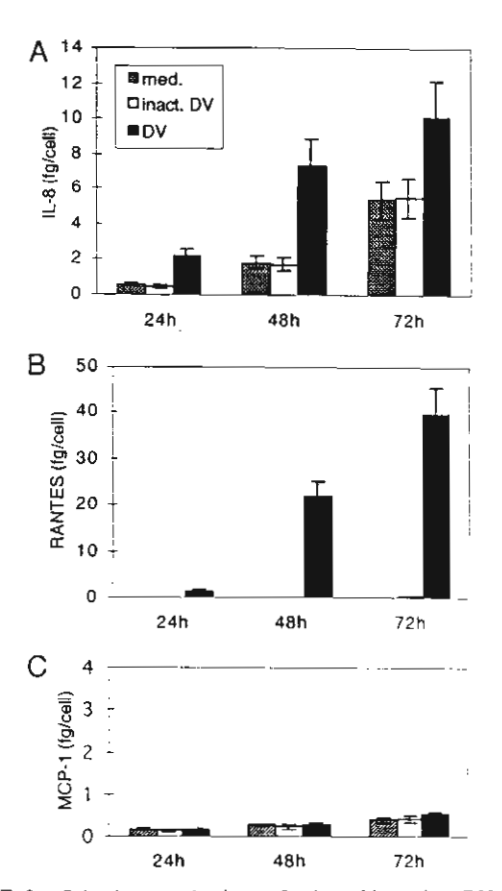


FIGURE 2. Selective production of chemokines by DV-infected ECV304 cells. Culture media were collected from untreated cells (med), from cells treated with heat-inactivated DV (intact.DV), or from DV-infected cells (DV) at 24, 48, and 72 h after infection, and assayed by ELISA. Results represent the accumulative amounts of IL-8 (A). RANTES (B), and MCP-1 (C) divided by the number of seeded cells. Data are displayed as the mean \pm SD from three independent experiments.

FACS or immunofluorescence microscopy (not shown). For DV-infected ECV304 cells, we also determined the release of infectious virions into culture supernatants by plaque-forming assays. The peak titer, obtained 2 days after infection of $2-3 \times 10^5$ ECV cells at an MOI of 0.1 was 19×10^5 PFU/ml (SD $\pm 2 \times 10^5$, n = 4).

Induction of RANTES and IL-8 in dengue-infected endothelial cells

To analyze cytokine production in response to DV, we collected supernatants of infected ECV304 cells after 24, 48, and 72 h from parallel cultures, and screened them by ELISA. No virus-mediated induction was found for MCP-1, IL-1 β , IL-1 α , IL-7, IL-15, and GM-CSF, and only minimal induction of TNF- α was noted (data not shown). In contrast, a marked time-dependent increase of RANTES and IL-8 became detectable in supernatants of DV-infected ECV304 cells (Fig. 2). Likewise, untransformed EC from umbilical vein or dermal microvascular EC, cultured in media with 2% FCS, produced significant amounts of RANTES only upon DV infection (Fig. 3). IL-8 levels were increased twofold in supernatants of HUVEC 96 h after infection as compared with controls (not shown). On a per infected cell basis, ECV304 cells produced roughly five times more RANTES than did primary cells.

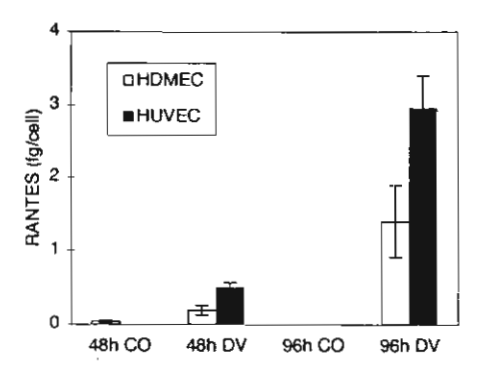


FIGURE 3. DV infection induces RANTES in primary endothelial cells. Human umbilical vein endothelial cells or human dermal microvascular endothelial cells were cultured in media of low serum content in the presence of DV or of inactivated DV (CO). Supernatants were assayed for RANTES by ELISA. The data represent the mean ± SD from three independent experiments.

Transcriptional up-regulation of RANTES and IL-8 during dengue infection of endothelial cells

RT-PCR for IL-8 and RANTES with total RNA from uninfected and control cells revealed increased steady state levels of specific mRNAs in infected cells (Fig. 4). We therefore investigated whether IL-8- and RANTES-mRNA accumulation could be attributed to transcriptional up-regulation of their promoters. Transient transfections with promoter/reporter hybrid constructs were performed. A 4.9-fold induction of transfected pIL-8(-420/+102)LUC was observed 2 days after infection with DV of ECV304 cells and a 10- to 20-fold activation with pRANTES (-935/+73) (Fig. 5).

Chemokines in samples from DSS patients

The results of the in vitro assays prompted us to analyze PF and plasma samples of DSS patients for the presence of IL-8, MCP-1, and RANTES. ELISAs were performed twice on each sample with virtually identical results. As shown in Table I, IL-8 in plasma and PF of DSS patients were all markedly increased over the healthy donor controls; the difference exceeded 2 logs in some cases. Combined treatment of cell-rich plasma from healthy donors with inulin, 50 mg/ml at 37°C for 1 h (to activate complement), and 0.1% Triton X-100 for an additional 30 min at RT (to liberate any cell-bound IL-8) led to increased plasma IL-8 levels of up to 627 pg/ml. MCP-1 levels in the patients' samples were also markedly elevated. Presumably due to the activation of platelets during sampling, RANTES was detectable in all plasma samples of DSS patients and healthy donors, with concentrations ranging between

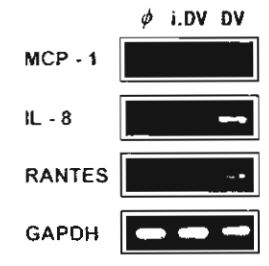


FIGURE 4. Selective induction of IL-8 and RANTES mRNA in DV-infected ECV304 cells. RT-PCR was performed on total RNA isolated 24 h after initiation of cultures from untreated cells (ϕ), cells treated with inactivated DV (i.DV), or DV (DV). The constitutively expressed GAPDH gene served as a control. The same results were reproduced in two further experiments.

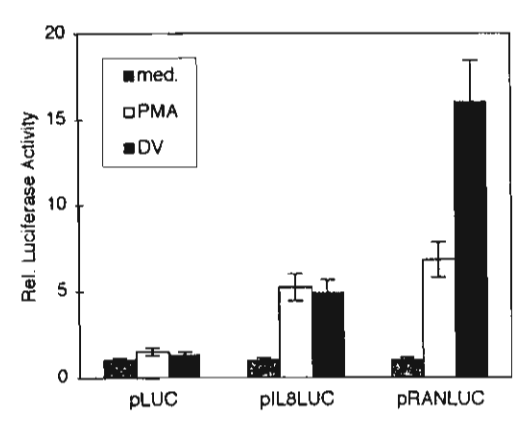


FIGURE 5. Up-regulation of the IL-8 and the RANTES promoter in transiently transfected ECV304 cells following infection with DV. Promoter/reporter hybrid plasmids pIL8(-420/+102)LUC or pRANTES(-935/+73)LUC were transiently transfected into ECV304 cells using Lipofectin Life Technologies. Luciferase activity was measured in cell lysates from parallel cultures that were either treated with DV for 48 h (DV) or with PMA at 50 ng/ml for 16 h (PMA) as a positive control or left untreated (med.). The data shown represent the mean of three independent experiments ± SD, each done in triplicate, and are reported as the fold activation over the untreated control.

750 and 1500 pg/ml. Plasma RANTES determinations were considered uninformative. In contrast, RANTES concentrations in PF of DSS patients 1 through 6 were: 34, 1018, 530, 13, 12, and 60 pg/ml, respectively. Thus, the two samples with the highest amounts of IL-8 also displayed the highest levels of RANTES.

Cell death of ECV304 after infection with DV

On microscopic inspection of infected ECV304 or primary cells we regularly noted rounding, detachment, and nuclear condensation of many cells after 48–72 h. Measurements of intracellular ATP and propidium iodide-uptake were performed. DV led to approximately 50% ATP reduction after 48 h and to >73% reduction by 72 h postinfection (Fig. 6). The number of propidium iodide-positive cells increased from 7% at 24 h to almost 40% at 72 h. The morphology of dying cells in DV-infected cultures suggested that they succumbed to programmed cell death. Nicking of the DNA by endogenous endonucleases is another hallmark of apoptosis (22), and the TUNEL method was next used to detect intrachromosomal DNA strand breaks. As a control, cells were treated with TNF- α , and anti-TNF Abs were employed to detect cytokine-dependent apoptosis. In the experiment of Fig. 7, controls incubated without (Fig. 7A) or with anti-TNF Abs (Fig. 7B) contained less than 1%

Table I. Chemokines in body fluids of DSS patients

	IL-8 (pg/ml)		MCP-1 (pg/ml)	
	Plasma	Pleural fluid	Płasma	Pleural fluid
DSS patient				
1	1,795	1,200	1,966	3,597
2	13,798	15,977	ND	3,692
3	10,973	19,009	3,643	3,780
4	3,338	639	3,294	3,471
5	977	1,089	1,037	2,808
6	20,000	2,164	4,316	2,810
Controls				
t	4		35	
2	161		40	
3	0		ND	
4	284		ND	

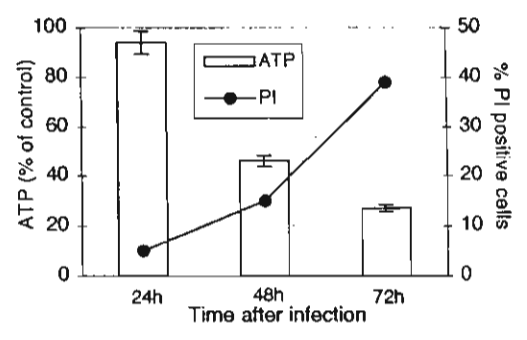


FIGURE 6. DV infection causes cell death in ECV304 cells. At 24, 48, and 72 h after infection, ECV304 cells (pool of adherent cells and cells in culture fluid) were harvested and stained with propidium iodide prior to analysis by flow cytometry. No significant change in the number of propidium iodide-positive cells was observed in uninfected cultures (not shown). In parallel experiments, DV-infected ECV304 monolayers were analyzed for the level of intracellular ATP. The data shown are representative of two experiments showing the average of six measurements ± SD.

apoptotic cells. Treatment with TNF- α plus cycloheximide (10 μ g/ml) for 16 h caused apoptosis in about 5–10% of cells (Fig. 7C), and this effect was inhibited by anti-TNF Abs (Fig. 7D). DV infection led to apoptosis of 15–25% of the cells after 24 h (not shown) and 50–60% of the cells after 48 h (E), and anti-TNF Abs were unable to suppress this effect (Fig. 7F). Thus, apoptosis of DV-infected cells appeared not to be dependent on TNF- α secreted by ECV304. Apoptosis of hepatoma cells following DV infection has been reported recently (23).

NF-KB activation following DV infection of ECV304 cells

The crucial role of transcription factor NF-kB for the control of immune responses, including the production of chemokines, is well documented and NF-kB has recently also been recognized to be a central player in the regulation of cell death (24). We therefore investigated whether DV-infected ECV304 cells activate NF-kB. First, double-immunofluorescence staining for viral Ag and NF-kB p65 was performed (Fig. 8). Nuclei of untreated cells are essentially negative for p65, some cytoplasmic staining is seen (Fig. 8A). Positive staining with Ab to the viral Ag NS1 proved that virtually all cells were infected (Fig. 8B). Double staining for NS1 and for p65 revealed that p65 was translocated to the nuclei in some of the cells and to different degrees. Most of the cells exhibiting intense nuclear staining for NF-kB and complete translocation were characterized by a strong and focal perinuclear staining for NS1 and appeared condensed (Fig. 8C). Orange to yellow staining resulted from double exposure with the two fluorescent dyes. Thus, NF-κB p65 activation occurred in infected cells.

The time course of NF- κ B activation was assessed by EMSA. (Fig. 9A); extracts from cultures infected for 24 and for 48 h showed increased binding activity, at least in part due to increased p65 binding. No induction was seen at 12 h or earlier. While competition with a 200-fold molar excess of unlabeled oligonucleotides showed that complexes with either extracts from uninfected or DV-infected cells were specific for the probe, immunosupershift experiments clearly demonstrated that binding of both NF- κ B p65 and of p50 was markedly activated in virus-treated cells (Fig. 9B). C1 disappeared after preincubation with anti-p65 and thus probably represents a p65 homodimer while C2 was reduced after either preincubation with anti-p50 or anti-p65 and thus may be a p50/p65 heterodimer. Preincubation with both Abs (lane 6) led to a decrease of C2, SC1, and SC2, suggesting that these complexes comprise p50 and p65, the major activating form of NF- κ B.

The Journal of Immunology 6343

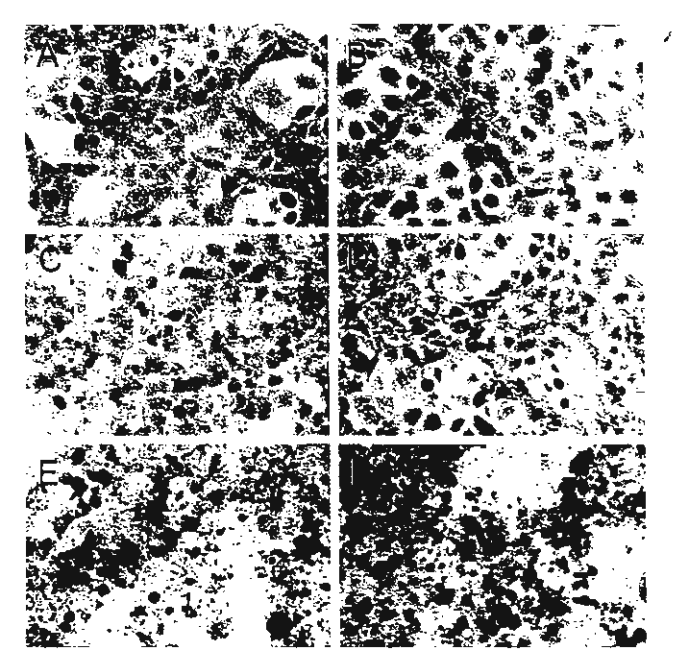


FIGURE 7. TUNEL staining of DV-infected ECV304 cells. Cells were fixed and stained after 48 h of cultures. A, Control cells; B, control cells incubated with anti-TNF Abs; C, cells treated with TNF- α /cycloheximide; D, cells treated with TNF- α /cycloheximide plus Abs against TNF- α , showing reduction of apoptosis as compared with C; E, cells 48 h after DV infection without or with (F) Abs against TNF- α . Approximately 50% of the DV-infected cells were apoptotic in both E and F. Virtually identical results were obtained in two experiments.

Dengue virus-infected endothelial cells are capable of activating complement

A marked reduction of complement proteins and a concomitant increase in complement fragments is observed in DHF/DSS, and the degree of complement activation correlates with the severity of the disease (5, 25, 26). Therefore, we investigated whether DVinfected EC activate complement in vitro. DV-infected ECV304 cells were incubated in the presence and absence of anti-dengue Abs with human complement for 1 h at 37°C. Ab-dependent deposition of C3dg fragments on the surface of infected cells was observed using a mAb specific for a neoantigen that is exposed in C3bi and C3dg (27) (Fig. 10A). This necepitope is expressed only after cleavage of substrate-bound complement C3b by factor I, in the presence of factor H, upon binding to a complement-activating surface (28). Positive staining for C3dg was time dependent: staining was not observed when cells that had been infected for only 12 h were analyzed. The latter negative finding at the same time provided an important control. Deposition of C3dg fragments was also not seen when infected ECV304 cells were incubated with anti-dengue Abs and heat-inactivated nonimmune serum (not shown), or with nonimmune serum alone (Fig. 10B). Together, these results indicated that activation of complement by dengueinfected ECV304 cells is Ab dependent.

Activation of complement does not always lead to the generation of membrane attack complexes, C5b-9. Circulating SC5b-9 complexes have been detected particularly in patients with severe disease (P. Malasit, J. Mongkolsapaya, S. Nimmannitya, and S. Bhakdi, unpublished observations). Their origin is not known. Small surfaces, such as soluble immune complexes, are less efficient in terms of C5b-9 complex generation than large activator surfaces, e.g., cells (29). Therefore, in the next experiments, the formation of C5b-9 complexes on control or DV-infected ECV304

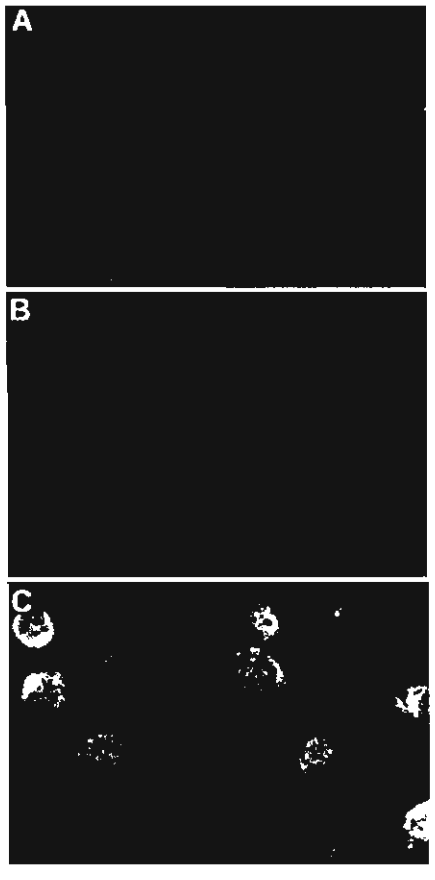


FIGURE 8. DV induces nuclear translocation of NF- κ B p65 in ECV304 cells. A, Untreated cells; B and C, cultures infected for 48 h with DV. Cells were fixed and stained for NF- κ B p65 using a conjugate of the red dye Cyt3 as the secondary Ab (A, C). The viral nonstructural Ag NS1 was stained with a specific mAb and a DTAF-conjugate conferring green fluorescence (B and C). One representative experiment out of three is shown.

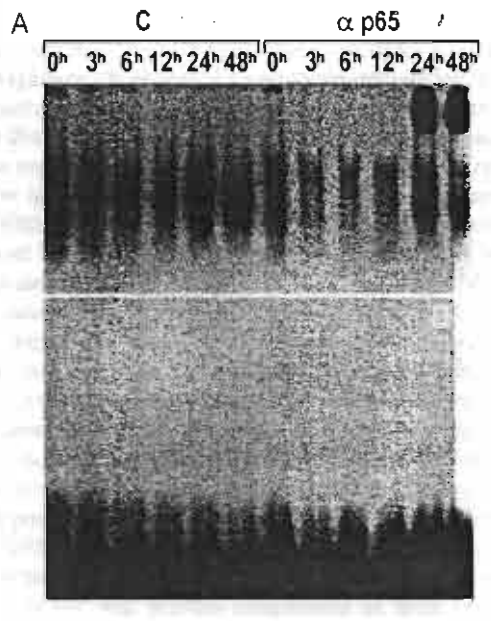
cells treated with anti-dengue Abs plus complement were analyzed. DV infection led to C5b-9 formation (Fig. 10C). Activation occurred via both classical and alternative pathways since adding EGTA-MgCl₂ only partially abolished the formation of C5b-9 complexes (data not shown).

Since the formation of C5b-9 complexes on the surface of cells may lead to cell lysis, measurements of cellular ATP were undertaken. No changes were observed after incubation of infected cells with anti-dengue Abs and complement (data not shown). This result indicated that no direct cytotoxic effect occurred after complement activation of dengue-infected ECV304 cells.

Discussion

Short-lived plasma leakage occurring selectively at serosal sites, and massive complement consumption are hallmarks of DSS. The objective of the present study has been to seek for possible explanations and causal links between these phenomena. As in all previous studies on DV pathogenesis, we were restricted to model studies in vitro; however, these led to a directed search and to the novel finding of high IL-8 levels in plasma and PF of DSS patients.

Based on the collective data, several pathways are envisaged that possibly converge to cause the massive but transient leakage syndrome. First is a selective action of cationic chemokines on the vascular endothelium in serosal tissues, which may be mediated via their interaction with heparan sulfate expressed at these sites.



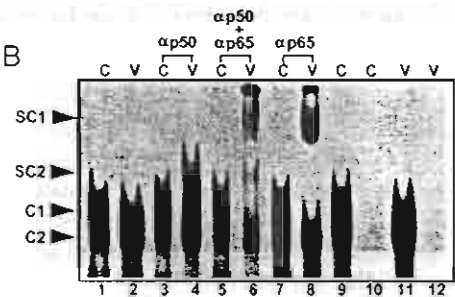


FIGURE 9. A, Time course of DV-induced NF-κB activation. At various times after infection with DV, ECV304 cells were harvested and whole cell extracts were prepared. EMSA was performed with equal amounts of protein per lane. Note the increased binding at 24 and 48 h. The data on the right half of panel A were obtained with Ab against p65 in the binding reaction. B, Immunosupershift and competition with unlabeled oligonucleotides. Lanes marked with a C contained binding reactions performed with extracts from control cells (treatment with inactivated DV); in lanes marked V, binding reactions with extracts from DV-infected cultures were analyzed. Extracts were obtained 48 h after initiation of cultures. SC1 and SC2 indicate supershifted complexes generated after preincubation of extracts with Abs against p65 or p50, respectively, from complexes C1 and C2. The experiments shown in both panels, A and B, were reproduced once.

A second mechanism is the activation of complement on the surface of infected cells, and the third is apoptotic cell death.

The cellular source of chemokine production remains an open question. In line with the classic Ab dependent enhancement concept, which envisages non-neutralizing Abs to augment infection of macrophages, these cells may provide a source of these chemokines. However, the present study raises another possibility, i.e., that EC may also be major producers of IL-8 and RANTES. This hypothesis derives from two findings: first, EC are effectively infected by DV, and second, DV-infected EC selectively up-regulate transcription and secretion of IL-8 and RANTES.

That EC can be infected by DV has been shown previously, and we confirm that the virus replicates to high titers in cultured EC, independent of the presence of enhancing Abs. The reason for differential susceptibility of ECV304 and HUVEC remains to be elucidated. Possibly ECV304 express a higher density of DV receptor. That DV-infected EC liberate large amounts of IL-8 and RANTES is a novel finding. Transcriptional up-regulation was

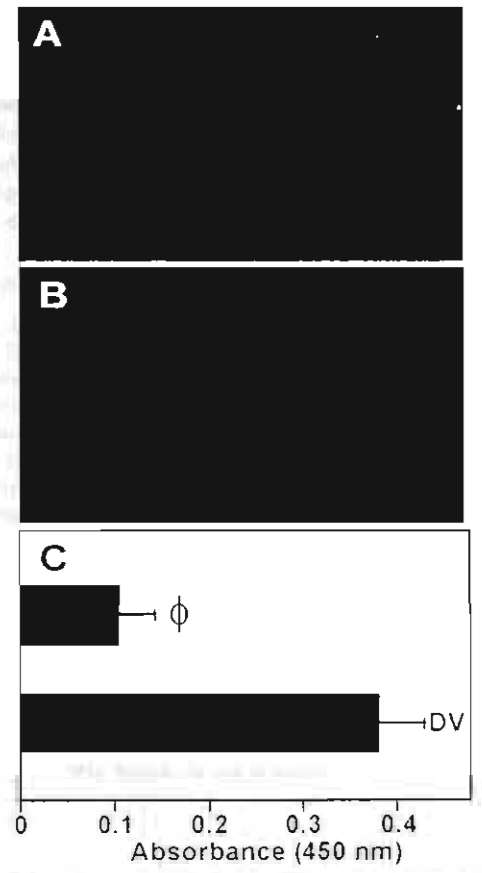


FIGURE 10. Deposition of C3dg and C5b-9 on the surface of DV-infected cells. A, Detection of C3dg by immunofluorescence. DV-infected cells were incubated with pooled dengue hyperimmune sera plus complement, and C3dg was subsequently detected by the use of a mAb specific for a neoantigen. B, No fluorescence was detected in DV-infected cells treated with complement alone. Representative photomicrographs from one out of two experiments are shown in A and B. C. Detection of cell-bound C5b-9 by ELISA. DV-infected or control cells were incubated with anti-dengue Ab and complement, subsequently washed, and lysed with detergent. Cell lysates were subjected to ELISA for the detection of C5b-9 complexes. The ELISA signal obtained in lysates from controls (Ø) ranged at background levels whereas positive signals were observed in lysates of infected cells (DV). No C5b-9 complexes were detected when control or DV-infected ECV304 cells were incubated with complement without anti-dengue Abs, in the presence of EGTA/MgCl2, or with heat-inactivated complement (not shown). The data represent the average of four experiments ± SD.

demonstrated with the use of reporter gene constructs, and secreted proteins were quantified by ELISA. Quite remarkably, chemokine production occurred selectively, and there was no virus-mediated induction of MCP-1, IL-1 β , IL-1 α , IL-15, or GM-CSF. The selective induction of cytokine synthesis is now emerging as a common theme that possibly directs pathology in many diseases. The underlying mechanism in the case of DV will be the subject of future studies, but the very fact that the virus selectively induces endothelial production of IL-8 and RANTES harbors potentially significant consequences. It is known that IL-8 binds to heparan sulfate (30) and to EC of serosal tissues (31) that express this proteoglycan (32). It is also known that both IL-8 and RANTES increase vascular permeability via transient recruitment and local activation of neutrophils (33). That the chemokines are indeed produced in quantity during viral infection became evident from IL-8 measurements in plasma and pleural fluids from DSS patients. Very high levels of circulating IL-8 were detected in all cases.

These could not have derived from circulating Granulocytes, because maximal IL-8 levels in control blood samples were two orders of magnitude lower despite Granulocyte-stimulation via complement activation with inulin combined with cell lysis with Triton X-100 to liberate any nonsecreted IL-8. We believe it is reasonable to assume that the high chemokine levels in DSS patients reflected production in infected cells, with EC representing attractive candidates. While MCP-1 levels in supernatants of ECV304 cells were not induced by DV, all plasma and PF samples of DSS patients displayed elevated levels of this chemokine. Levels of MCP-1 in PF from various clinical conditions have previously been shown to correlate with the numbers of monocytes (34). Thus, monocytes might also be an important source of the chemokines in PF of DSS patients. Cytologic studies with PF from DSS patients are in progress now. Of note, high levels of IL-8 have been detected in patients with pleural effusion of other etiology, whereby the values measured in our study markedly exceed those previously published (34). The presence of large amounts of RANTES in two out of six PF from DSS patients complements the findings on IL-8.

Once infection of EC has occurred, cross-reacting, non-neutralizing Abs to DV will activate complement on these cells. This provides a second possible mechanism leading to vascular leakage. Complement attack on virus-infected cells is, of course, not conceptually novel, but its possible involvement in DSS has not received much consideration hithertofore. In an early hypothesis, one of us pointed out that such auto-attack would result in local liberation of anaphylatoxins and the generation of C5b-9 complexes (10). Both processes could contribute to disease. Here, the Ab-dependent deposition of activated C3 and C5b-9 on DV-infected cells was demonstrated. Our results indicate that the terminal complexes were not directly cytocidal, and it is known that subcytocidal C5b-9 attack increases vascular permeability of endothelial cell monolayers (35). C5b-9 generation can only occur in conjunction with the liberation of anaphylatoxins. In this context, high levels of C3a and C5a have indeed been detected in PF of DSS patients (P. Malasit, unpublished observation). C3a induces histamine release from mast cells, and thus would indirectly enhance vascular permeability. It is of interest that high histamine concentrations have actually been measured in urine samples of DSS patients (36). In addition to activating phagocytes, C5a induces shedding of heparan sulfate from EC (37). In the context of DV pathogenesis, this may be important because, if chemokines are targeted to serosal EC via binding to heparan sulfate, C5ainduced shedding might represent a counteracting factor. Furthermore, if heparan sulfate represents a binding site for DV on EC (38), shedding might also serve to limit infection.

The third putative pathway to vascular leakage could derive from apoptosis of infected cells. Massive reduction in cellular ATP, accompanied by positive TUNEL stainings for nicked DNA occurred after 3-4 days of infection. Apoptosis of DV-infected EC would acutely enhance local vascular leakage. Furthermore, apoptosis would be followed by rapid removal of infected cells, which would explain the difficulties in detecting the infectious agent in tissue specimens. Apoptosis of infected EC and complement-induced shedding of the viral receptor heparan sulfate from bystander cells would also nicely explain the abrupt termination of infection

In summary, there are three major findings in this study that can be accommodated in a coherent hypothesis of the DSS leakage syndrome. First, EC are highly permissive to DV infection and respond by the selective production of chemokines IL-8 and RAN-TES. These may accumulate at serosal sites, causing local vascular leakage. Second, cross-reacting but non-neutralizing Abs to DV will activate complement on the surface of infected EC, causing liberation of anaphylatoxins and deposition of C5b-9. Of these, C3a may mediate histamine release, and C5a will induce shedding of heparan sulfate. The latter might counteract infection and reduce chemokine binding. Third, infected EC eventually undergo apoptosis. This would augment vascular leakage, and also provide a mechanism for the sudden disappearance of the infectious agent, explaining the short-lived duration of disease and the eradication of clues to the nature of the infected cells in vivo.

Acknowledgments

We thank Dr. Peter J. Lachmann for providing mAbs C3dg neoepitope (clone 9), Dr. Anan Nisalak for pooled dengue hyperimmune serum and dengue-2 hyperimmune mouse ascitic fluid; Dr. Mariam Klouche for primers and help in performing RT-PCR experiments; Dr. Sirijitt Vasanawathana and Dr. Kulkanya Chokephaibulkit for collection of the PF and providing clinical data of the patients at Khonkaen and Siriraj Hospitals respectively; Dr. Suchitra Nimmannitya for her comments throughout the research project; Dr. Iwan Walev for advice and support, Petra Jehnichen for technical assistance, Dr. Dirk Peetz for albumin determinations, and Klaus Adler for outstanding photographic help and artwork.

References

- 1. Henchal, E. A., and J. R. Putnak. 1990. The dengue viruses. Clin. Microbiol. Rev. 3:376
- 2. Their, S., M. M. Aung, T. N. Shwe, M. Ave, A. Zaw, K. Ave, K. M. Ave, and J. Aaskov. 1997. Risk factors in dengue shock syndrome. Am. J. Trop. Med. Hvg.
- 3. Monath, T. P. 1994. Dengue: the risk to developed and developing countries. Proc. Natl. Acad. Sci. USA 91:2395.
- 4. Nimmannitya, S. 1987. Clinical spectrum and management of dengue haemor-
- rhagic fever. Southeast Asian J. Trop. Med. Public Health 18:392.
 Bokisch, V. A., F. H. Top, Jr., P. K. Russell, F. J. Dixon, and H. J. Muller-Eberhard. 1973. The potential pathogenic role of complement in dengue hemorrhagic shock syndrome. N. Engl. J. Med. 289:996.
- 6. Innis, B. L. 1995. Dengue and dengue hemorrhagic fever. In Exotic Viral Infection. J. S. Porterfield, ed. Chapman & Hall, London, p. 103.
- 7. Halstead, S. B. 1989. Antibody, macrophages, dengue virus infection, shock, and hemorrhage: a pathogenetic cascade. Rev. Infect. Dis. 11 (Suppl. 4):S830.
- 8. Kurane, I., A. L. Rothman, P. G. Livingston, S. Green, S. J. Gagnon, J. Janus, B. L. Innis, S. Nimmannitya, A. Nisalak, and F. A. Ennis. 1994. Immunopathologic mechanisms of dengue hemorrhagic fever and dengue shock syndrome Arch. Virol. Suppl. 9:59
- 9. Halstead, S. B., and E. J. O'Rourke 1977. Dengue viruses and mononuclear phagocytes. I. Infection enhancement by non-neutralizing antibody. J. Exp. Med. 146:201.
- 10. Bhakdi, S., and M. D. Kazatchkine. 1990. Pathogenesis of dengue: an alternative hypothesis. Southeast Asian J. Trop. Med. Public Health 21:652.

 11. Butthep, P., A. Bunyaratvej, and N. Bhamarapravati. 1993. Dengue virus and
- endothelial cell; a related phenomenon to thrombocytopenia and granulocytopenia in dengue hemorrhagic fever. Southeast Asian J. Trop. Med. Public Health 24:246.
- 12. Andrews, B. S., A. N. Theofilopoulos, C. J. Peters, D. J. Loskutoff, W. E. Brandt. and F. J. Dixon. 1978. Replication of dengue and Junin viruses in cultured rabbit and human endothelial cells. Infect. Immun. 20:776.
- 13. World Health Organization. Dengue Hemorrhagic Fever: Diagnosis, Treatment and Control. WHO, Geneva, 1986.
- 14. Chomczynski, P., and N. Sacchi. 1987. Single-step method of RNA isolation by acid guanidinium thiocyanate-phenol-chloroform extraction. Anal. Biochem. 162: 156.
- 15. Klouche, M., S. Gottschling, V. Gerl, W. Hell, M. Husmann, B. Dorweiler, M. Meßner, and S. Bhakdi. 1998. Atherogenic properties of enzymatically degraded low density lipoprotein: selective induction of MCP-1 and cytotoxic effects on human macrophages. Arterioscler. Thromb. Vasc. Biol. 18:1376.
- 16. Bhakdi, S., M. Muhly, S. Korom, and G. Schmidt. 1990. Effects of Escherichia coli hemotysin on human monocytes: cytocidal action and stimulation of interleukin 1 release. J. Clin. Invest. 85:1746.
- Husmann, M., P. Jehmchen, B. Jahn, D. Schlosshan, E. Romahn, and J. Marx. 1996. A novel SP-1 site in the human interleukin-1 beta promoter confers preferential transcriptional activity in keratinocytes. Eur. J. Immunol. 26:3008.
- 18. Hugo, F., S. Kramer, and S. Bhakdi. 1987. Sensitive ELISA for quantitating the terminal membrane C5b-9 and fluid-phase SC5b-9 complex of human complement. J. Immunol. Methods. 99:243.
- 19. Cardiff, R. D., and J. K. Lund. 1976. Distribution of dengue-2 antigens by electron immunocytochemistry. Infect. Immun. 13:1699
- 20. Catanzaro, P. J., W. E. Brandt, W. R. Hogrefe, and P. K. Russell. 1974. Detection of dengue cell-surface antigens by peroxidase-labeled antibodies and immune cytolysis. Infect. Immun. 10:381.
- 21. Ng, M. L., and L. C. Corner. 1989. Detection of some dengue-2 virus antigens in infected cells using immuno-microscopy. Arch. Virol. 104:197.

- Gavrieli, Y., Y. Sherman, and S. A. Ben Sasson. 1992. Identification of programmed cell death in situ via specific labeling of nuclear DNA fragmentation. J. Cell. Biol. 119:493.
- Marianneau, P., A. Cardona, L. Edelman, V. Deubel and P. Desprès, 1997. Dengue virus replication in human hepatoma cells activates NF-κb which in turn induces apoptotic cell death. J. Virol. 71:3244.
- Baichwal, V. R., and P. A. Baeuerle. 1997. Activate NF-κB or die? Curr. Biol. 7-R9
- Anonymous. 1973. Pathogenetic mechanisms in dengue haemorrhagic fever: report of an international collaborative study. Bull. W. H. O. 48:117.
- Malasit, P. 1987. Complement and dengue haemorrhagic fever/shock syndrome. Southeast Asian J. Trop. Med. Public Health 18:316.
- Lachmann, P. J., R. G. Oldroyd, C. Milstein, and B. W. Wright. 1980. Three rat monoclonal antibodies to human C3. *Immunology* 41:503.
- Lachmann, P. J., M. K. Pangburn, and R. G. Oldroyd. 1982. Breakdown of C3
 after complement activation: identification of a new fragment C3g, using monoclonal antibodies. J. Exp. Med. 156:205.
- Bhakdi, S., W. Fassbender, F. Hugo, M. P. Carreno, C. Berstecher, P. Malasit, and M. D. Kazatchkine. 1988. Relative inefficiency of terminal complement activation. J. Immunol. 141:3117.
- Witt, D. P., and A. D. Lander. 1994. Differential binding of chemokines to glycosaminoglycan subpopulations. Curr. Biol. 4:394.

- Rot, A., E. Hub, J. Middleton, F. Pons, C. Rabeck, K. Thierer, J. Wintle, B. Wolff, M. Zsak, and P. Dukor. 1996. Some aspects of IL-8 pathophysiology. III. Chemokine interaction with endothelial cells. J. Leukocyte Biol. 59:39.
- Erlinger, R. 1995. Glycosaminoglycans in porcine lung: an ultrastructural study using cupromeronic blue. Cell Tissue Res. 281:473.
- Rampart, M., J. van Damme, L. Zonnekeyn, and A. G. Herman. 1989. Granulocyte chemotactic protein/interleukin-8 induces plasma leakage and neutrophil accumulation in rabbit skin. Am. J. Pathol. 135:21.
- Anthony, V. B., S. W. Godbey, S. L. Kunkel, J. W. Hott, D. L. Hartman, M. D. Burcick, and R. M. Strieter. 1993. Recruitment of inflammatory cells to the pleural space. J. Immunol. 12:7216.
- Saadi, S., and J. L. Platt. 1995. Transient perturbation of endothelial integrity induced by natural antibodies and complement. J. Exp. Med. 181:21.
- Tuchinda, M., B. Dhorranintra, and P. Tuchinda. 1977. Histamine content in 24-hour urine in patients with dengue haemorrhagic fever. Southeast J. Trop. Med. Public Health 8:80.
- Platt, J. L., A. P. Dalmasso, B. J. Lindman, N. S. Ihrcke, and F. H. Bach. 1991.
 The role of C5a and antibody in the release of heparan sulfate from endothelial cells. Eur. J. Immunol. 21:2887.
- Chen, Y., T. Maguire, R. E. Hileman, J. R. Fromm, J. D. Esko, R. J. Linhardt, and R. M. Marks, 1997. Dengue virus infectivity depends on envelope protein binding to target cell heparan sulfate. *Nat. Med.* 3:866.

Distal Renal Tubular Acidosis and High Urine Carbon Dioxide Tension in a Patient With Southeast Asian Ovalocytosis

Charoen Kaitwatcharachai, MD, Somkiat Vasuvattakul, MD, Pa-thai Yenchitsomanus, PhD, Peti Thuwajit, MD, Prida Malasit, MD, Duangporn Chuawatana, BSc, Sumitra Mingkum, BSc, Mitchell L. Halperin, MD, Prapon Wilairat, PhD, and Sumalee Nimmannit, MD

• Southeast Asian ovalocytosis (SAO) is the best-documented disease in which mutation in the anion exchanger-1 (AE1) causes decreased anion (chloride [Cl⁻]/bicarbonate [HCO₃⁻]) transport. Because AE1 is also found in the basolateral membrane of type A intercalated cells of the kidney, distal renal tubular acidosis (dRTA) might develop if the function of AE1 is critical for the net excretion of acid. Studies were performed in a 33-year-old woman with SAO who presented with proximal muscle weakness, hypokalemia (potassium, 2.7 mmol/L), a normal anion gap type of metabolic acidosis (venous plasma pH, 7.32; bicarbonate, 17 mmol/L; anion gap, 11 mEq/L), and a low rate of ammonium (NH₄⁺) excretion in the face of metabolic acidosis (26 μmol/min). However, the capacity to produce NH 4⁺ did not appear to be low because during a furosemide-induced diuresis, NH 4⁺ excretion increased almost threefold to a near-normal value (75 μmol/L/min). Nevertheless, her minimum urine pH (6.3) did not decrease appreciably with this diuresis. The basis of the renal acidification defect was most likely a low distal H ⁺ secretion rate, the result of an alkalinized type A intercalated cell in the distal nephron. Unexpectedly, when her urine pH increased to 7.7 after sodium bicarbonate administration, her urine minus blood carbon dioxide tension difference (U--B P co₂) was 27 mm Hg. We speculate that the increase in U-B P co₂ might arise from a misdirection of AE1 to the apical membrane of type A intercalated cells.

© 1999 by the National Kidney Foundation, Inc.

INDEX WORDS: Band 3 protein; anionic exchanger; NH 4+ excretion; NH4+ production; U-B Pco2; H+-ATPase.

HEREDITARY ovalocytosis (southeast Asian ovalocytosis [SAO]) is common in parts of southeast Asia and Melanesia. It is the best documented disease in which mutation in the anionic exchanger-1 (AE1)^{1,2} causes decreased anion transport³ and increased membrane rigidity.¹ The red blood cells (RBCs) in SAO are resistant to malarial invasion, and this has been attributed to their altered membrane mechanical properties.⁴

AE1 (or band 3 protein) is the major integral membrane protein of the human RBC. It is composed of two domains with separate functions. The N-terminal 40-kd portion is located in the cytoplasm and acts as an anchor site to the membrane for components of the RBC skeleton, a structure critical to RBC integrity and the binding of several glycolytic enzymes and hemoglobin. The C-terminal 55-kd portion spans the bilayer and performs the exchange of chloride (Cl⁻) for bicarbonate (HCO₃⁻) ions. ^{5,6} The AE1 gene that encodes this RBC anion exchanger is located on chromosome 17q21-qter. ⁷

AE1 is also found in the basolateral membrane of the type A, but not type B, intercalated cells of the kidney. 8.9 Most of the H⁺ in the distal nephron is secreted across the apical membrane of type A intercalated cells through vacuolar H⁺-adenosine triphosphatase (H⁺-ATPase). There is also a role for an H⁺, K⁺-ATPase in mediating

H⁺ secretion across the apical membrane of the type A intercalated cells. ¹⁰ It is likely that homozygosity for SAO band 3 is lethal, not only because of the effects on RBC function, but possibly because HCO₃ /Cl antiport is a critical component for H⁺ secretion in the distal portion of the nephron (Fig 1).

At least five studies implied that mutations of the AE1 gene affected renal acidification. Bae-

From the Renal Unit, Songklanakarin Hospital, Prince of Songkla University; Renal and Medical Molecular Biology Units, Siriraj Hospital; Faculty of Medicine, Department of Biochemistry, Faculty of Science, Mahidol University, Bangkok, Thailand; and the Renal Division, St Michael's Hospital, University of Toronto, Canada.

Received January 23, 1998; accepted in revised form October 16, 1998.

P.M. is a recipient of the Senior Research Scholar Award of the Thailand Research Fund and the Suraphongchai Honorary Professor Chair of the Siriraj Foundation. The Medical Molecular Biology Unit has been partially supported by grants from the National Center for Genetic Engineering of the National Science and Technology Development Agency. This work has been supported in part by grant no. 5623 from the mm MRC, Toronto, Canada.

Address reprint requests to Somkiat Vasuvattakul, MD, Renal Unit, Department of Medicine, Siriraj Hospital, Mahidol University, Bangkok, Thailand. E-mail: sisva@mucc.mahidol.ac.th

© 1999 by the National Kidney Foundation, Inc 0272-6386/99/3306-0020\$3.00/0

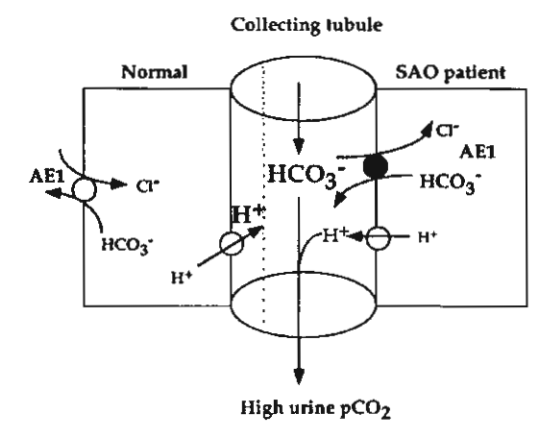


Fig 1. Proposed mechanism for a normal increased urine Pco₂ in the patient. Two possible explanations for the increased urine P co₂ are a greater secretion of H+ and/or a greater secretion of HCO₃. The barrelshaped structure is the collecting duct, and the rectangles represent type A intercalated cells (normal on the left and SAO patient on the right). The abnormality of AE1 in the patient with SAO results in mistargeting of the protein to the apical membrane, where it functions to secrete bicarbonate and thereby increase, rather than decrease, the U-B P co₂.

hner et al¹¹ reported that renal tubular acidosis (RTA) occurred in a single family with hereditary elliptocytosis. Rysava et al^{12,13} suggested that 2 of 10 patients with hereditary spherocytosis and a known AE1 gene mutation (substitution of G→A in the first nucleotide of intron 12, PRIBRAM band 3), had an incomplete form of RTA. Cope et al¹⁴ implied that both glycosylation abnormality and band 3 mutation may be necessary to produce familial distal RTA (dRTA). Bruce et al¹⁵ reported an association between familial dRTA and point mutations of the AE1 gene, and Jarolim et al¹⁶ described the association of the heterozygous hypomorphic AE1 mutation R589H with dominant dRTA and normal RBCs.

We report a case with SAO and dRTA in which the distal H⁺ secretory defect might arise from an altered anion (HCO₃ /Cl⁻) exchanger in the type A intercalated cells of the collecting duct. There was an unanticipated finding of a defect in distal H⁺ secretion, resulting in a high value for the urine minus blood carbon dioxide tension difference (U-B PCO₂). ¹⁷ Possible implications of this unexpected finding are discussed.

Table 1. Laboratory Values on Admission

	Serum	Urine	
рН	7.32	6.6	
Bicarbonate (mmol/L)	17		
Sodium (mmol/L)	139	86	
Potassium (mmol/L)	2.7	32	
Chloride (mmol/L)	111	113	
Anion gap (mEq/L)	11	5	
BUN (mg/dL)	10	_	
Creatinine (mg/dL)	0.7	_	
Osmolality (mOsm/kgH ₂ O)	294	450	

Abbreviations: BUN, blood urea nitrogen.

CASE REPORT

The chief complaint in a 33-year-old woman was generalized muscle weakness for the past 4 months. Her past medical history and review of systems were unremarkable. She was an elder sister in a family with two sibs. Only she and her father had SAO.

On admission, she was afebrile, blood pressure was 110/70 mm Hg while supine, respiratory rate was 20 breaths/min, and pulse rate was 86 beats/min. Postural changes in blood pressure and pulse rate were not detected. The patient was alert and oriented. The only abnormality on physical examination was a moderate degree of weakness of the proximal muscles in all extremities. Muscle bulk was normal, and the muscles were not tender. Cranial nerve function, sensory examinations, and deep tendon reflexes were normal.

On laboratory examination, her hematocrit was 39%, and ovalocytosis (75%) was prominent in the peripheral blood smear. The principal acid-base findings were metabolic acidosis with a normal anion gap in plasma (Table 1); a relatively low rate of excretion of NH₄+, together with a high urine pH (6.6) and a low rate of excretion of citrate (Table 2); an ability to increase the rate of excretion of NH₄+ threefold with a loop diuretic (Table 3); and a fractional excretion of bicarbonate of only 5% after a sodium bicarbonate load (Table 4). There was one surprising finding during the sodium bicarbonate load, which was a high value for urine PCO₂ (Table 4). There was also a high rate of excretion of potassium and transtubular [K+] gradient (TTKG)¹⁸ given the degree of hypokalemia (Table 2).

The results of analysis of AE1 gene by polymerase chain reaction¹⁹ showed that both the patient and her father were heterozygous for a 27-bp deletion in exon 11 (Fig 2), which confirmed that they had the mutation specific for SAO, whereas her mother and younger sister did not carry this mutation.

Table 2. Urine Values on Admission

Creatinine clearance (mL/min)	95
pH	6.6
NH4+ (µmol/min)	26
Citrate (µmol/min)	0.02
Potassium (µmol/min)	28
TTKG	7.7

Table 3. Urine Values After Oral Furosemide

	Control	After Diuresis
Flow rate (mL/min)	0.9	10
Sodium (µmol/min)	85	1080
Potassium (µmol/min)	28	73
pH	6.7	6.3
NH4+ (µmol/min)	26	75
Citrate (µmol/min)	0.17	< 0.01

³⁵S-sulfate influx studies³ for RBC anion transport of the patient and her father showed a 40% reduction in sulfate influx with normal 4,4-di-isothiocyanate-stilbene-2,2'-disulfonic acid (DIDS) sensitivity and pH dependence (Table 5).

DISCUSSION

The findings of hyperchloremic metabolic acidosis, hypokalemia with a relatively high TTKG and potassium excretion rate, a relatively low rate of excretion of NH₄⁺ and citrate, and high urine pH (>5.5) are all typical for a patient with a decreased rate of distal H⁺ secretion.²⁰ These results describe our patient with dRTA, whose disease is associated with the mutation of AE1 gene (deletion of 27-bp in exon 11). Nevertheless, no specific renal tissue was obtained because we could not do so on ethical grounds.

There are two major reasons why her rate of excretion of NH₄⁺ might be low: a low availability of ammonia in the renal medullary interstitium and/or a low rate of H+ secretion in the distal nephron. The high urine pH suggests there was a low rate of distal H+ secretion.20 To assess whether there was also a low [NH3] in the medullary interstitium, the patient was administered a loop diuretic, and the rate of excretion of NH4+ was measured as described by Vasuvattakul et al.21 Because the rate of excretion of NH₄⁺ increased by almost threefold during the furosemide-induced diuresis (Table 3) to typical values in healthy subjects with chronic acid loading,²¹ this indicates that the rate of production of NH4+ in the patient's proximal tubular cells was not appreciably depressed. That her urine pH did not decrease to the range of 4 to 5 with this diuresis is consistent with the suspicion that her major defect was a low net rate of H+ secretion in her distal nephron.22,23 There did not seem to be a major defect of H+ secretion in her proximal tubule because the fractional excretion of HCO₃ after sodium bicarbonate administration was close to 5% when her plasma bicarbonate level was 27 mmol/L (Table 4). Therefore, all these results were consistent with the impression that her major defect should be a reduced rate of H⁺ secretion in the distal nephron. This lesion would be anticipated if there was an impaired exit of HCO₃⁻ from these cells because of the AE1 defect, with the net result of a more alkaline intracellular pH.

Measurement of the U-B PCO2 in alkaline urine can provide a qualitative reflection of the secretion of H+ in the distal nephron. 17,24 After sodium bicarbonate loading (Table 4), the patient's plasma bicarbonate level was 27 mmol/L, urine pH increased to 7.7, and urine PCO2 was 66 mm Hg (U-B PCO₂, 27 mm Hg). The urine PCO₂ and U-B PCO2 in the two patients with hereditary spherocytosis and incomplete dRTA coinherited with a mutation in the AE 1 gene¹³ were also reported to be within the normal range after bicarbonate loading. There are three possible explanations for this normal increased urine Pco2 in the face of a defect in distal net H+ secretion. First, a reduction in luminal [H⁺] by the sodium bicarbonate load could permit more distal H+ secretion if the luminal [H+] influences net H+ secretion.25 However, this sodium bicarbonate load should also alkalinize type A intercalated cells further, and this should augment the depression of H+ secretion. Moreover, when the patient was administered an ammonium chloride (NH 4Cl) load for 3 days, NH₄+ excretion was very low because of the low distal H+ secretion. Second, a gradient defect, caused by an enhanced luminal membrane permeability of the collecting tubule to permit the back diffusion of H+, is also associated with dRTA and a normal ability to increase

Table 4. Urine Values After Oral Sodium Bicarbonate Loading With a Urine pH >7.4

	Blood	Urine
рH	7.44	7.74
Bicarbonate (mmol/L)	26.9	92.4
Creatinine (mg/dL)	0.7	49
Pco ₂ (mm Hg)	39	66
(U-B) Pco ₂ (mm Hg)	2	27
FE HCO ₃ - (%)		5

Abbreviation: FE HCO ₃⁻, fractional excretion of bicarba-

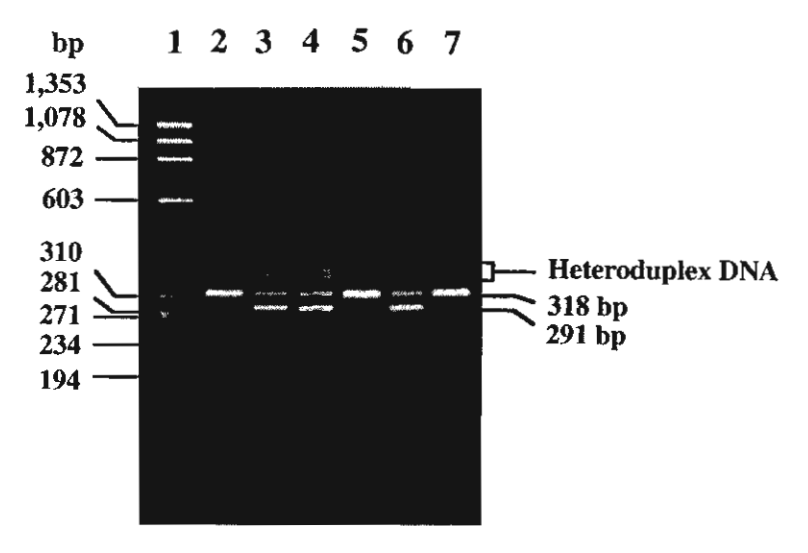


Fig 2. Agarose gel electrophoresis of polymerase chain reaction (PCR) products after amplifications of exon 11 of AE1 gene by PCR using exon 11 specific primers (AE1E ×11L/AE1E×11R). Lane 1 is PhiX 174 DNA/HaellI markers. Lanes 2 through 7 are PCR products resulted from amplifications of DNA samples of a healthy person, an individual with only SAO, patient's father, patient's mother, patient with dRTA and SAO, and patient's younger sister. The normal DNA sample gave PCR product with the size of 318 bp (lane 2), whereas that from the individual with SAO showed PCR products with the sizes of 318 and 291 bp, as well as heteroduplex DNA (lane 3). The DNA samples from the patient's father (lane 4) and the patient (lane 6) produced the PCR products the same as those of the individual with SAO, whereas those from the patient's mother (lane 5) and the patient's younger sister (lane 7) gave the PCR products the same as that of the healthy individual.

the urine PCo₂.^{17,24} A similar association has been reported in primary dRTA in an infant not previously exposed to amphotericin B²⁶ and in a patient with an early stage of primary Sjögren's syndrome²⁷ who also had the inability to decrease urinary pH in response to furosemide and markedly increased urinary excretion of NH₄⁺. For this mechanism to operate, the urine pH must be much greater than the mid-6 range because

the highest rates of NH₄⁺ excretion occur when the urine pH is in the low-6 range in subjects with chronic metabolic acidosis (NH₄Cl loading, ²⁸ chronic fasting). ²⁹⁻³¹ There is a problem relating the urine pH to that in the lumen of the distal nephron when bicarbonate is the principal urine buffer because of the absence of luminal carbonic anhydrase in this nephron segment (for review, see^{17,32,33}). As emphasized by Knepper

Table 5. 35S-Sulfate Influx Studies for RBC Anion Transport

		SO ₄ 2- Uptake (10 ⁻⁷ mol/L/min/cell)*		D*
	Phenotype	No DID\$	+ 1.5 µmoVL DIDS†	%‡
Father	SAO	4.8 ± 0.02§	0.1 ± 0.00	1.1
Mother	Normal	8.1 ± 0.1	3.7 ± 0.5	45.3
Patient	SAO	5.1 ± 0.1	0.1 ± 0.02	1.8
Sister	Normal	7.7 ± 0.3	3.4 ± 0.3	44.8
Mean of 2 SAOs		4.9 ± 0.2	0.1 ± 0.01	1.5 ± 1
Mean of 5 controls		6.3 ± 0.5	4.9 ± 1.5	58.6 ± 12

^{*}Initial rate of sulfate (SO 42-) uptake of the erythrocyte when incubated at 37°C with 3 mmol/L of [35S] sodium sulfate, 70 mmol/L of sodium citrate, 10 mmol/L of Tris, pH 7.4 buffer.

[†]The erythrocytes were incubated at 37°C with 1.5 µmol/L of DIDS for 15 minutes before SO 42- uptake

[‡]Percent of rate of SO 42- uptake, comparing with and without DIDS.

[§]Mean ± SD in duplicated experiment.

and Good,34,35 one should expect high local carbonic acid concentrations in luminal fluid, and thus the [H+] in vivo will be much greater here than in the urine. Therefore, a greater luminal [H+] in the distal nephron would likely be present with bicarbonaturia and make the gradient limit for H+ secretion a less likely explanation for the high urine PCO2 in our patient. Third, the normal ability to increase urine Pco2 during a bicarbonate diuresis could be the result of secretion of HCO₃ by type A intercalated cells in these patients with AE1 abnormality (Fig 1). To explain why HCO3 might be secreted by type A intercalated cells, we suggest, as did Bruce et al,15 that mistargeting of an active AE1 to the apical membrane of the type A intercalated cells might explain a decrease in net H+ (really HCO₃-) secretion in patients with familial dRTA.36 We hypothesize that the mutant AE1 protein in our patients was mistargeted to the apical membrane of the type A intercalated cells. The secretion of HCO₃ would not only cause a high urine Pco₂, but it should also cause an alkaline disequilibrium pH, making it even more difficult to trap ammonia in the luminal compartment. Secretion of HCO₃ by type B intercalated cells is also a possible mechanism for the normal increased urine PCO2. Nevertheless, because AE in these cells is a different gene product and is not involved in the SAO abnormality, these cells probably do not have abnormal function in this patient. Moreover, if HCO₃ were secreted by type B intercalated cells during a sodium bicarbonate load, the urine PCO2 would be increased in most patients with a defect in distal H⁺ secretion, but this is not consistent with the published data. 17

The incidence of metabolic acidosis in SAO patients is low. However, the degree to which the maximum rate of excretion of NH₄⁺ is decreased in SAO has never been studied. An incomplete form of dRTA might not produce clinical evidence of acidemia if there is enough capacity to excrete NH₄⁺ relative to the acid load of the diet, especially if the subject is not on a high-protein diet. Future studies, including U-B PCO₂ measurements, are planned in affected persons with SAO.

The presenting feature in this patient was related to hypokalemia (weakness). Although her daily intake of potassium was not high (42 mmol/L/d), the major reason for her hypokalemia was excessive excretion of potassium (>10 to 15 mmol/L/d, reviewed in ¹⁸). Because her osmole

excretion rate was not high, the flow rate in her cortical collecting duct was not excessively high.³⁷ Hence, a high [K⁺] in the lumen of the cortical collecting duct was the principal reason for her high rate of excretion of potassium (TTKG, 7.7 [Table 2], rather than <2¹⁸). Because her urine consistently contained HCO₃ (Table 2), perhaps the high TTKG reflected the kaliuretic actions of aldosterone when HCO₃ remained in the lumen of the CCD because of low distal H⁺ secretion, and possibly the secretion of HCO₃⁻, as previously suggested.^{23,38}

In summary, we report a case in which dRTA occurred in conjunction with SAO. The most likely explanation for the low rate of excretion of NH₄⁺ was a low rate of H⁺ secretion in the distal nephron, the result of an alkalinized type A intercalated cell consequent to impaired exit of HCO₃. There was an unanticipated high value for U–B PCO₂, perhaps the result of secretion of HCO₃⁻, which itself could also reduce the net rate of secretion of H⁺ in the distal nephron. The explanation might be from a mistargeting of the Cl /HCO₃ exchanger to the luminal membrane of the type A intercalated cells.

ACKNOWLEDGMENT

The authors thank Nunghathai Sawasdee for her laboratory assistance.

REFERENCES

- 1. Mohandas N, Winardi R, Knowles D, Leung A, Рагта M, George E, Conboy J, Chasis J: Molecular basis for membrane rigidity of hereditary ovalocytosis. A novel mechanism involving the cytoplasmic domain of band 3. J Clin Invest 89:686-692, 1992
- 2. Tanner MJA, Bruce L, Martin PG, Rearden DM, Jones DI: Melanesian hereditary ovalocytosis has a deletion in red cell band 3. Blood 78:2785-2787, 1991
- 3. Schofield AE, Reardon DM, Tanner MJA: Defective anion transport activity of the abnormal band 3 in hereditary ovalocytic red blood cells. Nature 355:836-838, 1992
- 4. Mohandas N, Lie-injo LE, Friedman M: Rìgid membranes of Malayan ovalocytosis. Blood 63:1385-1392, 1984
- Tanner MJA: Molecular and cellular biology of the erythrocyte anion exchanger (AE1). Semin Hematol 30:34-57, 1993
- 6. Peters LL, Shivdasani RA, Liu SC, Hanspal M, John KM, Gonzalez JM, Brugnara C, Gwynn B, Mohandas N, Alper SL, Orkin SH, Lux SE: Anion exchanger 1 (band 3) is required to prevent erythrocyte membrane surface loss but not to form the membrane skeleton. Cell 86:917-927, 1996
- 7. Showe LC, Ballantine M, Huebner K: Localisation of the gene for the erythroid anion exchange protein, band 3 (EMPB3), to human chromosome 17. Genomics 1:71-76, 1987

- 8. Sabolic I, Brown D, Głuck SL, Alper SL: Regulation of AE1 anion exchanger and H+-ATPase in rat cortex by acute metabolic acidosis and alkalosis. Kidney Int 51:125-137, 1997
- 9. Alper SL, Natale J, Gluck S, Lodish HF, Brown D: Subtypes of intercalated cells in rat kidney collecting duct defined by antibodies against erythroid band 3 and renal vacuolar H+-ATPase. Proc Natl Acad Sci U S A 86:5429-5433, 1989
- 10. Wingo CS, Cain BD: The renal H,K-ATPase: Physiological significance and role in potassium homeostasis. Annu Rev Physiol 55:323-347, 1993
- 11. Baehner RL, Gilchrist GS, Anderson EJ: Hereditary elliptocytosis and primary renal tubular acidosis in a single family. Am J Dis Child 115:414-419, 1968
- 12. Rysava R, Tesar IV, Brabec IV, Jirsa IM, Merta IM, Jarolim P: Renal tubular acidosis associated with mutation in the AE1 gene, in Ritz E (ed): EDTA. Amsterdam, The Netherlands, p 17, 1996
- 13. Rysava R, Tesar V, Jirsa M, Brabec V, Jarolim P: Incomplete distal renal tubular acidosis coinherited with a mutation in the band 3 (AE1) gene. Nephrol Dial Transplant 12:1869-1873, 1997
- 14. Cope DL, Bruce LJ, Schofield AE, Unwin RJ, Wrong OM: Altered red cell anion exchanger (band 3, AE1) associated with familial distal renal tubular acidosis, in Grantham J (ed): Twenty-Ninth Annual ASN Meeting. Baltimore, MD, Williams & Wilkins, 1852;3028A, 1996 (abstr)
- 15. Bruce LJ, Cope DL, Jones JK, Schofield AE, Burley M, Povey S, Unwin RJ, Wrong O, Tanner MJA: Familial distal renal tubular acidosis is associated with mutations in the red cell anion exchanger (band 3, AE1) gene. J Clin Invest 100:1693-1707, 1997
- 16. Jarolim P, Shayakul C, Prabakaran D, Jiang L, Stuart-Tilley A, Rubin H, Simova S, Zavadil J, Herrin JT, Brouillette J, Somers MJG, Seemanova E, Brugnara C, Guay-Woodford LM, Alper SL: Autosomal dominant distal renal tubular acidosis is associated in three families with heterozygosity for the R589H mutation in the AE1(band 3) Cl-/HCO₃-exchanger. J Biol Chem 273:6380-6388, 1998
- 17. Halperin ML, Goldstein MB, Haig A, Johnson MD, Stinebaugh BJ: Studies on the pathogenesis of type 1 (distal) renal tubular acidosis as revealed by urine pCO₂ tensions. J Clin Invest 53:669-677, 1974
- 18. Ethier J, Kamel K, Magner P, LemannJJ, Halperin ML: The transtubular potassium concentration in patients with hypokalemia and hyperkalemia. Am J Kidney Dis 15:309-315, 1990
- 19. Jarolim P, Palek J, Amato D, Hassan K, Sapak P, Nursel GT, Rubin HL, Zhai S, Sahr KE, Liu SC: Deletion in erythrocyte band 3 gene in malaria-resistant southeast Asian ovalocytosis. Proc Natl Acad Sci U S A 88:11022-11026, 1991
- 20. Kamel KS, Briceno LF, Sanchez MI, Brenes L, Yorgin P, Kooh SW, Balfe W, Halperin ML: A new classification for renal defects in net acid excretion. Am J Kidney Dis 29:136-146, 1997
- 21. Vasuvattakul S, Gougoux A, Halperin ML: A method to evaluate renal ammoniagenesis in vivo. Clin Invest Med 16:265-273, 1993

- 22. Rastogi S, Crawford C, Wheeler R, Flanigan W, Arruda JAL: Effect of furosemide on urinary acidification in distal renal tubular acidosis. J Lab Clin Med 104:271-282, 1984
- 23. Carlisle EJF, Donnelly SM, Halperin ML: Renal tubular acidosis (RTA): Recognize the ammnonium defect and pH or get the urine pH. Pediatr Nephrol 5:242-248, 1991
- 24. Dubose TJ, Caffisch C: Validation of the difference in urine and blood carbon dioxide tension during bicarbonate loading as an index of distal nephron acidification in experimental models of distal renal tubular acidosis. J Clin Invest 75:1116-1123, 1985
- 25. Steinmetz PR, Anderson OS: Electrogenic proton transport in epithelial membranes. J Membrane Biol 65:155-174, 1982
- 26. Bonilla-Felix M: Primary distal renal tubular acidosis as a result of a gradient defect. Am J Kidney Dis 27:428-430, 1996
- 27. Zawadzki J: Permeability defect with bicarbonate leak as a mechanism of immune-related distal renal tubular acidosis. Am J Kidney Dis 31:527-532, 1998
- 28. Madison LL, Seldin DW: Ammonia excretion and renal enzymatic adaptation in human subjects, as disclosed by administration of precursor amino acids. J Clin Invest 37:1615-1627, 1958
- 29. Schloeder FX, Stinebaugh BJ: Urinary ammonia content as a determinant of urinary pH during chronic metabolic acidosis. Metabolism 26:1321-1331, 1977
- 30. Rapoport A, From GLA, Husdan H: Metabolic studies in prolonged fasting. I. Inorganic metabolism and kidney function. Metabolism 14:31-46, 1965
- 31. Kamel KS, Lin S-H, Cheema-Dhadli S, Marliss EB, Halperin ML: Prolonged total fasting: A feast for the integrative physiologist. Kidney Int 53:531-539, 1998
- 32. Berliner RW, Dubose TDJ: Carbon dioxide tension of alkaline urine, in Seldin DW, Giebisch G (eds). The Kidney, Physiology and Pathophysiology. New York, NY, Raven, 1992, pp 2681-2694
- 33. Maren T: Carbon dioxide equilibria in the kidney: The problems of elevated carbon dioxide tension, delayed dehydration, and disequilibrium pH. Kidney Int 14:395-405, 1978.
- 34. Knepper MA, Good DW, Burg MB: Mechanisms of ammonia secretion by cortical collecting ducts of rabbits. Am J Physiol 247:F729-F738, 1984
- 35. Knepper MA, Good DW, Burg MB: Ammonia and bicarbonate transport by rat cortical collecting ducts perfused in vitro. Am J Physiol 249:F870-F877, 1985
- 36. Schwartz GJ, Barasch J, Awqati AL: Plasticity of functional epithelial polarity. Nature 318:368-371, 1985
- 37. Steele A, deVeber H, Quaggin SE, Scheich A, Ethier J, Halperin ML: What is responsible for the diurnal variation in potassium excretion? Am J Physiol 36:R554-R560, 1994
- 38. Lin SH, Cheema-Dhadli S, Gowrishankar M, Marliss EB, Kamel KS, Halperin ML: Control of the excretion of potassium: Lessons from studies during prolonged fasting in human subjects. Am J Physiol 273:F796-F800, 1997

Autosomal recessive distal renal tubular acidosis associated with Southeast Asian ovalocytosis

Somkiat Vasuvattakul, Pa-thai Yenchitsomanus, Prayong Vachuanichsanong, Peti Thuwajit, Charoen Kaitwatcharachai, Vichai Laosombat, Prida Malasit, Prapon Wilairat, and Sumalee Nimmannit

Renal Division and Medical Molecular Biology Unit, Siriraj Hospital, Mahidol University; Songklanakarin Hospital, Prince of Songkla University; and Department of Biochemistry, Faculty of Science, Mahidol University, Bangkok, Thailand

Autosomal recessive distal renal tubular acidosis associated with Southeast Asian ovalocytosis.

Background. A defect in the anion exchanger 1 (AE1) of the basolateral membrane of type A intercalated cells in the renal collecting duct may result in a failure to maintain a cellto-lumen H⁺ gradient, leading to distal renal tubular acidosis (dRTA). Thus, dRTA may occur in Southeast Asian ovalocytosis (SAO), a common AE1 gene abnormality observed in Southeast Asia and Melanesia. Our study investigated whether or not this renal acidification defect exists in individuals with SAO.

Methods. Short and three-day NH₄Cl loading tests were performed in 20 individuals with SAO and in two subjects, including their families, with both SAO and dRTA. Mutations of AEI gene in individuals with SAO and members of the two families were also studied.

Results. Renal acidification in the 20 individuals with SAO and in the parents of the two families was normal. However, the two clinically affected individuals with SAO and dRTA had compound heterozygosity of 27 bp deletion in exon 11 and missense mutation G701D resulting from a CGG—CAG substitution in exon 17 of the AEI gene. Red cells of the two subjects with dRTA and SAO and the family members with SAO showed an approximate 40% reduction in sulfate influx with normal 4,4'-di-isothiocyanato-stilbene-2,2'-disulfonic acid sensitivity and pH dependence.

Conclusion. These findings suggest that compound heterozygosity of abnormal AEI genes causes autosomal recessive dRTA in SAO.

Southeast Asian ovalocytosis (SAO) is a hereditary condition that is widespread in parts of Southeast Asia and Melanesia. It has been shown that SAO results from a mutation in the red cell membrane band 3 or the anionic

Key words: band 3 protein, anion exchanger 1, AEI gene, DNA sequencing, renal acidification.

Received for publication November 17, 1998 and in revised form June 15, 1999
Accepted for publication June 16, 1999

© 1999 by the International Society of Nephrology

(HCO₃⁻/Cl⁻) exchanger 1 (AE1) [1, 2]. The N-terminal fragment of the abnormal band 3 migrates slower than normal in sodium dodecyl sulfate-polyacrylamide gel electrophoresis (SDS-PAGE) [3]. Sequencing of the abnormal erythrocyte AE1 gene in SAO showed that it contained two linked mutations: a deletion of codons 400 to 408 in the boundary of cytoplasmic and membrane domains and a point mutation in the first base of codon 56 (K56E), the Memphis I polymorphism [4].

Anion exchanger 1 is also found in the basolateral membrane of the type A intercalated cells of renal collecting ducts, which are involved in H⁺ secretion [5, 6]. Studies of human kidneys have indicated that, although the protein in the basolateral membrane of type A intercalated cells is reactive toward monoclonal antibodies to the membrane transport domain of AE1 [6, 7], several antibodies to the cytoplasmic domain of AE1 are unreactive [6], which is consistent with renal AE1 being truncated at the NH₂ terminus [8]. A promoter that gives rise to these kidney transcripts is present in erythroid intron 3 of the human AE1 gene [8, 9].

A defect in AE1 of the basolateral membrane of type A intercalated cells of the collecting duct may result in a failure to establish or maintain a cell-to-lumen H+ gradient, and leads to distal renal tubular acidosis (dRTA) [5,10]. Three studies and a review have shown that mutations of the AE1 gene affect renal acidification [11–14]. There are at least two reports indicating an association between dRTA and hereditary elliptocytosis [15, 16], which is uncommon among Caucasians, but a related condition, SAO, is widespread in parts of Southeast Asia, with a prevalence reaching 30% in certain ethnic groups [17].

To examine the possibility that a defect in renal acidification may be associated with subjects with SAO, the renal acidification function and a detailed characterization of the AEI gene were studied in SAO individuals and members of two unrelated families with dRTA and

SAO. In this report, we describe a novel compound heterozygosity of mutated AEI genes in the subjects with SAO and dRTA, and an autosomal recessive mode of inheritance of the abnormal genes associated with the two combined defects.

METHODS

Subjects

The study population consisted of 20 individuals with SAO, two unrelated subjects with SAO and dRTA (as defined by a low rate of NH₄⁺ excretion and an inability to lower the urine pH below 5.5 in the presence of systemic acidosis, HCO₃⁻ < 20 mEq/liter) and their family members and 11 individuals with normal red blood cell morphology living in the same region as the control subjects. All subjects were placed on a normal diet, and medications were terminated one week prior to the study. This investigation was approved by the Human Ethics Committee of the Prince of Songkla University, Thailand.

Clinical studies

Renal acidification was studied using a short acid loading by administration of 0.1 g/kg NH₄Cl, as previously described by Wrong and Davies [18], in 10 individuals with SAO, the two family members and seven normal control subjects; simultaneously, a chronic acid loading was achieved by administration of 0.1 g/kg/day NH₄Cl for three days with diuresis on the fourth day induced by furosemide (20 mg p.o.) [19] in another 10 individuals with SAO and four normal control subjects. To achieve urinary osmolality \geq 800 mOsm/kg H₂O, intranasal 1-deamino-D-arginine vasopressin (DDAVP) was given after 16 hours of water deprivation [20].

Venous blood pH was measured using blood gas analyzer (model 178, Corning). The concentration of bicarbonate in plasma was calculated using the pK value of 6.10 and a solubility factor of 0.0301 [21, 22]. Analytical methods for determination of NH₄⁺, sodium, potassium, chloride, creatinine, and osmolality were as previously described [23].

The clearance of creatinine provided an approximation of the glomerular filtration rate [24]. The transtubular K concentration gradient (TTKG) was calculated to reflect the driving force for K secretion [25].

Values were reported as mean ± SEM, and comparisons between groups were made by analysis of variance (ANOVA).

DNA analysis

Polymerase chain reaction primers. The sequence of AE1 gene was retrieved from Entrez database (Gen-Bank, NCBI). Nineteen pairs of polymerase chain reaction (PCR) primers were designed for amplifications of

AUTHOR: Please answer

two overlapping regions in intron 3 (one for the potential kidney promoter and another for the possible 5' sequence of transcript expressed in kidney) and 17 regions in exons 4 to 20 of the AEI gene (Table 1). The primers for each exon would anneal to sequences in introns, flanking both sides of the exon. The sizes of PCR products obtained from amplifications using these primers were usually less than 400 bp, except those for the two regions in intron 3. These primers were synthesized by BioService Unit of the National Center for Genetic Engineering and Biotechnology (Biotec, Bangkok, Thailand).

DNA samples. Leukocyte genomic DNAs were prepared from 10 ml ethylenediaminetetraacetic acid (ED TA) blood samples by standard DNA extraction method, which consisted of steps of proteinase K digestion, phenol-chloroform extractions, and ethanol precipitation [26]. DNA samples were finally dissolved in sterile distilled water, and their amounts were estimated from absorbances measured by ultraviolet-visible spectrophotometer at wavelength 260. A small part of stock DNA sample was diluted to 50 ng/µl for using in PCR.

Polymerase chain reaction. Polymerase chain reaction was performed by mixing 125 ng DNA sample, 2.5 µl of 10 × buffer (Perkin-Elmer Cetus, Norwalk, CT, USA), 1.5 µl of 25 mm MgCl₂, 2.5 µl of 2 mm dNTP mix, 12.5 pmol each of forward (L) and reverse (R) primers, and 0.25 units of Tag polymerase (Perkin-Elmer Cetus) in a total volume of 25 µl. The reaction mixture was overlaid with one drop of mineral oil, and amplification was performed for 35 cycles in Thermal Cycler 480 (Perkin-Elmer Cetus). Each cycle was comprised of denaturation at 94°C for one minute (5 min for the first cycle), annealing at 58 to 70°C (depending on pair of primers; Table 1) for one minute, and extension at 72°C for one minute (5 min for the final cycle). After amplifications, PCR products were examined by running on 2% agarose gel electrophoresis and ethidium bromide staining.

Single strand conformational polymorphism (SSCP). Two microliters of the PCR product were mixed with 8 µl of sample running buffer (containing 95% formamide, 0.05% bromophenol blue, 0.05% xylene cyanol, 20 mm EDTA, and 10 mm NaOH). The mixture was heated at 95°C for 10 minutes to denature DNA into single strands and was then cooled on ice for five minutes before loading onto nondenaturing polyacrylamide gel. The polyacrylamide gel with the size of 90 × 80 mm and thickness of 1 mm contained 10% acrylamide:bis-acrylamide (49:1). Electrophoresis was run in 1 × TBE buffer at 20 mA for two to six hours at room temperature. Double-stranded DNA might also be run by mixing 2 µl of the PCR product with 8 µl sample running buffer (without 10 mm NaOH) and loading onto the same gel without heating.

After electrophoresis, the gel was fixed with 40% methanol for 10 minutes, soaked in 160 mm HNO₃ for

Table 1. Oligonucleotide primers for amplifications of the AEI gene

Exon	PCR primer sequence	Position	Annealing temp	Product size
Intron 3.1	5'-CAGTTTGGGACAAGGGCGTG-3'	6995-7014	67	491
	5'-TGATGAAGTGAAGGGACCTCTCC-3'	7463-7485		
Intron 3.2	5'-TGGGAGGAGAGAAGGGAGTCTG-3'	7364-7383	67	402
	5'-CGGTGTCGTGAGCTGAAAACC-3'	7745-7765		
Exon 4	5'-GTCTCTGAGGCTCACAGTGGATG-3'	7673-7695	63	226
	5'-ATCCCCTTGCTCCTCTCTCC-3'	7878–7898		
Exon 5	5'-TGAGCACCCACTATGCCCTG-3'	8522-8541	63	299
	5'-CAGCACCCCACAACAATCCTC-3'	8800-8820		
Ехоп 6	5'-AGATGAGGATTGTTGTGGGGTG-3'	8796-8817	63	262
	5'-CAAGTGGGCTGGGGAAGTG-3'	9039-9057		
Exon 7	5'-CACCACTGATAGCTCAGCCTGAAC-3'	9407-9430	60	243
	5'-TGAGAAAGCTCTCTCCTTGCCC-3'	9628-9649		
Exon 8	5'-GAGAATGGGAAGGGAGGATG-3'	9739-9760	60	244
	5'-GGTCCAGGCTGAGGGAAAGAC-3'	9963-9983		
Exon 9	5'-TCTTCAGCACACCCACCCTG-3'	9998-10017	60	299
	5'-TCAGCCACCATGCAGGTCC-3'	10278-10296		
Exon 10	5'-TCCTTTCCCTCCGCAGGTC-3'	10726-10744	58	332
	5'-ACAGAGGCTACGCTGAGGTGTC-3'	11036-11057		
Exon 11	5'-CCTCACCTCCTCCAGCTACTCC-3'	11163-11184	62	318
	5'-CAGAAGTTGGGGCTGAGACAGAG-3'	1145811480		
Exon 12	5'-GCTCTATGGGCTCCTGGAAATG-3'	11529-11550	58	293
	5'-AAAGGGTCTTGGGGCAAGG-3'	11803-11821		
Exon 13	5'-CTGTCATGTCCCCCGCAC-3'	11765-11782	58	339
	5'-TGTCTCAGTCTTATACACAACCTCC-3'	12079-12103		
Exon 14	5'-TGGTGGTATTTTCCAGCCCAAG-3'	13484-13505	60	320
	5'-GCACTGAGGAATTTGGAGCGG-3'	13783-13803		
Exon 15	5'-AAGGCAGGAGGTGGGGAGTGACTG	14045-14078	70	201
	5'-GGAAATGAGGACCTGGGGGGTATC	14222-14245		
Exon 16	5'-TCCTGCTCCCACCCTTCCCC-3'	14673-14692	68	276
	5'-TCTGCCTCCCACCCTCCCAG-3'	14929-14948		
Exon 17	5'-TGGAGGAGGCAGGGGAGAAC-3'	15980-15999	70	347
	5'-GGGGCAGGAGGATGGTGAAG-3'	16307-16326		
Exon 18	5'-ATATGGTGCCTGTGTTTTATTCCC-3'	17705-17728	65	332
	5'-TGCCTATCACACCCCAGCAC-3'	18017-18036		
Exon 19	5'-GGTACAGGACCCTTTTCTGG-3'	17973-17992	60	334
	5'-GCCTGCCCTAGTTCTGAGAC-3'	18287-18306		
Exon 20	5'-TCTCACCCTGTCTCTCTCCTG-3'	18819-18839	65	198
	5'-GAGGTGCCCATGAACTTCTG-3'	18997-19016	55	170

six minutes, washed with deionized water, and soaked in deionized water for five minutes. It was then stained in 0.2% AgNO₃ solution for 20 minutes with gentle shaking, washed with deionized water, and soaked in deionized water for five minutes. The AgNO₃ solution and washing water were pooled and added with a few drops of HCl to convert AgNO₃ to AgCl before discarding. The gel was, soaked in developer containing 3% Na₂CO₃ and 0.0175% formamide in deionized water for 4 to 10 minutes. When DNA bands were clearly observed, a solution of 10% citric acid in deionized water was immediately added into the developer to stop the staining reaction. The SSCP pattern on the gel was recorded into a computer by scanning with a scanner. The gel was also dried on a piece of filter paper for long-term storage.

Mobility shift of ssDNA from the normal pattern indicated the presence of a possible mutation. The PCR product of the exon that showed mobility shift was analyzed by direct DNA sequencing.

Direct DNA sequencing. To identify mutation in the exons of AEI gene observed in the PCR-SSCP analysis, the PCR product was purified from a preparative agarose gel and sequenced by manual direct DNA sequencing using Thermo Sequenase Cycle Sequencing Kit (Amersham Life Science Inc., Arlington, Heights, IL, USA) or by an automated sequencing machine (ABI-PRISM[™] 310 Genetic Analyzer; ABI, USA) using an ABI PRISM[™] Dye Terminator Cycle Sequencing Ready Reaction Kit.

ED: COMMA WANTE

Red cell anion transport studies

³⁵S-SO₄ influx into red blood cells was measured in the two patients with SAO and dRTA and their family members, and normal controls in the presence and absence of the inhibitor, 4,4'-di-isothiocyanato-stilbene-2,2'-disulfonic acid (DIDS). The studies were performed at 37°C in buffer of 70 mm sodium citrate, 3 mm sodium asulfate, and 10 mm Hris, ipH.7.4 [13].

Table 2. Renal acidification function after three days of NH₄Cl loading in individuals with Southeast Asian <u>ovalcytosis</u> (SAO) compared with controls

	SAO	Controls
	(N=10)	(N = 4)
Serum		
Creatinine mg/dL	0.9 ± 0.1	1.1 ± 0.1
К⁺ ты	3.8 ± 0.1	3.7 ± 0.1
HCO₃⁻ mм		
Pre-acid loading	26 ± 0.8	27 ± 0.1
Post-acid loading	20 ± 0.7	20 ± 1.6
Venous pH		
Pre-acid loading	7.35 ± 0.02	7.37 ± 0.03
Post-acid loading	7.32 ± 0.01	7.29 ± 0.02
Urine		
Cc, ml/min	93 ± 6	87 ± 9
рĤ		
Pre-acid loading	6.0 ± 0.1	6.0 ± 0.3
Post-acid loading	5.0 ± 0.1	4.9 ± 0.1
After furosemide	4.5 ± 0.1	4.4 ± 0.1
NH, + µmol/min		
Pre-acid loading	22 ± 0.3	23 ± 4
Post-acid loading	65 ± 6	65 ± 4
After-furosemide	75 ± 6	63 ± 7

RESULTS

Clinical studies

Renal acidification was performed in 20 individuals with SAO and the 11 controls. The NH₄⁺ excretion rate and urine pH after a three-day NH₄Cl load are shown in Table 2. Neither subject groups (10 individuals vs. 4 controls) had a statistical significant difference in the NH_4^+ excretion rate (65 ± 6 vs. 65 ± 4 μ mol/min) or urinary pH (5.0 \pm 0.1 vs. 4.9 \pm 0.1) following the acid load. After diuresis with oral furosemide on the fourth day of the acid load, the urinary pH decreased significantly in both groups, but there was no significant difference between the two groups $(4.5 \pm 0.1 \text{ vs. } 4.4 \pm 0.1)$. The increment of NH₄⁺ excretion during the peak diuresis was not significantly different between the two groups $(75 \pm 6 \text{ vs. } 63 \pm 7 \text{ } \mu\text{mol/min})$. The maximum urine osmolality after 16 hours of water deprivation and intranasal DDAVP administration was also not significantly different between the two groups (940 ± 41 vs. 850 ± 46 mOsm/kg/H₂O).

Table 3 provides a summary of the results of urinary acidification studies after the short acid load. Blood pH values after the acid loading of 10 SAO and 7 control subjects were less than 7.35. Urine pH and NH_4^+ excretion rate after the acid load between both groups were not significantly different (5.0 \pm 0.1 vs. 4.9 \pm 0.1 and 39 \pm 6 vs. 37 \pm 4 μ mol/min, respectively).

Pedigrees (KSN and YAT) of two subjects with SAO and dRTA are shown in Figure 1. Propositi (II-1 in both families) presented with history of growth retardation, SAO, and hypokalemia (Table 4). Complete dRTA was diagnosed by low NH₄⁺ excretion rate in both propositi

Table 3. Renal acidification after short acid loading in individuals with Southeast Asian ovalocytosis (SAO) compared with controls

	SAO	Controls
	(N = 10)	(N=7)
Serum		-
Creatinine mg/dL	1.1 ± 0.1	1.0 ± 0.2
K+ mM	3.8 ± 0.04	3.9 ± 0.1
HCO ₃ - mm		
Pre-acid loading	25 ± 0.7	25 ± 0.9
Post-acid loading	20 ± 0.6	22 ± 0.8
Venous pH		
Pre-acid loading	7.37 ± 0.02	7.35 ± 0.01
Post-acid loading	7.31 ± 0.05	7.30 ± 0.02
Urine		
C _G ml/min	83 ± 6	90 ± 14
pH		
Pre-acid loading	5.9 ± 0.1	5.6 ± 0.1
Post-acid loading	5.0 ± 0.1	4.9 ± 0.1
NH ₄ + μmol/min		
Pre-acid loading	28.6 ± 3	21.5 ± 6
Post-acid loading	39.4 ± 6	36.7 ± 4

(3.3 and 4.3 μ mol/min, respectively) as well as by the inability to lower the urine pH below 5.5 (7.3 and 6.7, respectively) in the presence of metabolic acidosis (venous pH 7.26 and 7.27 and serum HCO₃⁻ 9 and 14 mEq/ liter, respectively). No abnormal renal acidification was detected in both sets of parents (I-1 and I-2).

Screening and characterization of AE1 gene mutations

Polymerase chain reaction-SSCP was used to screen for mutations in exons 4 to 20 of the AEI gene and in intron 3, the promoter region of the kidney isoform. DNA samples from the propositi, siblings, as well as the parents of the two families were also analyzed. Figure 1 shows the results of PCR-SSCP analysis for exons 11 and 17 of one normal individual (N) and members of the two families. In the YAT family, the father (I-1) showed a mobility shift in exon 17, and the mother (I-2) showed a mobility shift in exon 11. In the KSN family, the father (I-1) demonstrated a mobility shift in exon 11, whereas the mother (I-2) showed a shift in exon 17. The DNA samples of both KSN and YAT families revealed mobility shifts in both exons 11 and 17. Except for a mobility shift of exon 4 (caused by the Memphis I polymorphism, confirmed by sequencing; Fig. 5), the PCR-SSCP patterns of all other exons, including intron 3, were normal (data not shown).

Because the mobility shifts of exons 11 and 17 of AEI gene detected by PCR-SSCP in the two patients were the same, amplified DNA of these two exons from the propositus of KSN family were sequenced. Exon 11 had a deletion of 27 bp corresponding to codons 400 to 408 (Fig. 2), whereas exon 17 contained a nucleotide substitution of G to A in codon 701 (CGG—CAG), resulting in an amino acid change from glycine 10 aspartic acid (G701D) (Fig. 3). Thus, the AEI gene of the propositi of

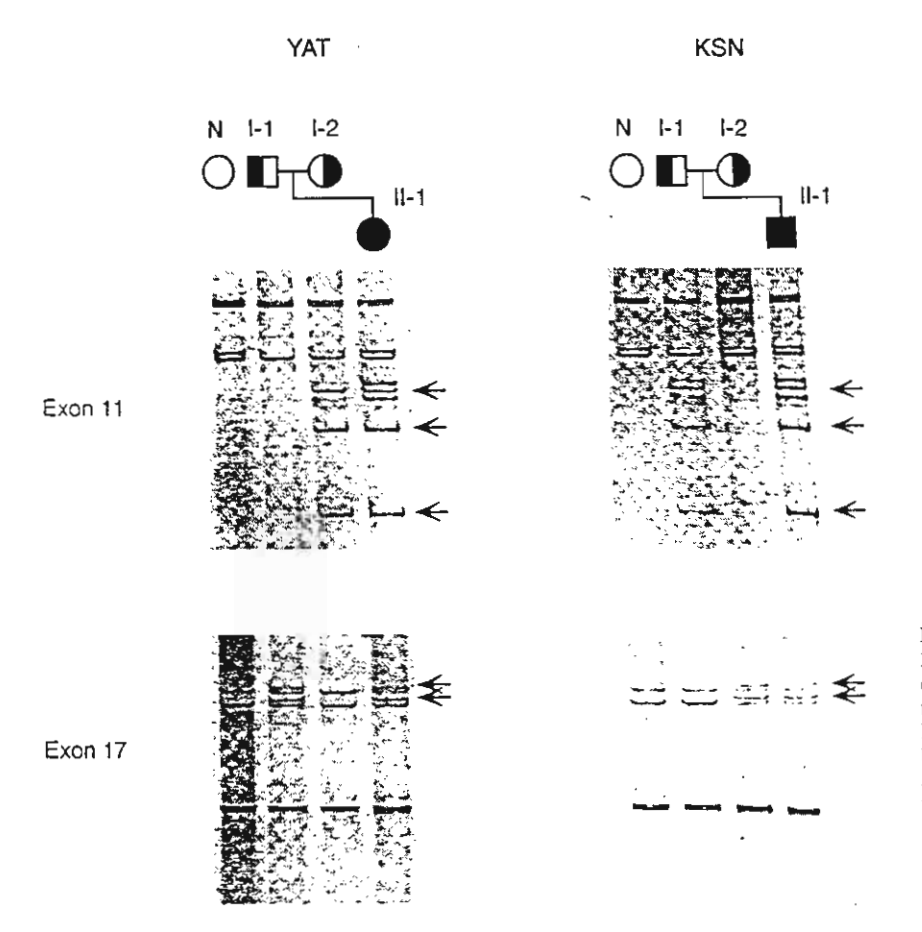


Fig. 1. Screening of mutations in exons 11 and 17 of the AEI gene in the two patients with Southeast Asian ovalocytosis (SAO) and distal renal tubular acidosis (dRTA) and their parents by the PCR-SSCP technique. The two patients (II-1 in both families) had mobility shifts of single-stranded DNAs in both exons 11 and 17 (arrows), whereas their parents had the mobility shifts in either exon 11 (I-2 in family of YAT and I-1 in family of KSN) or exon 17 (I-1 in family of YAT and I-2 in family of KSN). "N" is normal individual.

Table 4. Values in blood and urine collections from the two patients with SAO and dRTA

	KSN: II-1	YAT: II-1	
Serum			
Creatinine mg/dL	0.5	0.6	
BUN mg/dL	13	13	
Na+ mm	137	141	
K ⁺ тм	3.3	3.4	
Cl- mм	116	111	
HCO ₃ - mm	8.7	14	
Venous pH	7.26	7.27	
Urine			
TTKG	10.4	10.3	
Flow rate ml/min	0.4	0.8	
р Н	7.3	6.7	
NH ₄ + µmol/min	3.3	4.3	

Abbreviations are: SAO, Southeast Asian ovalocytosis; dRTA, distal renal tubular acidosis; BUN, blood urea nitrogen; TTKG, transtubular K concentration gradient.

both families was a compound heterozygosity of 27 bp deletion in exon 11 and missense mutation (CGG—CAG) in exon 17. The sequencing results also showed the presence of homozygous band 3 Memphis I (Fig. 4) in the two patients. The presence of exon 11 deletion and exon 17 missense mutation in both patients was also confirmed by the detection of a shorter PCR product and elimina-

tion of *HpaII* restriction site on the amplified DNA, respectively, by gel electrophoresis (Fig. 4). Mutations of *AEI* gene were also analyzed by PCR-SSCP in 20 individuals with SAO and in normal subjects (Fig. 5). SAO individuals had mobility shifts in exons 4 and 11.

Anion transport property of the red cells of the two families

An influx of [35S] sulfate into the red cells of members of the two families was compared with that of red cells from 10 normal controls taken at the same time. Red cell samples from the propositi of the KSN and YAT families and family members with SAO showed a consistently lower anion transport activity than the normal samples in both the presence and absence of DIDS (Table 5). Family members with only the exon 17 mutation had normal anion transport and DIDS activity.

DISCUSSION

Mutation of the AEI gene in SAO has been the subject of a number of studies [1, 4, 27]. The underlying molecular defect is a 27 bp deletion in exon 11 of the AEI gene, resulting in the loss of 9 amino acids (codons 400 to 408) in the band 3 protein, which is also associated with the

The second of the second of the second of the

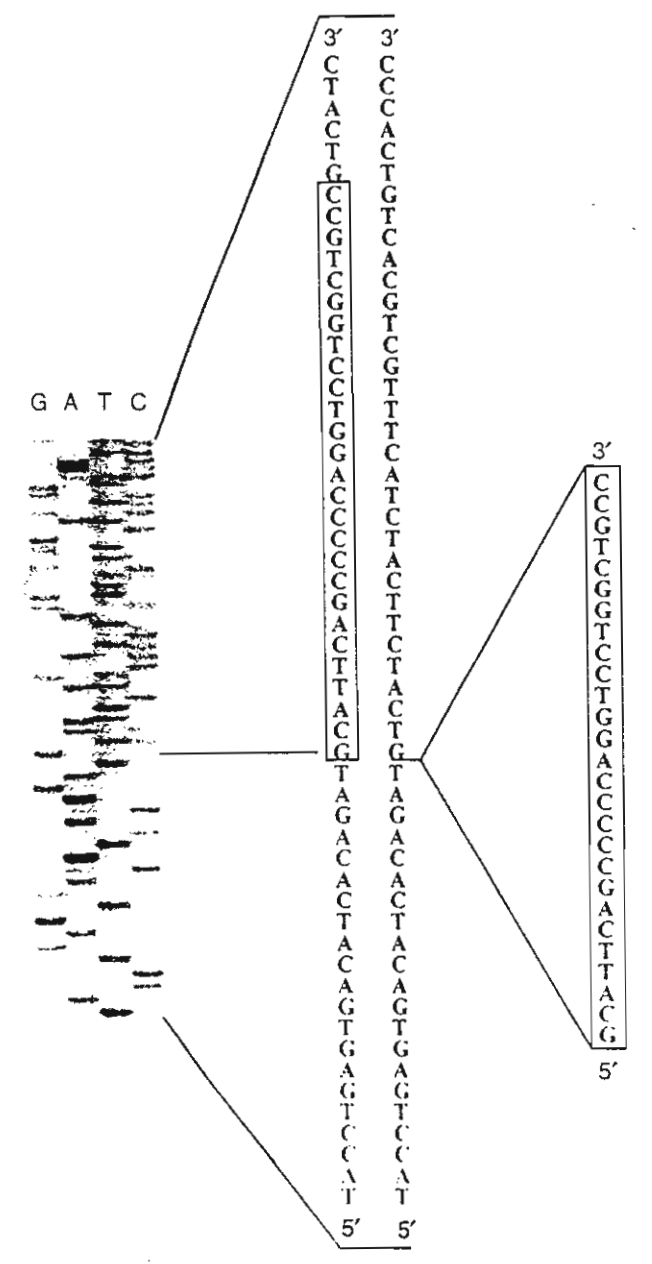


Fig. 2. Sequencing analysis of exon 11 of the AEI gene in the patient with dRTA and SAO (II-1, family of KSN), showing nucleotide sequence of exon 11 with 27 nucleotide deletion superimposing the normal sequence. Identical 27 nucleotides in the normal and deleted alleles of the latter is separated from the nucleotide stretch) are blocked. The deletion of 27 nucleotides in one allele resulted in shifting of the remaining nucleotide sequence superimposing the normal sequence in the autoradiogram.

Memphis I (K56E) polymorphism. Although SAO occurs with high frequency in parts of Southeast Asia and Melanesia, no homozygous individual for the AEI mutation has been identified, suggesting that homozygosity for this mutation may be lethal [1].

Anion exchanger 1 in red cells is important for the transport of carbon dioxide from the tissue to the lung

and for acid secretion in type A intercalated cells of the kidney [28]. Total deficiency of red cell band 3 caused by a nonsense mutation has been reported in cattle [29]. Animals showed a moderate uncompensated anem-(bb ia with hereditary spherocytosis and retarded growth, which was attributed to mild acidosis. The band 3-deficient animals had defective renal acid secretion and could not acidify urine pH below 7.5 despite metabolic acidosis. In dRTA, acid secretion in the distal nephron is impaired, leading to the development of metabolic acidosis [10, 30]. Recently, several studies have demonstrated associations of the AEI mutations and dRTA: Rysava et al reported that 2 out of 10 patients with hereditary spherocytosis and band 3 PRIBRAM (G→A in the first nucleotide of intron 12) had an incomplete form of dRTA [14]; Bruce et al reported an association between familial dRTA and point mutations of the AEI gene, namely, R589H, R589C, and S613F [12]. The AEI mutation, R589H, has also been reported in two other studies [13, 31]. An intragenic 13 bp duplication resulting in deletion of the last 11 amino acids of AEI gene in one dRTA subject has also been demonstrated [31]. Mutations in the AEI gene appear to cause autosomal dominant dRTA [12, 13, 31], but the molecular mechanism is unknown.

There have been two previous studies showing the association between dRTA and elliptocytosis or SAO [15, 16]. The presence of the two conditions in the same individuals suggests that there may be a common underlying molecular defect. However, mutation of the AE1 gene in individuals with both of these conditions was not demonstrated. In this study, 20 individuals with SAO, confirmed by the presence of 27 bp deletion in exon 11 of the AE1 gene, showed no abnormal renal acidification following the three-day NH₄Cl loading (N = 10; Table 2) or by short acid loading (N = 10; Table 3). The rate of excretion of NH₄⁺ increased by almost threefold, and the urine pH decreased below 5.0 after three-day acid loading and during the furosemide-induced diuresis to typical values of normal subjects [19]. This suggests that the rate of production of NH4+ in the proximal tubular cells was not appreciably depressed. Thus, SAO mutation of the AEI gene in the heterozygous condition is not sufficient to cause dRTA.

The two clinically affected unrelated patients in the KSN and YAT families with dRTA and SAO showed a low rate of NH₄⁺ excretion and an inability to lower the urine pH below 5.5 in the presence of systemic acidosis (Table 4). There was also a high transtubular [K⁺] gradient (TTKG) [25] given the degree of hypokalemia. No abnormal renal acidification was detected in either set of parents. Analysis of AEI gene mutation by PCR-SSCP showed that the two patients (II-1 in both families) had the same mobility shifts in exons 11 and 17, whereas the parents had mobility shift in either exon 11 (I-2 in

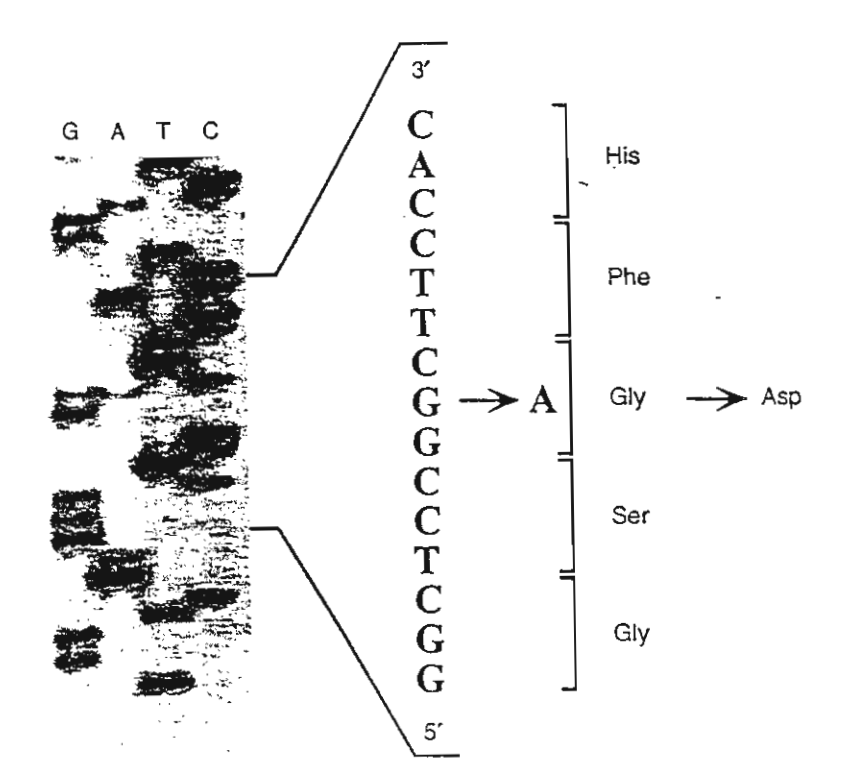


Fig. 3. Sequencing analysis of exon 17 of AEI gene in the patient with SAO and dRTA (II-1, family of KSN). A substitution from G to A in the second nucleotide of codon 701 was observed. This substitution results in missense mutation changing the amino acid at the position 701 from glycine to aspartic acid (G701D).

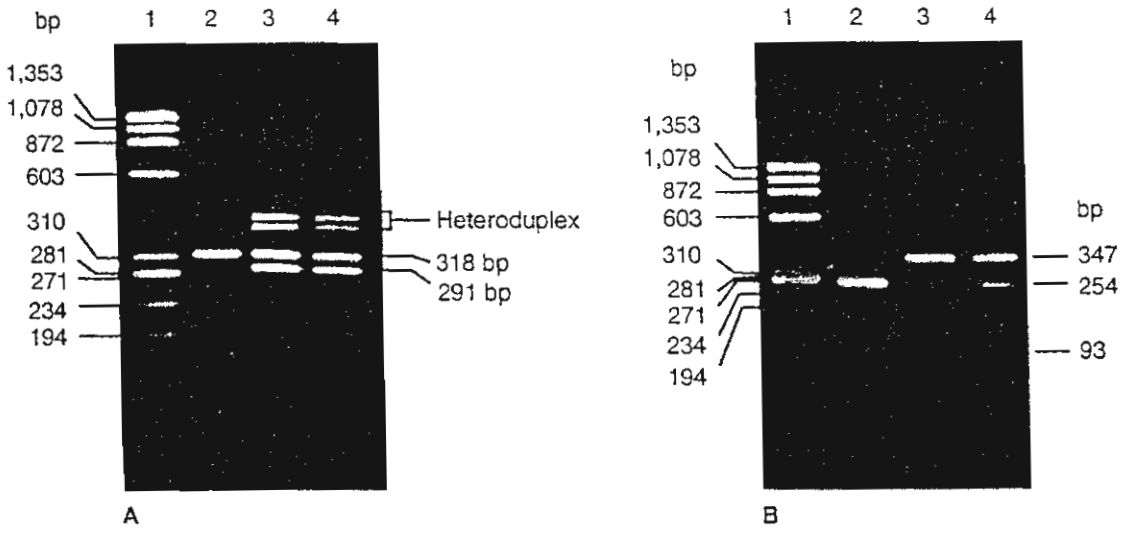


Fig. 4. Detection of exon 11 deletion and exon 17 (CGG—CAG) missense mutation in the patients (II-1) of KSN and YAT families by agarose gel electrophoresis. (A) PCR products from amplifications of exon 11 of AEI gene with AEIEx11L/AEIEx11R primers. Normal control sample (lane 2) showed only a PCR product with the size of 318 bp. DNA samples from the patients of the KSN (lane 3) and YAT (lane 4) families who had 27 bp deletion in exon 11 in one allele of the AEI genes resulted in PCR products with the sizes of 318 and 291 bp, and also their heteroduplexes. (B) PCR products from amplifications of exon 17 with AEIEx17L/AEIEx17R primers and digestions with HpaII restriction endonuclease, which could digest the normal (CCGG) but not the mutant (CCAG) sequences. A normal control sample (lane 2) showed digested fragments with the sizes of 254 and 93 bp. DNA samples from the patients of the KSN (lane 3) and YAT (lane 4) families who had exon 17 missense mutation in one allele of the AEI gene revealed both digested (254 and 93 bp) and undigested (347 bp) PCR products. Lane 1 in both sets is Phix174 DNA/ HaeIII markers.

family YAT and I-1 in family KSN) or exon 17 (I-1 typical of SAO [4] and exon 17 had a single nucleotide in family YAT and I-2 in family KSN; Fig. 1). DNA substitution of G to A in the second nucleotide of codon sequencing (Figs. 2 and 3) and gel electrophoresis (Fig. 117701 (CGG—CAG), resulting in a G701D missense muta-4) revealed that exon 11 contained a 27 bp deletional rion This is the first report of a compound heterozygosity

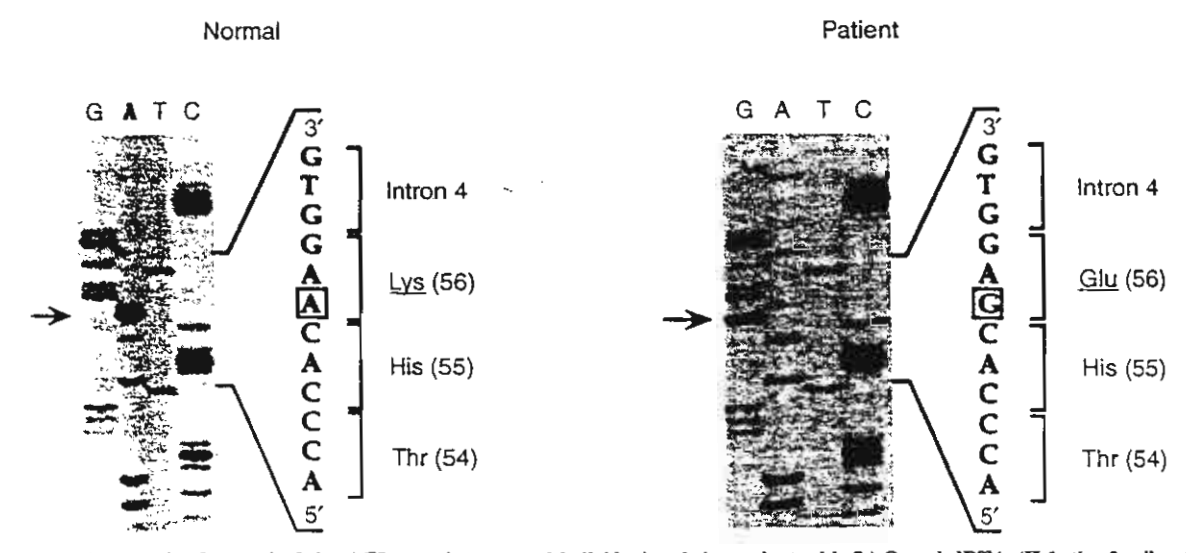


Fig. 5. Sequencing analysis of exon 4 of the AEI gene in a normal individual and the patient with SAO and dRTA (II-1, the family of KSN). The normal individual had AAG (code for lysine), but the patient had GAG (code for glutamic acid) at codon 56. The band 3 variant that had glutamic acid at the patient of 56 was previously described as band 3 Memphis I. The patient who had the 27 bp deletion in exon 11 and the G-A substitution in codon 281 in exon 17 was homozygous for band 3 Memphis I. Therefore, these two mutations were linked to band 3 Memphis I polymorphism.

Table 5. Characteristion of [35]SO4 influx into red cells from members of families of YAT and KSN, compared with healthy control cells

			SO ₄	SO ₄ uptake 10-17 mol/min/cell	
	Genotype	Phenotype	No DIDS	1.5 µм DIDS	%
YAT family					
I-1	G701D		6.45	2.12	32.9
I-2	Ex 11Δ27	SAO	4.78	0.08	1.7
$\Pi-1$	Ex11\(\Delta\)27/G701D	SAO + RTA	4.77	0.13	2.7
KSN family					
I-1	Ex 11Δ27	SAO	3.57	1.48	24.1
I2	G701D		6.56	2.35	35.8
II-1	Ex11\(\Delta\)27/G701D	SAO + RTA	4.03	0.15	3.7
Controls			6.0 ± 0.8		

for AEI mutations associated with SAO and dRTA, to our knowledge. The sequencing results also showed the presence of homogous band 3 Memphis I (Fig. 5) in the two patients, indicating that the two mutations linked with band 3 Memphis I polymorphism. Studies of the influx of [PS] sulfate into red cells of the two patients and their family members with SAO indicated a consistently lower amon transport activity than the normal red cells (Table 5). Individuals with exon 17 mutation had normal red cell amon transport activity.

Glycine 701 is located at the beginning of membrane span 9 of band 3, which is in a highly conserved region in the AE protein family across several species [28], which indicates its structural or functional importance. Although the presence of both SAO and G701D mutations had no additional affect on the influx of [35] sulfate into red cells than the presence of the SAO mutation alone, the HCO₃-ACI⁻ anion exchanger activity in the type A intercalated cells of the renal collecting duct in

garage and the strong

individuals with the combined mutations may be abnormal. Two siblings with dRTA and hemolytic anemia have recently been found to carry a homozygous G701D missense mutation of the AEI gene, which causes recessively transmitted dRTA in this kindred with apparently normal erythroid anion transport in the parents and affected children [32].

An expression study of the G701D mutation in Xenopus oocytes has shown that the mutant protein was not transported to the surface of the cell membrane [32]. However, when it was co-expressed with glycophorin A, the erythroid band 3 chaperonin, both AE1 surface expression and AE1-mediated Cl⁻ transport were rescued. This suggests that the G701D mutation may lead to decreased or absent AE1 accumulation at the basolateral membrane of the type A intercalated cells in the collecting duct. Therefore, the presence of both SAO and G701D mutations would have a greater effect to the type A intercalated cells than the presence of either mutation alone,

and this would explain the abnormal urinary acidification in the patients with the compound heterozygosity.

Although mutations of the AEI gene have been reported to be associated with autosomal dominant dRTA [12, 13, 31], the presence of the compound heterozygosity of AEI mutations associated with SAO and dRTA shown in our study, and of homozygosity of AEI mutation associated with dRTA and hemolytic anemia in that of Tanphaichitr et al [32] indicate an autosomal recessive mode of inheritance.

ACKNOWLEDGMENTS

This study has been supported by grants from Research Development and Medical Education Fund of the Faculty of Medicine, Siriraj Hospital. P. Malasit and P. Wilairat are recipients of the Senior Research Grant of The Thailand Research Fund (TRF). The Medical Molecular Biology Laboratory also operates as a Medical Biotechnology Unit of the National Center for Genetic Engineering (BIOTEC) of the National Science and Technology Development Agency (NSTDA), Thailand. We thank Miss Duangporn Chuawatana, Sumitra Mingkum, and Nunghathai Sawasdee for their technical assistance.

Reprint requests to Somkiat Vasuvattakul, M.D., Renal Unit, Department of Medicine, Siriraj Hospital, Mahidol University, Bangkok 10100, Thailand.

E-mail: sisva@mucc.mahidol.ac.th

REFERENCES

- LIU S, ZHAI S, PALEK J, GOLAN DE, AMATO D, HASSAN K, NURSE GT, BABONA D, COETZER T, JAROLIM P, ZAIK M, BORWEIN S: Molecular defect of the band 3 protein in Southeast Asian ovalocytosis. N Engl J Med 323:1530–1538, 1990
- Jones GL, Edmundson HM, Wesche D, Saul A: Human erythrocyte band 3 has an altered N-terminus in malaria resistant Melanesian ovalocytosis. Biochim Biophys Acta 1096:33–40, 1991
- SCHOFFELD AE, REARDON DM, TANNER MIA: Defective anion transport activity of the abnormal band 3 in hereditary ovalocytic red blood cells. Nature 355:836–838, 1992
- JAROLIM P, PALEK J, AMATO D, HASSAN K, SAPAK P, NURSEL GT, RUBIN HL, ZHAI S, SAHR KE, LIU SC: Deletion in erythrocyte band 3 gene in malaria-resistant Southeast Asian ovalocytosis. Proc Natl Acad Sci USA 88:11022-11026, 1991
- ALPER SL, NATALE J, GLUCK S, LODISH HF, BROWN D: Subtypes of intercalated cells in rat kidney collecting duct defined by antibodies against erythroid band 3 and renal vacuolar H⁺ ATPase. Proc Natl Acad Sci USA 86:5429–5433, 1989
- WAGNER S, VOGEL R, LIETZKE R, KOOB R, DRENCKHAHN D: Immunochemical characterization of a band 3-like anion exchanger in collecting duct of human kidney. Am J Physiol 253:213–221, 1987
- WAINWRIGHT SD, TANNER MJA, MARTIN GEM, YENDLE JE, HOLMES C: Monoclonal antibodies to the membrane domain of the human erythrocyte anion transport protein. Biochem J 258:211–220, 1989
- Kollerton-Jons A, Wagner S, Hubner S, Appelhans H, Drenckhahn D: Anion exchanger 1 in human kidney and oncocytoma differs from erythroid AE1 in its NH2 terminus. Am J Physiol 265:F813-F821, 1993
- Schoffeld AE, Martin PG, Spillett D, Tanner MJA: The structure of the human red blood ceil anion exchanger (EPB3, AE1, band 3) gene. Blood 84:2000–2012, 1994
- WRONG O, UNWIN R, COHEN E, TANNER M, THAKKER R: Unraveling the molecular mechanisms of kidney stones. Lancet 348:1561–1565, 1906
- BATLLE D, FLORES G: Underlying defects in distal renal tubular acidosis; New understandings. Am J Kidney Dis 27:896–915, 1996
- 12. BRUCE LJ, COPE DL, JONES JK, SCHOPIELO AE, BURLEY M, POVEY S, UNWIN RJ, WRONG O, TANNER MJA: Familial distal renal tubular

- acidosis is associated with mutations in the red cell anion exchanger (band 3, AE1) gene. J Clin Invest 100:1693-1707, 1997
- 13. JAROLIM P, SHAYAKUL C, PRABAKARAN D, JIANG L, STUART-TILLEY A, RUBIN H, SIMOVA S, ZAVADIL J, HERRIN JT, BROUILLETTE J, SOMERS MJG, SEEMANOVA E, BRUGNARA C, GUAY-WOODFORD LM, ALPER SL: Autosomal dominant distal renal tubular acidosis is associated in three families with heterozygosity for the R589H mutation in the AE1 (band 3) CI-/HCO₃ exchanger. J Biol Chem 273:6380-6388, 1998
- RYSAVA R, TESAR V, JIRSA M, BRABEC V, JAROLIM P: Incomplete distal renal tubular acidosis coinherited with a mutation in the band 3 (AE1) gene. Nephrol Dial Transplant 12:1869–1873, 1997
- THONG MK, TAN AAL, Lin HP: Distal renal tubular acidosis and hereditary elliptocytosis in a single family. Singapore Med J 38:388— 390, 1997
- BAEHNER RL, GILCHRIST GS, ANDERSON EJ: Hereditary elliptocytosis and primary renal tubular acidosis in a single family. Am J Dis Child 115:414-419, 1968
- LIE-INIO LE, FIX A, BOLTON JM, GILMAN RH: Haemoglobin Ehereditary elliptocytosis in Malayan aborigines. Acta Haematol 47: 210–216, 1972
- Wrong O, Davies H: The excretion of acid in renal disease. Q J Med 28:259-313, 1959
- VASUVATTAKUL S, GOUGOUX A, HALPERIN ML: A method to evaluate renal ammoniagenesis in vivo. Clin Invest Med 16:265–273, 1993
- VASUVATTAKUI, S., NIMMANNIT S., CHAOVAKUL VWS, SHAYAKUL C., MALASIT P: The spectrum of endemic renal tubular acidosis in the northeast of Thailand. Nephron 74:541–547, 1996
- Van Slyke DD, Linder GS, Hiller A, Letter L, McIntosh JF: The excretion of ammonia and titrable acid in nephritis. J Clin Invest 2:255-288, 1926
- HASTINGS AB, SENDROY J: The effect of variation in ionic strength on the apparent first and second dissociation constants of carbonic acid. J Biol Chem 65:445-455, 1925
- HALPERIN ML, VINAY P, GOUGOUX A, PICHETTE C, JUNGUS RL: Regulation of the maximum rate of renal ammoniagenesis in the acidotic dog. Am J Physiol 248:F607-F615, 1985
- CAMARA AA, ARN KD, REIMER A, NEWBURGH LH: The twentyfour hourly endogenous creatinine clearance as a clinical measure of the functional state of the kidneys. J Lab Clin Med 37:743

 –763, 1951
- ETHIER J, KAMEL K, MAGNER P, LEMANN JJ, HALPERIN ML: The transtubular potassium concentration in patients with hypokalemia and hyperkalemia. Am J Kidney Dis 15:309–315, 1990
- GRUNEBAUM L, CAZENAVE J-P, CAMERINO G, KLOEPFER C, MANDEL J-L, TOLSTOSHEV P, JAYE M, DE LA SHALLE H, LECOCQ J-P: Carrier detection of hemophilia B by using a restriction site polymorphism associated with the coagulation factor IX gene. J Clin Invest 73:1491–1495, 1984
- TANNER MJA: Molecular and cellular biology of the erythrocyte anion exchanger (AE1). Semin Hematol 30:34–57, 1993
- TANNER MJA: The structure and function of band 3 (AE1): Recent developments. (review) Mol Membr Biol 14:155–165, 1997
- 29. INABA M, YAWATA A, KOSHINO I, SATO K, TAKEUCHI M, TAKAKUWA Y, MANNO S, YAWATA Y, KANZAKI A, JI S, BAN A, KI O, MAEDE Y: Defective anion transport and marked spherocytosis with membrane instability caused by hereditary total deficiency of red cell band 3 in cattle due to a nonsense mutation. J Clin Invest 97:1804–1817, 1996
- MORRIS RC, IVES HEA INHERITED DISORDERS OF THE RENAL TUBULE, IN The Kidney, edited by Brenner BM, Philadelphia, W. B. Saunders, 1996, pp 1764–1827
- 31. KARET FE, GAINZA FJ, GYORY AZ, UNWIN RJ, WRONG O, TANNER MJA, NAYIR A, ALPAY H, SANTOS F, HULTON SA, BAKKALOGLU A, OZEN S, CUNNINGHAM MJ, DI PIETRO A, WALKER WG, LIFTON RP: Mutations in the chloride-bicarbonate exchanger gene AE1 cause autosomal dominant but not autosomal recessive distal renal tubular acidosis. Proc Natl Acad Sci USA 95:6337-6342, 1998
- TANPHAICHITR VS, SUMBOONNANONDA A, IDEGUCHI H, SHAYAKUL C, BRUGNARA C, TAKAO M, VEERAKUL G, ALPER SL: Novel AE1 mutations in distal renal tubular acidosis: Loss-of-function rescued by glycophorin A. J Clin Invest 102:2173–2179, 1998

WIL



Author / Typesetter Queries *Kidney Int* 56:5 November 1999 KID99756 Vasuvattakul

[VGC1]Dr. Vasuvattakul, It is journal style to mention the city location of each affiliation/institution. Is Songklanakarin Hospital also in Bangkok?

[Q2]Au: Please provide complete source location (city, country). [Q3]Au: Please provide complete source location (city, country).

[Q4]Typesetter: insert Table 1 near here

[Q5]Au: Please define (spell out) first use of ssDNA

[Q6]Au: Please provide complete source location (city, state).

[Q7]Typesetter: insert Table 2 near here [Q8]Typesetter: insert Table 3 near here [Q9]Typesetter: insert Figure 1 near here

[Q10]Typesetter: insert Table 4 near here

[Q11]Typesetter: insert Figure 2 near here

[Q12]Typesetter: insert Figure 3 near here

[Q13]Typesetter: insert Figure 4 near here

[VGC14] Typesetter: insert Fig. 5 nearby. [Q15] Typesetter: insert Table 5 near here

[Q16]Au: Please verify page range and year.

Title: Red cell microvesicles in Thalassemia

Running title: Microvesicles in Thalassemia

Key words: Thalassemia, microvesicles, complement, pathogenesis

Prapat Suriyaphol P, Prida Malasit, Prapon Wilairat,* Suthat Fucharoen,** and Sucharit Bhakdi°

Medical Molecular Biology Unit, Office for Research and Development, Faculty of Medicine, Siriraj Hospital, Mahidol University, Bangkok Noi, Bangkok, Thailand

- * Department of Biochemistry, Faculty of Science, Mahidol University, Phayathai, Bangkok, Thailand
- **Institute of Science and Technology for Research and Development, Mahidol University, Salaya, Nakorn Pathom, Thailand
- ° Institute of Medical Microbiology and Hygiene, Johannes Gutenberg University, Mainz, Germany.

Financial support:

The Senior Research Scholar Award to P Malasit, the Thailand Research Fund

Corresponding Author and Address:

Prida Malasit, M.D., F.R.C.P.

Medical Molecular Biology Unit, Office for Research and Developemnt, Siriraj Hospital, Faculty of Medicine, Prannok, Bangok 10700.

Tel and Fax 662 4184793

E mail sipml@mahidol.ac.th

Abstract

Many biochemical and structural defects were found in RBC from thalassemic patients, including depletion of cytoplasmic ATP, oxidative damage to the membrane and complement activation on the surfaces. RBC would response to the cited abnormalities, if induced artificially, by shedding of the membrane in the form of small vesicles. Employing the technique of flow cytometry and using fluorochrome labeled antiglycophorin antibody, significant amount of circulating red cell vesicles were found, highest in splenectomized β thalassemia/HbE patients, followed by non-splenectomized β -thalassemia/HbE, non-splenectomized α -thalassemia.

Erythrocytes from patients with thalassemia produced significantly more vesicles *in vitro* when incubated in buffers. The vesicles were spherical in shape, with an average size of 0.3 µm when examined with electron microscopy. Analysis by polyacrylamide gel electrophoresis revealed that the vesicles were free of spectrin. The vesicles were shown by flow cytometry to bind fluorochrome-labeled annexin V - a protein which binds specifically to phosphotidyl serine.

The vesicles were shown to efficiently activate the complement system via the alternative pathway. Complement split product, C3b, was detected by two dimensional gel immunoelectrophoresis when vesicles were incubated with autologous serum in the presence of EGTA Mg⁺⁺. Vesicles bound C3b was demonstrated by flow cytometry and Western-blot analysis of the red cell membrane.

These findings are unique and significant. They served as a linkage between the defective hemoglobin synthesis and red cell perturbation and a group of clinical complications as found in thalassemia. Thalassemic patients, particularly those who had been splenectomized, were more susceptible for repeated infections. Acquired complement deficiency has also been reported. The fact that significant amount of red cell vesicles has been found to be constantly generated *in vivo*, and the vesicles were functionally active in complement activation, they therefore represent important factors responsible for the complications as described.

Introduction

The primary defect in thalassemia syndromes is reduced or absent production of one or more globin chains of the hemoglobin tetramer, which results in a relative excess of the unpaired chain. The excess unmatched globin chains precipitate and incur damage to the cell. The underlying mechanisms are not well understood, but oxidative membrane damage is believed to be of main importance. concentrations of polyunsaturated fatty acids are regularly decreased, and membrane protein thiols are reduced as a reflection of their pathological oxidation. Intracellular Ca²⁺ levels are increased, which may be a consequence of enhanced Ca²⁺ flux across the damaged membrane. Further to these findings, little is known on pathological cell biology of the diseased erythrocytes. Moreover, an explanatory model does not exist to account for the systemic afflictions, in particular of the coagulation and complement system, that are characteristic of thalassemia patients. In particular, it has remained an enigma why a hypercoagulable state exists in these patients, leading to increased incidents of thrombotic events. Further, thalassemic patients have chronically low complement levels, a finding that also lacks a satisfactory explanation.

Membrane vesiculation is a physiological process that occurs during cell aging. Vesiculation can readily be observed in vitro, e.g. during storage of erythrocytes. Thereby, small lipid vesicles are released from the cells. They contain integral membrane proteins, phospholipids and cholesterol, but are almost devoid of the spectrum cytoskeleton. Enhanced vesiculation can be artificially induced in normal erythrocytes by treating the cells with Ca²⁺ ionophore, or by subjecting cells to attack by permeabilizing agents such as complement. Thalassemic RBC contain elevated Ca2⁺ concentrations, and activated components have also been detected on their surface. Hence, we questioned whether the diseased cells might exhibit an enhanced tendency to vesiculate. Abnormal vesiculation *in vitro* has previously been observed in sickle cells, although the possible physiological relevance thereof has remained unexplored. Here, we report that RBC vesicles exist *in vivo*, that their concentrations are elevated in patients with thalassemia, and that thalassemic cells exhibit abnormally high vesiculation rates. It is shown that vesicle formation can be

induced *in vitro*, and that the isolated vesicles activate both the complement and the coagulation system. A concept is advanced in which major clinical findings in thalassemic patients may be traced to the pathological tendency of their RBC to vesiculate. In particular, a simple explanation is offered for the characteristically low complement levels, which predispose these patients to infections, and for the hypercoagulable state that is often manifested in thrombotic complications.

Materials and Methods

Buffers and solutions. phosphate-buffered saline (PBS). 137 mM NaCl, 3 mM KCl, 10 mM Na₂HPO₄, 2 mM KH₂PO₄, pH 7.4; tris-buffered saline (TBS).140 mM NaCl, 20 mM Tris, pH 7.4; barbitone buffer. 22 mM barbitone, 127.5 mM sodium barbitone

Antibodies. Phycoerythrin(PE)-labeled anti-glycophorin A and FITC labeled anti-GpIIb/IIIa was purchased from Immunotech (Cedex,France)

Patients and controls

Thirty six β-thalassemia/hemoglobin E (β thal/HbE) patients were recruited: 21 had had splenectomy, 8 had non-splenectomized α thalassemia (HbH), and 7 patients had non-splenectomized α thalassemia constant spring (HbH/CS). The diagnosis of thalassemia was based on accepted criteria, including the characteristic clinical and hematological manifestations and hemoglobin type determined by starch gel electrophoresis. The study was conducted at the hematology clinic of the Department of Medicine, Siriraj Hospital. All patients had not had blood transfusion at least 3 months prior to the study. Fourteen normal healthy volunteers were included as controls.

Identification and quantification of vesicles

1 ml samples of venous blood were collected into a tube containing 50 μl of 1% glutaraldehyde solution and 25 μl of 0.2M EDTA (final concentration of 0.05% and 5mM, respectively). Platelet-rich plasma (PRP) was prepared by centrifugation of the fixed blood at 200g for 10 min at 25°C.

4 μl of PRP were diluted 1:5 by addition of phosphate buffered saline (PBS). 4 μl of PE-labeled anti-glycophorin A and 2 μl of FITC-labeled anti-GP IIb/IIIa were used to stain red blood cell (RBC) vesicles and platelets in the PRP, respectively. After incubation at room temperature for 30 min in the dark, the samples were diluted with 500 μl of PBS and analyzed by flow cytometer.

Samples were analyzed using a Beckton Dickinson FACSORT flow cytometer (Becton Dickinson Immunocytometry systems, California U.S.A). Instrument parameters were set to focus on the platelet population. Light scatter and fluorescence channels were set at logarithmic gain. Forward scatter threshold was set to avoid noise signal. Figure 1a shows a scattergram of the forward (FSC) versus sideward scatter (SSC) signals from PRP of a thalassemic patient. The distribution of dots indicated one homogenous population of signals, which correspond well with the size of platelets. Platelets (R1) and vesicles (R2) were distinguished according to the fluorescent intensity (Figure 1b-c). The ratio of platelet to vesicle in each sample was determined from the number of platelets in R1 and vesicles in R2.

The concentration (conc.) of RBC vesicles in the PRP samples was calculated by the following formula:-

conc. of vesicles = conc. of platelets x ratio of vesicles/platelets

The concentration of platelets was determined by Technicon H1 machine, which has been tested that it measures the accurate number of platelets in the vesicle-containing samples (data not shown).

Statistical analysis

All calculations were carried out on an IBM-PC computer with the StatView statistical package. Comparison of data between different groups was performed using ANOVA. A "p value" of <0.05 was regarded as significant.

Morphological study of vesicles by electron microscope

Fresh PRP was prepared by centrifugation of EDTA blood at 200 g for 10 min. After 3 washes with PBS, PRP was fixed with 2% glutaraldehyde overnight at 4 °C. The samples were washed again 3 times with PBS and stained with 2% osmium tetroxide for 1 h at 4°C. After another wash, the samples were dehydrated by stepwise introduction of ethanol at 4°C. Finally, the samples were incubated for 10 min and washed 3 times in absolute ethanol. The dehydrated samples were treated

and embedded in epoxy resin. After complete polymerization of resin, the samples were cut and examined under transmission electron microscope.

In vitro generation of RBC vesicles

5 ml samples of blood from splenectomized β thal/Hb E patients were collected in a tube containing 250 μl of 0.2M EDTA (10 mM final concentration) as an anticoagulant. RBCs were pelleted by centrifugation at 200g for 10 min, and washed 3 times with PBS. After each wash, the buffy layer containing white cells was carefully discarded. An equal volume of PBS was added to the washed RBCs to obtain 50% hematocrit RBCs. After incubation at 37°C for 24 h, the remaining red cells (RBC remnants) were separated from the vesicle-containing supernatant by centrifugation at 200g for 10 min and washed 3 times with PBS. RBC vesicles in the supernatant were then pelleted by centrifugation at 15,000g for 10 min, and washed 3 times with PBS.

SDS-PAGE

SDS-PAGE was performed in a minigel apparatus using 10% separating gel and 3.85% stacking gel. Samples were treated with 4x reducing sample buffer and heated in boiling water for 5 min. Electrophoresis was performed in a vertical direction with a constant voltage of 150 V. The polypeptide bands were visualized with Coomassie brilliant blue staining or blotted onto a nitrocellulose membrane for immunoassay.

Annexin V staining assay

The samples were washed 3 times with annexin V-staining buffer (TBS with 2mM Ca⁺⁺), then stained with 2 µl of FITC-labeled annexin V (Bender MedSystems, Germany) in dark for 30 min. 4 µl of PE-labeled anti-glycophorin A were added to the vesicle samples and were used to identify vesicles. After incubation, the samples were diluted with 500 µl of annexin V-staining buffer and subjected to flow cytometry analysis.

Flow cytometry

Samples were analyzed using a Beckton Dickinson FACSORT flow cytometer (Becton Dickinson, Le Pont de Claix, France). The light scatter and the fluorescence

channels were set at logarithmic gain. Ten thousand signal data were acquired twice for each sample. The average number of signals was used.

Complement activation assay

10 μl of thalassemic RBCs (5 x 10⁶ cells/μl) and vesicles were added to 50 μl of autologous serum or EDTA serum (10 mM final concentration). After incubation at 37°C for 1 h, cells in the suspension were pelleted and washed 3 times with cold PBS at 4°C. Washed RBCs and vesicles were subjected to flow cytometry and Western blot analysis. The serum supernatants were analyzed by 2-D immunoelectrophoresis.

Flow cytometry analysis

RBCs (approximately 5 x 10^5 cells) and vesicles were stained with 2 μ l of FITC-labeled anti-C3c monoclonal antibody (DAKO, Denmark). 4 μ l of PE-labeled anti-glycophorin A were added to the vesicle sample and were used to identify vesicles. After incubation for 30 min in the dark, the samples were diluted with 500 μ l of PBS and analyzed by flow cytometry.

Western blot analysis

After SDS-PAGE, the proteins were transferred to a nitrocellulose membrane using a semi-dry blotter. The membrane was blocked with 5% skimmed milk in PBS (blocking buffer) for 30 min at room temperature. The membrane was incubated with rabbit monoclonal antibody to C3d (DAKO, Denmark) at 1:1000 dilution in the blocking buffer for 12 h. After 3 washes with PBS, each for 3-5 min, the nitrocellulose membrane was incubated with a swine anti-rabbit IgG conjugated with HRP (DAKO, Denmark) at 1:1000 dilution for 4 h at room temperature. The membrane was washed 3 times as described above. Chromogenic substrate was added to develop the enzymatic reaction for 5 min. The reaction was stopped by briefly rinsing membrane in distilled water. Positive reaction appeared as a dark brown bands on the membrane.

Two-dimensional crossed immunoelectrophoresis

The serum samples were tested for C3 conversion by two-dimensional crossed immunoelectrophoresis. The first dimension was run in 1% agar using barbitone buffer containing 0.01 M EDTA (pH 8.6) at 10 V/cm for about 1.5 h. The second

dimension was run against rabbit anti-human C3c (Dako immunoglobulins) at 1 V/cm overnight. The plates were dried, stained with 0.1% Coomassie brilliant blue and destained in methanol/acetone (1:1). The main peak represented native C3 and the smaller, faster migrating peak represented the C3b/iC3b conversion product.

Study of complement regulatory proteins (DAF, CD59)

RBCs and vesicles were stained with 5 μ l of either FITC-labeled anti-DAF or anti-CD59 (Serotec, England) in dark for 30 min at room temperature. 4 μ l of PE-labeled anti-glycophorin A were also added in vesicle samples. After incubation, the samples were diluted with 500 μ l of PBS and analyzed by flow cytometry.

Procoagulant activity of the vesicles

5 ml samples of blood from normal volunteers were collected in a tube containing 500 μl of 0.109M trisodium citrate anticoagulant. PRP was prepared by centrifugation of blood at 200g for 10 min at room temperature. Platelet-poor plasma (PPP) was prepared by centrifugation of PRP at 2,500 g for 15 min. RBC vesicles were prepared as described above. Coagulation activator (buffered suspension of kaoline 5 mg/ml) and samples were added to 100 μl of PPP in the cuvette, mixed, and incubated for 180 s at 37°C. After incubation, the cuvette was transferred into the light absorbance measurement chamber of Fibrinometer (Labor Fibrintimer Condata 1000, Hamburg, Germany). 100 μl of 25 mM Ca⁺⁺ were added to cuvette. The clotting time was measured by the Fibrinometer.

Results

Patients and Controls

A total 52 patients were studied: 36 were β thal/HbE of whom 21 were splenectomized, 9 non-splenectomized α thalassemia (Hb H disease), and 7 non-splenectomized α thalassemia with Constant Spring (HbCS). All subjects were devoid of any signs of infection or skin ulcer and did not receive any blood transfusion within three months prior to the study. The average age of the patients was 30.8 ± 1.7 years (\pm standard error) which was similar to that of normal controls (29.8 ± 1.5 years, p > 0.05). There was no difference in age between the three groups of patients. All thalassemic patients recruited in this study had significantly lower hemoglobin concentration than controls but there was no significant difference among patient groups (Table 1).

Quantitation of vesicles in plasma

A flow cytometry technique was employed to demonstrate the existence of RBC vesicles in circulation and to quantify their amounts. Consistently fewer than $20,000 \text{ vesicles/mm}^3$ were found in normal individuals (Figure 2 and Table 1). The highest numbers of vesicles were found in patients with β thal/Hb E disease, and this was the more pronounced in the splenectomized subjects. Among the α -thalassemic patients, only those with HbCS had significantly more vesicles than controls.

Vesicle morphology

Vesicles in PRP prepared from splenectomized β thal/HbE patients are depicted in Figure 3. Platelets were identified and differentiated from the RBC vesicles by their irregular shapes and their enclosed cytoplasmic organelles. RBC vesicles were characterized by their spherical or oval shapes with no cytoplasmic organelles and the presence of electron dense cytoplasm. The diameter of vesicles varied greatly from one tenth to equal that of platelets (1,000 nm), with an average dimension of 300 nm. Vesicles could also be seen budding out from red cells (Fig.3b).

Membrane Protein Characterization

Membrane proteins of *in vitro*-generated vesicles were compared with those of RBC ghosts by SDS-PAGE (Figure 3). Although it was difficult to visualize the

vesicle membrane protein components because vesicles were resistant to lysis buffer making it difficult to remove the hemoglobin before solubilizing the membrane, the lack of spectrin bands was apparent. Band 7 was present, indicating that there was sufficient amount of membrane proteins on the gel. Therefore, the absence of spectrin and other cytoskeletal proteins was not due to inadequate material.

Annexin V binding assay

Annexin V signals from the vesicles were stronger than those from thalassemic RBCs as demonstrated by the clear shift to the right (Figure 5). Using the histogram profile of annexin V of thalassemic RBCs as control, we calculated that 52.91% of vesicles have phosphatidylserine on their surface.

Complement activation by vesicles

Flow cytometry study

Normal RBCs showed no detectable binding of C3 on their surface (data not shown). All vesicles incubated in EDTA-serum had low fluoresent intensity of anti-C3c. Vesicles incubated in autologous serum could be divided into two populations (Figure 6): one group had low anti-C3c fluorescent intensity, similar to vesicles incubated in EDTA-serum, whereas the other population had high anti-C3c fluorescent intensity, indicating the presence of C3 molecules on their surface. This suggested that approximately half the vesicles activated the complement system in autologous serum.

Western blot analysis

High molecular weight bands, indicative of C3b molecules covalently bound to proteins, were detected on vesicles generated from thalassemic RBCs incubated with autologous serum, but not in vesicles incubated with EDTA-serum used as negative control (Figure 7). Such high molecular weight bands was detected in thalassemic RBC membrane. These findings support the notion that vesicles could activate the complement system in autologous serum.

Two-dimensional immunoelectrophoresis

Autologous serum showed one peak of C3 (Figure 8A), which remained intact in the presence of thalassemic RBC (Figure 8B). Incubation with vesicles cleaved C3 into C3a and C3b (Figure 8C), the latter being recognized by the antibody (Figure 8C,

right-shifted peak). A lower concentration of vesicles added to the suspension resulted in less cleavage of C3 (Figure 8D), and addition of EDTA to the serum blocked C3 cleavage by the vesicles (Figure 8E). However, in the presence of EGTA and Mg⁺⁺, cleavage of C3 occurred (Figure 8F), indicating that complement activation could still take place when the classical pathway was inhibited. Therefore, vesicles activated complement via the alternative pathway.

Complement Regulatory Proteins

The amount of DAF (CD55) on the surface of vesicles was significantly lower than on RBCs (Figure 9). Since the amount of DAF on the surface of vesicles varied from low to intermediate (Figure 10) and only a proportion of the vesicle population activated complement (Figure 6), it is possible that only those vesicles that expressed a low amount of DAF activated complement. To test this possibility, vesicles were incubated in autologous serum and subsequently stained with monoclonal antibodies against DAF and C3c. Vesicles that contained intermediate amounts of DAF could activate complement (Figure 11). Thus complement activation occurred despite the presence of complement inhibitory proteins.

Procoagulant activity of the vesicles

A clotting time of 35.8 sec was obtained using normal plasma in the presence of activator and cephalin. Without the activator and cephalin, clotting time was extended to 170.9 sec. Addition of vesicles which served as a phospholipid surface decreased the clotting time to 90.7 sec, which was similar to that when only activator was added (97.4 sec). The presence of both activator and vesicles resulted in a clotting time of 53.2 sec, which was similar to the normal clotting time. Vesicles could serve as a strong procoagulant surface.

Discussion

It has long been known that RBCs vesiculate upon aging in vitro. The possibility that vesiculation also occurs in vivo had been imminent, but direct detection of vesicles in freshly drawn blood samples has not been possible due to lack of appropriate methodology. In this communication, we describe a flow-cytometric technique that provide investigators with a new tool in this area. Vesicles can be detected on the basis of their size and positive staining for glycophorin. They can easily be quantified on the basis of platelet counts. We are not aware that this or any other method has been employed to detect and quantify RBC vesicles in blood samples before. We found that the number of vesicles in samples from healthy donors is 9664 ± 1206 per mm³. Levels exceeding 18000 vesicles per mm³ were never observed. Vesicle counts were elevated in B-thal HbE patients (30417 ± 3618 per mm³), and this finding was accentuated after splenectomy. Attention is drawn to the actual values shown in Fig.2. Whereas vesical counts never exceeded 18000 per mm³ in controls, this threshold was surpassed in 13 of 17 \(\beta \)-thal HbE patients with intact spleen, and in 21 of 25 patients with splenectomy. Some of the splenectomized patients had vesical counts 4-6-fold higher than in normal donors. The latter finding most likely reflects that the spleen is an important site of vesicle removal. Elevated vesicle concentrations were also found in HbH CS patients.

Vesicles could readily be identified because they carried typical RBC markers, e.g. glycophorin, DAF, and CD59. They were also directly detected by electron microscopy in platelet-rich plasma from splenectomized patients. Vesicles could be generated in vitro, and they similarly expressed glycophorin, DAF and CD59. The possibility of generating vesicles in vitro facilitated their further characterization. Vesicles were found to essentially lack spectrin, a finding that was in accord with results of earlier investigations on vesicles generated from aging erythrocytes. Further findings were novel and of distinct interest. First, we found that vesicles bound annexin V, as demonstrable by flow cytometry. This property was not displayed by intact thalassemic RBCs. The capacity to bind annexin V reflects exposure of phosphatidyl serine on the outer membrane leaflet. Thus, our finding indicates breakdown of phospholipid asymmetry in the membrane vesicles. It is known that

13

phosphatidyl serine enriched in the outer leaflet of platelets and artificial lipid vesicles is an important event underlying generation of a procoagulant surface. By analogy, we suspected that RBC vesicles might display procoagulatory activity, a possibility that has not been tested or considered hithertofore. When citrated PRP samples were spiked with purified vesicle preparations, coagulation times determined after recalcification indeed dropped. Another, equally important finding related to the capacity of vesicles to activate the alternative complement pathway. This was shown in experiments wherein C3 conversion in EDTA serum was found to be triggered by the vesicles. In the same experiments, deposition of C3 on vesicle membranes was shown by flow cytometry. The cause of complement activation is unknown at present, but its cholesterol-rich liposomes activate the alternative complement pathway. RBC vesicles quite likely mimick such liposomes, since they have a high content of cholesterol, a low content of membrane protein, and disrupted membrane asymmetry.

Now, it becomes possible to formulate a quite simple hypothesis that would explain some major clinical findings in thalassemia. In line with previous concepts, imbalance of globin change synthesis should lead to intracellular protein precipitation. Membrane damage is incurred perhaps through direct interaction with aggregated protein, and through oxidative processes. The damaged membranes permit enhanced flux of Ca2+ into the cells and this we propose enhances membrane vesiculation. Vesicles forming under physiologic conditions during aging are likely removed efficiently, so that detrimental consequences do not follow. Enhanced vesiculation rates in thalassemic patients probably results in an overload of the removal system. Elevated vesicle concentrations then cause systemic pathology via low grade activation of both coagulation and complement system. It is of interest to allude to previous descriptions of platelet and coagulation anomalies that have frequently been observed in thalassemic patients. Such observations included increased circulating platelet aggregates, shortened platelet life span, increased urinary excretion of thromboxin A2 metabolites, enhanced expression of p-selectin, raised plasma levels of thrombin/anti-thrombin 3 complexes, and low plasma levels of the natural anticoagulants, protein C and protein S. Isolated thalassemic erythrocytes had been reported to enhance thrombin generation, a finding that was attributed to the presence

14

of phosphatidyl serine on the thalassemic RBC outer surface. Our data suggest, however, that the phenomenon might rather be related to shedding of phosphatidyl-serine rich vesicles from the erythrocytes during the assay.

Constant activation of platelets by thrombin produced by red cell vesiculation may be a key factor leading to the formation of platelet microthrombi, especially on the right side of the systemic circulation. It is well-known that thalassemic patients characteristically suffer from thrombotic occasions within the pulmonary circulation, which leads to chronic hypoxemia.

Consequences of chronic complement consumption are also manifest. Thus, thalassemic patients characteristically have low complement levels. Previous findings have indicated that his may be due in part to binding of (auto)antibodies, which cause activation of the classical complement pathway on the cells. Now, a second possibility emerges that RBC vesicles also contribute to complement consumption. Quite satisfactorily, it is known that both classical and alternative complement components are reduced in the patients. Chronically low complement levels in turn may contribute to the known, enhanced predisposition of thalassemic patients to infectious disease.

In sum, it is proposed that pathological vesiculation rates that probably are a consequence of membrane damage and Ca²⁺ influx underlie major pathological sequelae in thalassemic patients. If correct, this concept may extent to other hemoglobinopathies such as sickle cell anemia, as well as to hereditary membrane anomalies of the red blood cell such as hereditary spherocytosis.

References

- 1. Schrier SL, Mohandas N. Globin-chain specificity of oxidation-induced changes in red blood cell membrane properties. Blood 1992;79(6):1586-92.
- 2. Schrier SL. Thalassemia: pathophysiology of red cell changes. Annu Rev Med 1994;45:211-8.
- 3. Advani R, Sorenson S, Shinar E, Lande W, Rachmilewitz E, Schrier SL. Characterization and comparison of the red blood cell membrane damage in severe human alpha- and beta-thalassemia. Blood 1992;79(4):1058-63.
- 4. Rachmilewitz E, Kahane I. The red blood cell membrane in thalassaemia. Br J Haematol 1980;46(1):1-6.
- 5. Rachmilewitz EA, Shinar E, Shalev O, Milner Y, Erusalimsky J, Schrier SL. Alterations in structure, function, and Ca++ content of thalassemic red blood cells. Biomed Biochim Acta 1983;42(11-12):S27-31.
- 6. Shalev O, Mogilner S, Shinar E, Rachmilewitz EA, Schrier SL. Impaired erythrocyte calcium homeostasis in beta-thalassemia. Blood 1984;64(2):564-6.
- 7. Wiley JS. Increased erythrocyte cation permeability in thalassemia and conditions of marrow stress. J Clin Invest 1981;67(4):917-22.
- 8. Allan D, Thomas P. Ca2+-induced biochemical changes in human erythrocytes and their relation to microvesiculation. Biochem J 1981;198(3):433-40.
- 9. Wagner GM, Chiu DT, Qiu JH, Heath RH, Lubin BH. Spectrin oxidation correlates with membrane vesiculation in stored RBCs. Blood 1987;69(6):1777-81.
- 10. Iida K, Whitlow MB, Nussenzweig V. Membrane vesiculation protects erythrocytes from destruction by complement. J Immunol 1991;147(8):2638-42.
- 11. Malasit P, Mahasorn W, Mongkolsapaya J, Singhathong B, Fucharoen S, Wasi P, et al. Presence of immunoglobulins, C3 and cytolytic C5b-9 complement components on the surface of erythrocytes from patients with beta- thalassaemia/HbE disease. Br J Haematol 1997;96(3):507-13.
- 12. Dumaswala UJ, Greenwalt TJ. Human erythrocytes shed exocytic vesicles in vivo. Transfusion 1984;24(6):490-2.
- Waugh RE, Narla M, Jackson CW, Mueller TJ, Suzuki T, Dale GL. Rheologic properties
 of senescent erythrocytes: loss of surface area and volume with red blood cell age.
 Blood 1992;79(5):1351-8.
- 14. Greenwalt T, Lau F. Evaluation of toluidine blue for measuring erythrocyte membrane loss during in vivo ageing. Br J Haematol 1978;39:545-50.
- Weatherall D, Clegg J. The Thalassaemia Syndromes. 3rd ed. ed. Oxford: Blackwell Scientific; 1981.
- 16. Wilairat P, Kittikalayawong A, Chaicharoen S. The thalassemic red cell membrane. Southeast Asian J Trop Med Public Health 1992;23(Suppl 2):74-8.
- 17. Peerapittayamongkol C, Bernini L, Wilairat P. Presence of alpha Constant Spring globin on membrane of red cell containing hemoglobin Constant Spring (CS). J Sci Soc Thai 1996;22:117-20.

- 18. Kruatrachue M, Sirisinha S, Pacharee P, Chandarayingyong D, Wasi P. An association between thalassaemia and autoimmune haemolytic anaemia (AIHA). Scand J Haematol 1980;25(3):259-63.
- 19. Winichagoon P, Fucharoen S, Wasi P. Increased circulating platelet aggregates in thalassaemia. Southeast Asian J Trop Med Public Health 1981;12(4):556-60.
- 20. Eldor A, Krausz Y, Atlan H, Snyder D, Goldfarb A, Hy-Am E, et al. Platelet survival in patients with beta-thalassemia. Am J Hematol 1989;32(2):94-9.
- 21. Eldor A, Lellouche F, Goldfarb A, Rachmilewitz EA, Maclouf J. In vivo platelet activation in beta-thalassemia major reflected by increased platelet-thromboxane urinary metabolites. Blood 1991;77(8):1749-53.
- 22. Del Principe D, Menichelli A, Di Giulio S, De Matteis W, Cianciulli P, Papa G. PADGEM/GMP-140 expression on platelet membranes from homozygous beta thalassaemic patients. Br J Haematol 1993;84(1):111-7.
- 23. Cappellini M, Coppola R, Bottasso B, Graziadei G, Fargion S, Mannucci P. Hypercoagulability in patients with thalassemia intermedia. Blood 1995;86 (Suppl. 1):643a.
- 24. Borenstain-Ben Yashar V, Barenholz Y, Hy-Am E, Rachmilewitz EA, Eldor A. Phosphatidylserine in the outer leaflet of red blood cells from beta-thalassemia patients may explain the chronic hypercoagulable state and thrombotic episodes. Am J Hematol 1993;44(1):63-5.
- 25. Chantharaksri U, Tonsuwonnont W, Fucharoen S, Wasi P. The pathogenesis of hypoxemia. Southeast Asian J Trop Med Public Health 1992;23 (Suppl.2):32-5.
- 26. Wasi P, Fucharoen S, Youngchaiyud P, Sonakul D. Hypoxemia in thalassemia. Birth Defects Orig Artic Ser 1982;18(7):213-7.

	Hb Concentration (g/dl)	Platelet Concentration (cell/mm ³)	Vesicle Concentration (cell/mm ³)
β thal/Hb E splenectomy	6.2 ± 0.2^{b}	$616,000 \pm 33.129^{a}$	34,473 ± 5,492 ^{b,c}
β thal/Hb E intact spleen	5.9 ± 0.5 ^b	315,633 ± 36,765 ^b	24,737 ± 3,777 ^b
Hb H intact spleen	7.4 ± 1.2 ^b	353,388 ± 52,903 ^b	$18,960 \pm 4,027^{c}$
Hb H/CS intact spleen	6.6 ± 0.6 ^b	313,929 ± 39,666 ^b	$35,583 \pm 10,902^{b}$
Control	15.0 ± 0.3	204,000 ± 10,759	9,664 ± 1,206

Table 1. Levels of hemoglobin, number of platelets, vesicle concentration in different groups of thalassemic patients

The values are shown as mean±standard error. The category in each group is compared with others and normal controls

- a. Significantly different from other corresponding categories and normal controls, P<0.01
- b. Significantly different from normal controls, P<0.05
- c. Significantly different from HbH with intact spleen, P<0.05
- d. Not different from normal controls, P<0.05

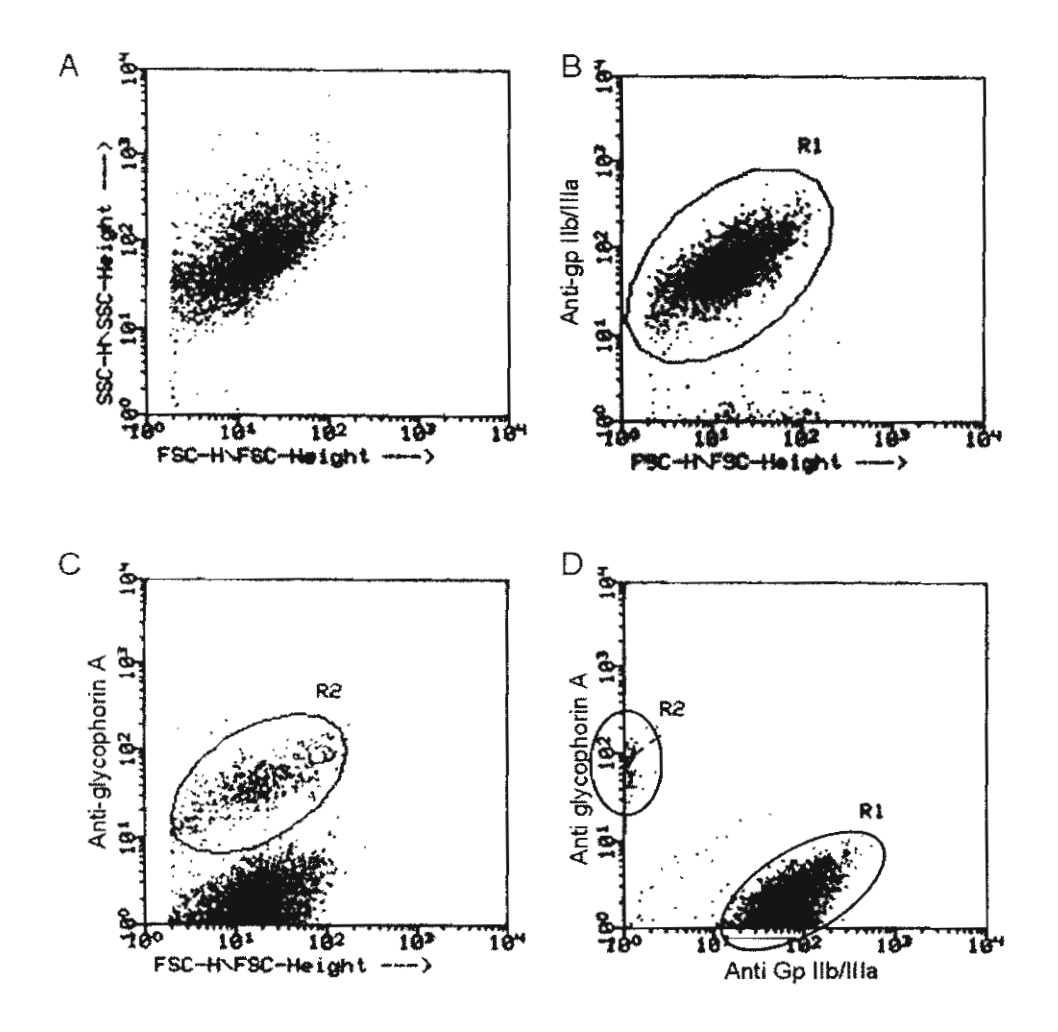


Figure 1. Typical flow cytometry scattergrams of a patient with thalassemia

a) Forward and sideward scatter of the platelet-rich plasma (PRP) shows one homogenous population. b) Forward scatter (FSC) vs. FL1, which represents signals from FITC-labeled anti-platelet GP IIb/IIIa. The platelets with high FL1 signals are labeled "R1". c) FSC vs. FL2 which represents signals from phycoerythrin (PE)-labeled anti-glycophorin A. The vesicles with high FL2 were labeled "R2". The ratio of glycophorin A-positive signals (R2) to GP IIb/IIIa-positive signals was used to calculate the amount of vesicles found *in vivo* by using platelet concentration as obtained from the H1 analysis.

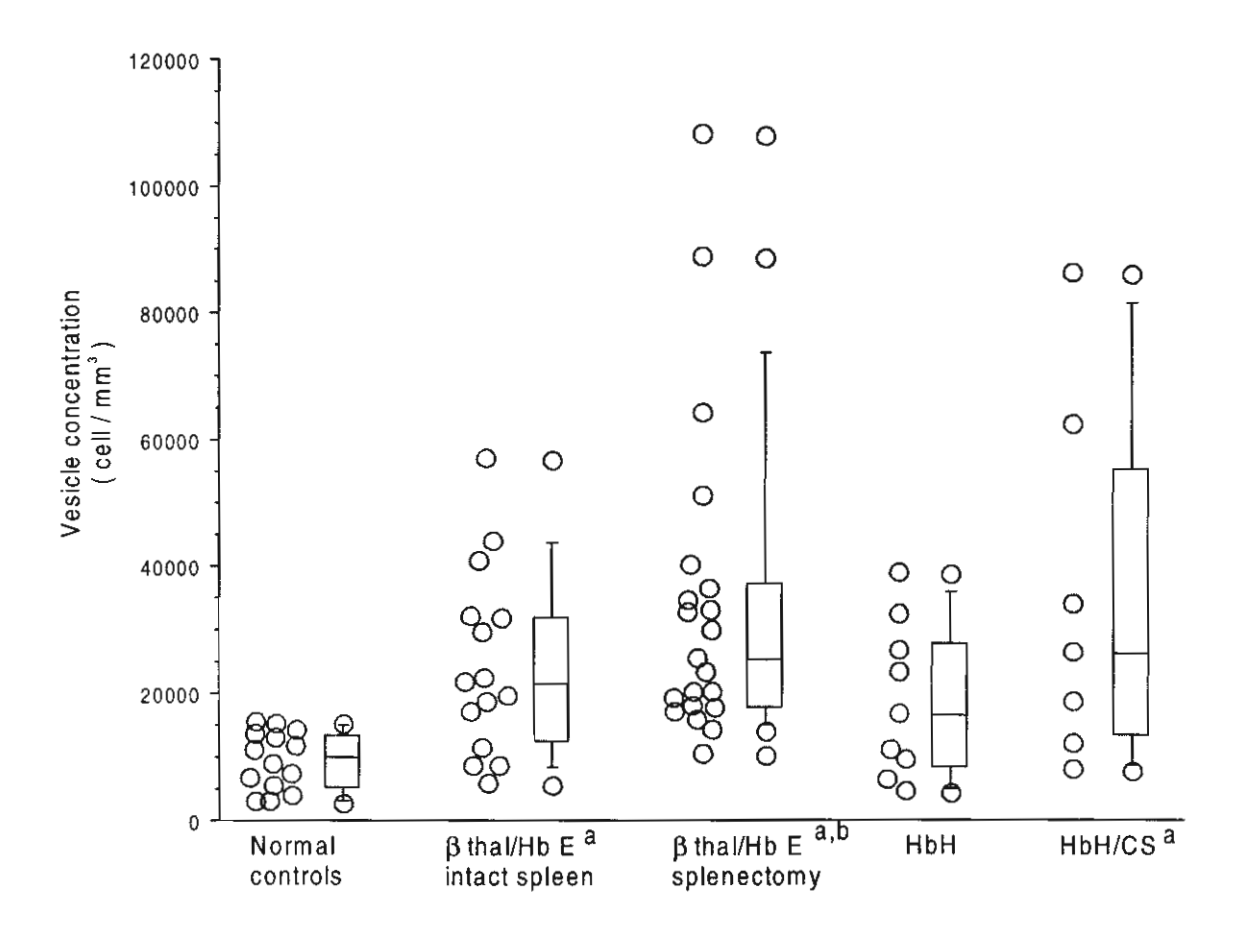


Figure 2. Vesicle concentration in normal controls and different groups of patients with thalassemia

The values were calculated from the absolute values of platelet count and the ratio of platelets to vesicles as assayed by flow cytometry.

- a Significantly different from normal controls, P < 0.05.
- b Significantly different from Hb H intact spleen, P < 0.05.

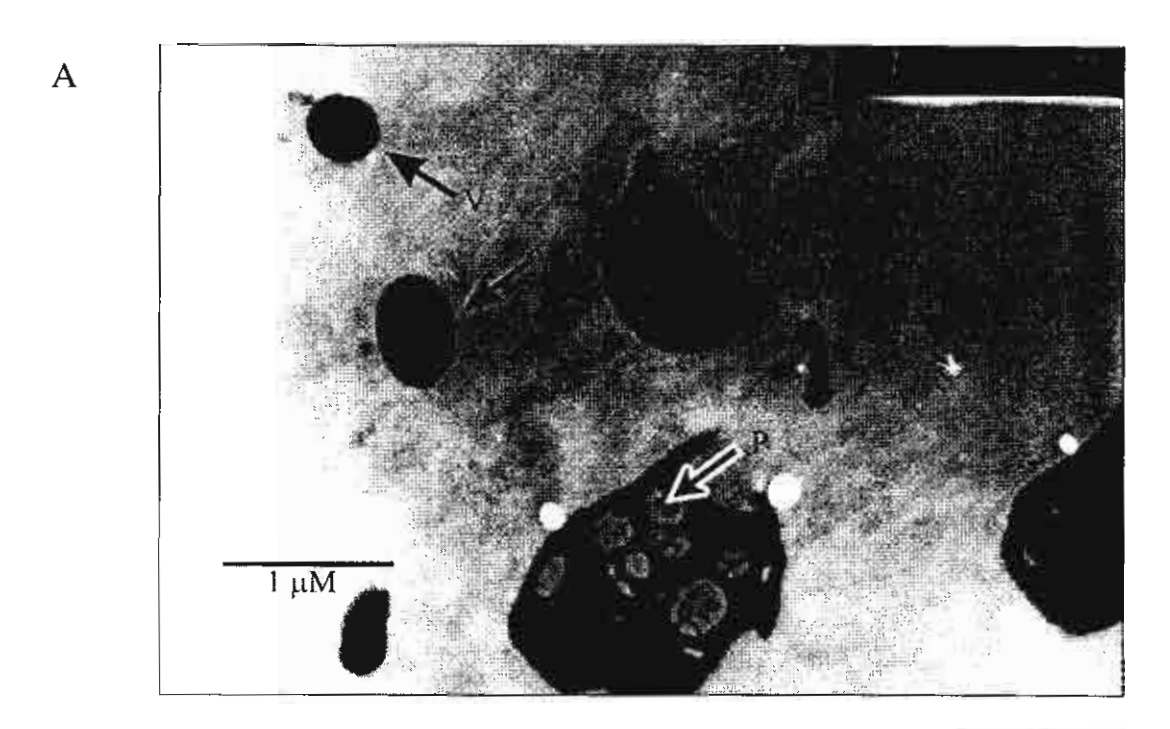




Figure 3. Electron micrograph of platelet-rich plasma from a patient with splenectomized β thalassemia/Hb E

A) Platelets (P) were identified by their irregular shape and enclosed organelles and cytoplasmic vesicles. RBC vesicles (V) were spherical or oval with no organelles. The cytoplasm of the vesicles had homogenous electron-dense pattern due to the high hemoglobin content. B) Vesicles budding from RBCs.

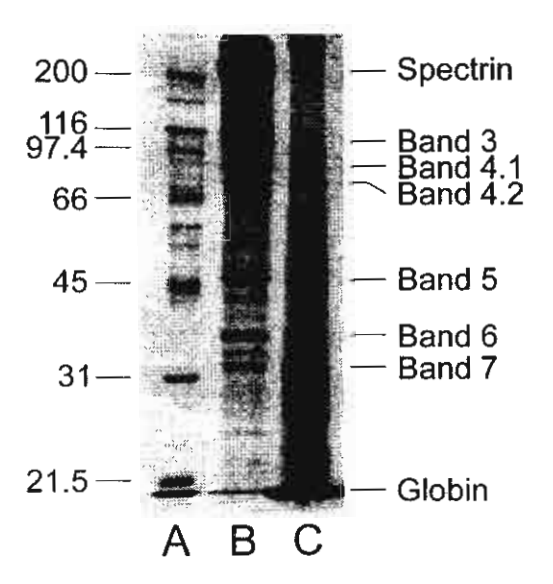


Figure 4. A representative SDS-polyacrylamide gel of normal erythrocyte ghosts and thalassemic RBC vesicles.

- (A) Molecular weight marker
- (B) Normal erythrocyte ghosts
- (C) Thalassemic RBC vesicles

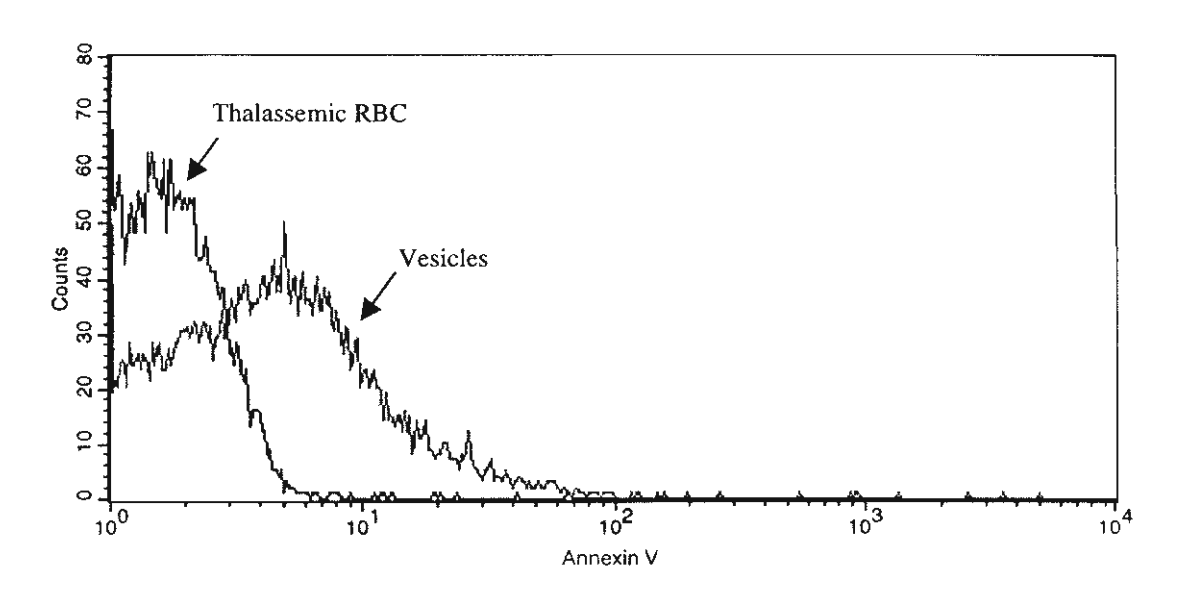


Figure 5. Annexin V staining of thalassemic RBCs and vesicles

Thalassemic RBCs and vesicles were incubated with annexin V and analyzed by flow cytometry. A representative histogram from one of three experiments is shown.

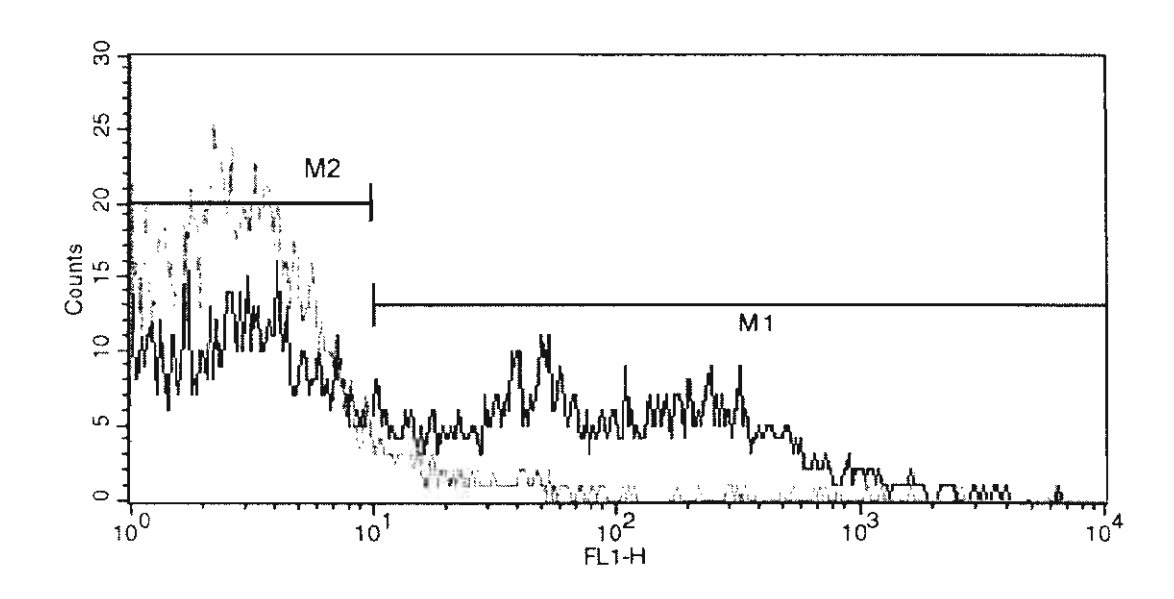


Figure 6. Complement activation of autologous serum by vesicles

After incubation in autologous serum and EDTA serum, vesicles were incubated with anti-C3c and analyzed by flow cytometry. A representative set of histogram profiles from one of three experiments is shown. Vesicles incubated in EDTA serum were used as negative controls (M2 gate). Forty five percent of vesicles contained C3 on their surface as indicated by high anti-C3c fluorescent intensity compared with negative control (M1 gate).

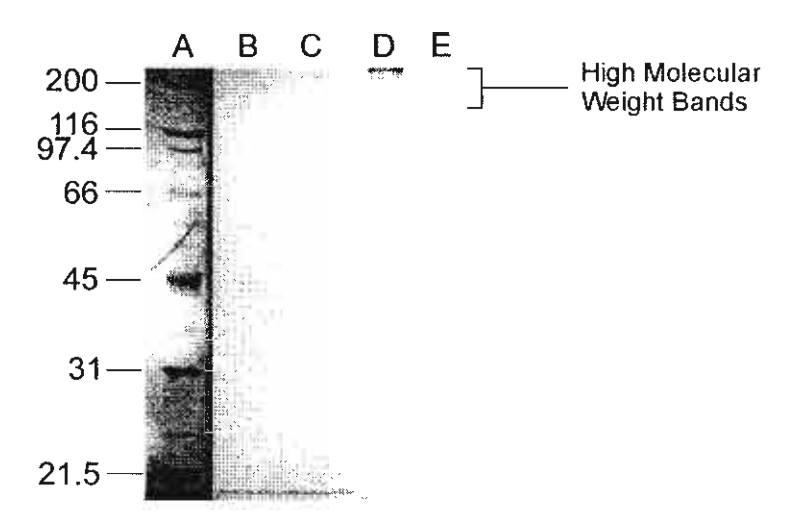


Figure 7. High molecular weight bands were detected on RBC vesicles incubated with autologous serum

A) Molecular weight marker. B) Thalassemic RBCs incubated with autologous serum. C) Thalassemia RBCs incubated with EDTA autologous serum. D) Vesicles incubated with autologous serum. E) Vesicles incubated with EDTA autologous serum.

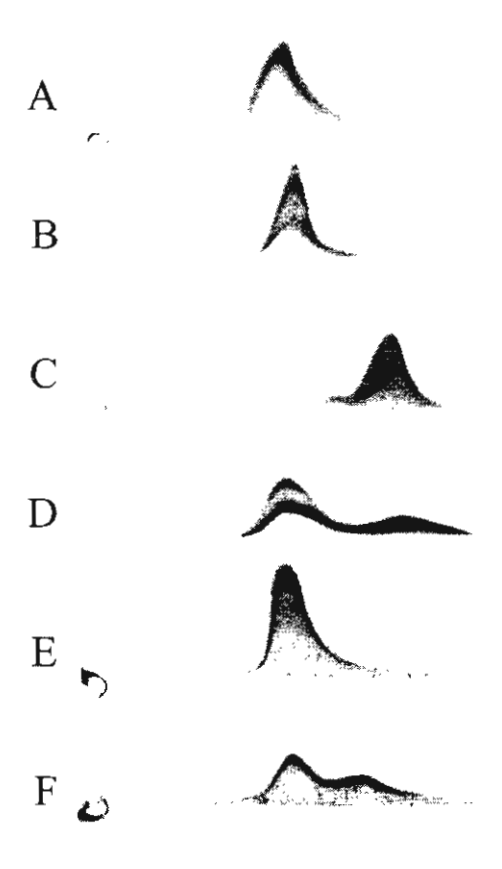


Figure 8. Vesicles could activate the complement system via the alternative pathway

A) Control serum. B) Serum incubated with thalassemic RBCs. C) Serum incubated with 10 μ l of vesicles. D) Serum incubated with 4 μ l of vesicles. E) EDTA serum incubated with vesicles. F) EGTA & Mg⁺⁺-added serum incubated with vesicles.

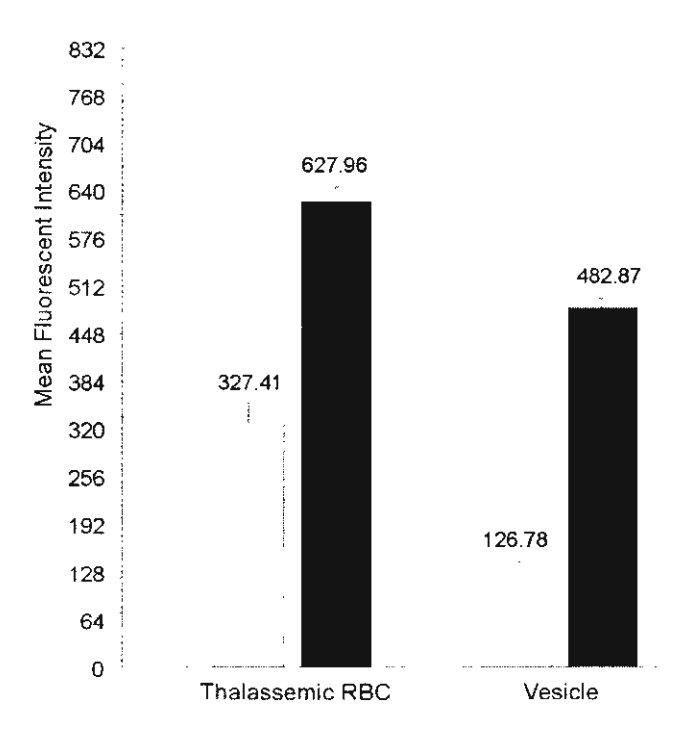


Figure 9. Mean fluorescent intensity of anti-CD55 (DAF) (□) and CD59 (■) of thalassemic RBCs and vesicles

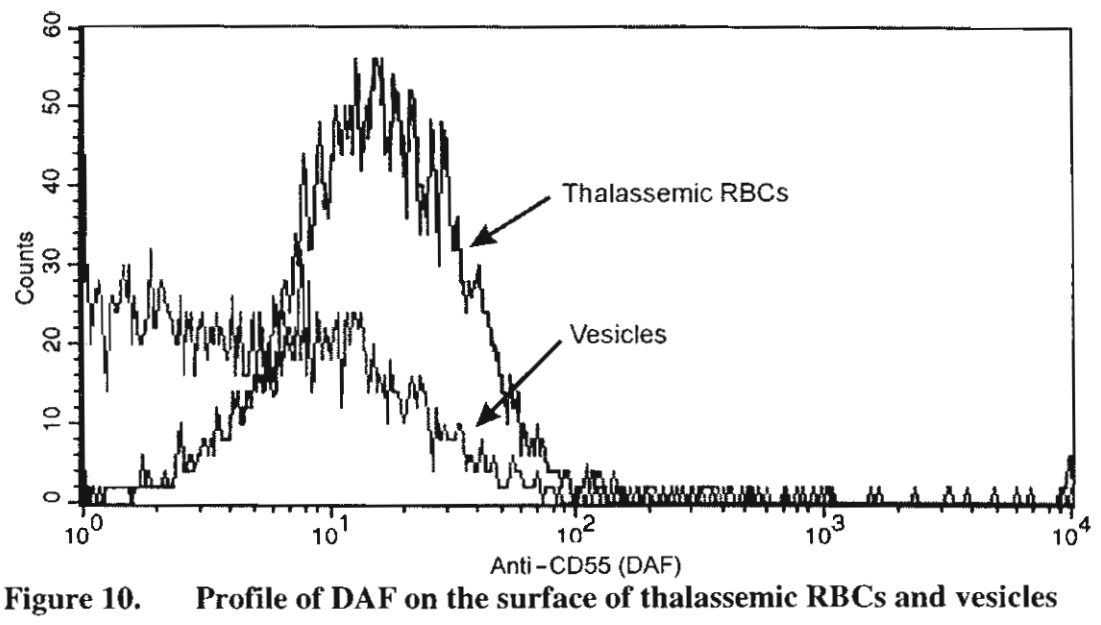


Figure 10.

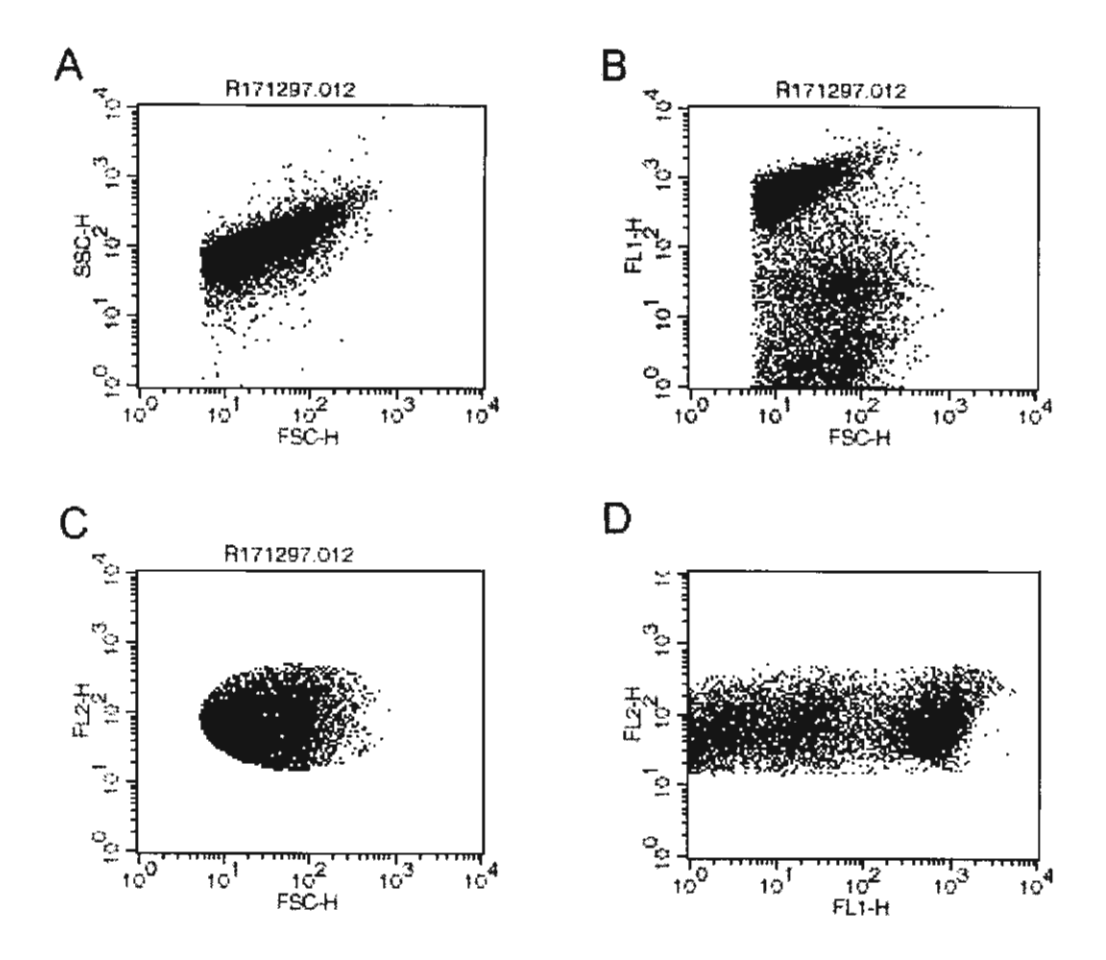


Figure 11. Flow cytometry scattergram of doubled-stained vesicles with monoclonal antibody to DAF and C3c.

After incubation in autologous serum, vesicles were stained with monoclonal antibody to DAF and C3 and analyzed by flow cytometry. DAF-positive (FL2) vesicles were gated (Panel C) and analyzed for C3 binding. A Proportion of DAF-positive vesicles contained C3 on their surface as demonstrated by anti-C3 binding (FL1) (Panel B)

Panel A: Forward scatter (FSC-H) vs Sideward scatter (SSC-H).

Panel B: Forward scatter (FSC-H) vs Anti-C3 (FL1).

Panel C: Forward scatter (FSC-H) vs Anti-DAF (FL2).

Panel D: Anti-C3 (FL1) vs Anti-DAF (FL2).

COMPARISON OF THE EFFICACY OF FOUR RT-PCR TESTS FOR THE DETECTION OF DENGUE VIRUS

BOONYOS RAENGSAKULRACH¹, ANANDA NISALAK¹, NIWAT MANEEKARN³, PA-THAI YENCHITSOMANUS², PRIDA MALASIT², NOPPORN SITTISOMBUT³, CHANDHANA LIMSOMWONG¹, AROONROONG JAIRUNGSRI², VIPA THIRAWUTH¹, SHARONE GREEN⁴, SIRIPEN KALAYANAROOJ⁵, SAROJ SUNTAYAKORN⁶, DAVID W. VAUGHN^{1*}

- Department of Virology, U.S. Army Medical Component, Armed Forces Research Institute of Medical Sciences, Bangkok, Thailand,
- Siriraj Medical Molecular Biology Center, Mahidol University, Bangkok, Thailand,
- Department of Microbiology, Chiang Mai University, Chiang Mai, Thailand,
- Division of Infectious Diseases and Immunology, University of Massachusetts, Worcester, MA
- Queen Sirikit National Institute of Child Health (Bangkok Children's Hospital), Bangkok, Thailand
- ⁶ Kampheng Phet Provincial Hospital, Kamphaeng Phet, Thailand
- * Current affiliation as shown below.

Corresponding author: LTC David W. Vaughn

Department of Virus Diseases

Walter Reed Army Institute of Research

14th & Dahlia St. N.W.

Washington, DC 20307-5100

Phone: 202-782-1243, Fax: 202-782-0442

e-mail: d.w.vaughn@usa.net

ABSTRACT

Sensitivity and specificity of dengue virus isolation by mosquito inoculation and 4 published polymerase chain reaction (PCR) procedures to detect dengue viral RNA (Henchal, Morita, Lanciotti, and Yenchitsomanus PCR) were evaluated using coded clinical specimens. Analysis of specimens from serologically confirmed dengue cases (n = 69) and non-dengue cases (n = 46) revealed the sensitivity of mosquito inoculation, Henchal, Morita, Lanciotti, and Yenchitsomanus PCR to be 55%, 51%, 71%, 75%, and 85%; and the specificity to be 100%, 98%, 96%, 100%, and 100%, respectively. Using Lanciotti PCR positive and/or serology positive specimens (n = 162) as a reference, no difference in sensitivity was observed between mosquito inoculation and Henchal, mosquito inoculation and Morita PCR, and Lanciotti and Yenchitsomanus PCR (p > 0.05) while other pairs of comparison showed significant difference ($p \le 0.05$). Typing results by each method showed substantial agreement (70-82% concordance, kappa = 0.63-0.77). Sensitivity of virus isolation and Henchal PCR dropped by days after the onset and by increasing amount of serum dengue antibody while sensitivity of the Morita, Lanciotti, and Yenchitsomanus PCR dropped slightly. Our study suggested that the Yenchitsomanus and Lanciotti PCR be the methods of choice for routine virus surveillance or research uses.

INTRODUCTION

Dengue virus types 1-4, members of the family Flaviviridae, are transmitted between humans by the mosquito vector, principally *Aedes aegypti*. Infection can give rise to a wide spectrum of disease ranging from a mild, self-limiting febrile illness to more severe vascular and hemostatic abnormalities known as dengue hemorrhagic fever and dengue shock syndrome (DHF and DSS, World Health Organization, 1986). Dengue infections constitute a significant cause of morbidity and mortality throughout tropical and subtropical regions (Halstead, 1988; Henchal and Putnak, 1990; Innis 1995; Gubler 1997).

Conventional dengue diagnosis is based on the detection of virus-specific antibody or the isolation and identification of virus from patient serum or plasma. The most commonly used serologic tests include the hemagglutination inhibition (HAI; Clarke and Casals, 1958) assay and the IgM capture enzyme immunoassay (EIA; Innis et al., 1989). However, neither is rapid nor easy to perform and furthermore they do not identify the dengue virus type responsible for the infection owing to the high cross-reactivity between antibodies induced by the different dengue virus serotypes. The traditional method to determine the infecting virus type is by virus isolation in cell culture (Gubler et al., 1984) or live mosquitoes (Rosen and Shroyer, 1985), followed by immunofluorescent staining with dengue type-specific monoclonal antibodies (Henchal et al., 1982). However, virus isolation takes from days to weeks and the success rate is often low because of factors such as inappropriate handling of specimens, formation of

virus-antibody complexes, and low numbers of viable virus (reviewed in Vorndam and Kuno, 1997; Gubler, 1998).

The polymerase chain reaction (PCR) technique has been widely applied for the rapid and sensitive detection of many infectious agents including dengue viruses. A number of reverse transcriptase PCR (RT-PCR) procedures to detect and to identify dengue serotypes have been reported (Deubel et al., 1990; Henchal et al., 1991; Morita et al., 1991; Lanciotti et al., 1992; Chang et al., 1994; Yenchitsomanus et al., 1996; Meiyu et al., 1997; Sudiro et al., 1997). These PCR methods vary somewhat in terms of gene regions of the genome amplified, methods to detect the RT-PCR products, and methods of virus typing. For example, the method developed by Henchal et al (Henchal PCR) selectively amplifies the 482 nucleotide sequence in the NS1 region of the dengue virus genome using degenerate-base dengue primers followed by blot hybridization with typespecific probes (Henchal et al., 1991). The method reported by Morita et al (Morita PCR) utilized 4 pairs of type-specific primers selected from the E-NS1-NS2A-NS2B gene regions to simultaneously detect and identify the dengue types in a single tube (Morita et al 1991).

Lanciotti et al and, more recently, Yenchitsomanus et al employed similar strategies - a RT-PCR using universal dengue primers followed by a type-specific nested PCR (Lanciotti et al., 1992; Yenchitsomanus et al., 1996). However, the two methods differ in the gene regions amplified (C-prM region for the Lanciotti PCR and E region for the Yenchitsomanus PCR). Applicability of these PCR procedures on the clinical specimens has been investigated to a certain extent (Henchal et al., 1991; Morita et al.,

1991; Lanciotti et al., 1992; and Yenchitsomanus et al., 1996); nevertheless, the procedures have never been compared in a diagnostic laboratory setting.

Here, we report the results of a multi-center study to evaluate the relative sensitivity and specificity of the 4 PCR methods described above (Henchal, Morita, Lanciotti, and Yenchitsomanus PCR) using the same set of coded clinical specimens. Standard dengue serology and standard virus isolation by mosquito inoculation were used as methods of reference. Except for the Lanciotti PCR, all other PCR methods were performed in the laboratories that either developed the procedures (Henchal and Yenchitsomanus PCR) or had a published report based on the procedure (Mortia PCR, Maneekarn et al., 1993).

MATERIALS AND METHODS

Patient specimens

Blood specimens were obtained from pediatric patients with suspected dengue infection admitted to the Queen Sirikit National Institute of Child Health (The Bangkok Children's Hospital, Bangkok, Thailand) and the Kamphaeng Phet Provincial Hospital (Kamphaeng Phet, Thailand) during 1994 and 1995. Sera or plasma were kept as 120-µl aliquots and stored at -70°C within 4 hours of collection. Specimens collected at admission were examined by virus isolation in live mosquitoes and the four PCR methods described below. Dengue serology was performed on admission and discharge specimens. All assays were performed at the Armed Forces Research Institute of Medical Sciences (AFRIMS) except the Morita and Yenchitsomanus PCR that were done at the Department of Microbiology, Chiang Mai University, Chiang Mai, Thailand and Siriraj Medical Molecular Biology Center, Mahidol University, Bangkok, Thailand, respectively. Over 300 specimens were distributed to each laboratory under code. Only specimens from serologically confirmed dengue and non-dengue cases (see criteria below) were selected for further analysis.

Serology

IgM and IgG to dengue and Japanese encephalitis (JE) viruses were determined by antibody capture enzyme immunoassay (EIA) as described by Innis et al (1989). An acute dengue infection was defined as the presence of 40 units or more of dengue IgM in the single specimen (with dengue IgM greater than JE IgM) or rising of dengue IgM from less than 15 units in the admission specimen to more than 30 units in the discharge specimen. In the absence of dengue IgM of \geq 40 units, a 2-fold increase in dengue IgG with an absolute value of \geq 100 units indicated an acute secondary dengue infection. Specimens were considered negative for serologic evidence for a recent dengue virus infection if paired specimens were collected at least 7 days apart and lacked dengue-specific antibody as defined above.

Virus isolation in mosquitoes

Dengue virus was isolated from sera or plasma by intrathoracic inoculation into live *Toxorhynchites splendens* mosquitoes (Rosen L. and Shroyer D.A., 1985). 0.34 ul of sample was used. After 14 days of incubation, mosquito heads were examined for dengue virus using an indirect immunofluorescence assay (IFA). Mosquito bodies from the mosquitoes positive by IFA were triturated and placed in C6/36 cell culture. After 7 days of incubation, the cell culture supernatant was assayed for the presence of dengue virus by antigen-capture ELISA using dengue and Japanese encephalitis virus typespecific monoclonal antibodies (Henchal et al., 1982).

Extraction of RNA

All RT-PCR methods described below were set up using RNA extracted by an acid guanidinium isothiocyanate phenol chloroform method of Chomczynski and Sacchi (1987). The amount of RNA used in the RT-PCR varied as indicated for each PCR method, depending on the set-up of each laboratory to obtain optimal results.

Lanciotti PCR

RNA equivalent to 10 ul of sample was used for each RT-PCR reaction. RT-PCR was performed according to the protocol of Lanciotti et al. (1992) except for the following modifications. pH of Tris buffer was reduced from 8.5 to 8.3. Reverse transcriptase from avian myeloblastosis virus (AMV RT, Promega, Madison, WI) was used instead of rav-2 recombinant RT as described by Lanciotti et al (1992). In addition, to reduce the nonspecific background bands on the gel, concentrations of primers used in the RT-PCR and nested reactions were reduced by half and nested PCR amplification was set for 16 cycles rather than 20.

Henchal PCR

The same RNA preparations that were used in the Lanciotti PCR were subjected to a PCR procedure described by Henchal et al (1991) with some modifications. Briefly,

5 μl of RNA (equivalent 10 ul of sample) was mixed with 10 pmol of an AD3 antisense primer in a 10 μl reaction volume. The mixture was heated to 68°C for 3 minutes and cooled on ice. The RT-PCR was set up by adjusting the RNA-primer mixture to 10 mM Tris (pH 8.3), 50 mM KCl, 3.5 mM MgCl₂, 25 pmol each of AD3 and AD4 primers, 40 units of RNAsin (Promega, Madison, WI), 2 units of reverse transcriptase, and 2.5 units of AmpliTag (Perkin Elmer, Norwalk, CT) in a final volume of 100 μl. The RT was carried out at 42°C for 45 minutes. Then the mixture was heated at 94°C for 3 minutes followed by 40 cycles of PCR at 94°C (1 min), 45°C (1 min), and 72°C (1 min). The last cycle was extended at 72°C for 5 min.

Fifty microliters of the PCR product was extracted once with chloroform-isoamyl alcohol and treated with 4 ul of 3M NaOH for 30 min at 70°C. Samples were then neutralized with equal volume of 2M ammonium acetate. A one-fourth volume of each sample was slotted onto 4 separate sheets of Nytran membrane according to the manufacturer's instructions (Schleicher&Schuell, Keene, NH). Membranes were soaked at 42°C for 10 minutes in a hybridization buffer [5X SSC (1x SSC = 0.15 M sodium chloride, 0.015 M sodium citrate), 0.5% hybridization blocking reagent (Amersham, Arlington Heights, IL), 0.1% sarcosyl, 0.02% sodium dodecyl sulfate]. Four separate hybridizations were carried out at 42°C for 1 hour in the hybridization buffer containing 20 ng/ml of each dengue virus type specific chemiluminescent probe (D1 to D4, Henchal et al., 1991). The probes were synthesized from thiol modified oligonucleotides using a 5'thiol oligolabelling system (Amersham, Arlington Heights, IL). Blots were washed and

the hybridization was detected by an ECL gene detection kit (Amersham, Arlington Heights, IL).

Morita PCR

The RT-PCR was performed as originally described by Morita et al (1991) and modified by Maneekarn et al (1993) except that the reverse transcription was done at 45°C for 30 min and the RT-PCR was set up in 4 separate reactions using specific primers for each dengue serotype instead of mixed primers. RNA equivalent to 25 ul of sample was used in each virus type specific RT-PCR.

Yenchitsomanus PCR

The Yenchitsomanus PCR was performed as described previously (Yenchitsomanus et al., 1996). PCR primers used in this study were the sets used to amplify dengue sequences in the E region. RNA equivalent to 100 ul sample was used in each RT-PCR.

Data analysis

The sensitivity and specificity for each assay were calculated using serology as the criterion standard. A McNemar statistic test was performed to find the correlation

between each method of virus detection. Agreement between types of dengue virus identified using each method was determined by Kappa statistic. A Kappa value of 1 indicates perfect agreement while 0 indicates that agreement is no better than that expected by chance.

RESULTS

This study was conducted using 2 panels of specimens. The first panel comprised 235 serum specimens from suspected dengue patients and the testings were done prospectively without prior knowledge of any test results. The second panel consisted of 43 and 93 acute specimens that were negative and positive for dengue infections by serology, respectively. Data from each panel were analyzed as follows.

Sensitivity and specificity for dengue virus detection based on Panel 1 specimens

Criterion testing (AFRIMS EIA) of the first 235 unselected specimens revealed that 145 patients experienced acute dengue infections, 14 did not experience a recent flavivirus infection, and 76 had indeterminate results (i.e., the acute serum was non-diagnostic serologically and an adequate follow-up specimen was not available). Virus isolation, Henchal, Lanciotti, and Yenchitsomanus PCR were done on all 235 specimens, however, the Morita PCR was done on 98 specimens (out of 235). Using serology as a gold standard, sensitivity and specificity of each method of virus detection were calculated according to data completed by all tests (Table 1). It should be noted that some specimens that yielded indeterminate results by any of the PCR assays were also excluded from the analysis. A total of 69 acute sera from serologically confirmed dengue patients and 3 from patients with non-flavivirus infections were available for analysis.

Sensitivity and specificity for dengue virus detection based on Panel 2 specimens

From the panel 1 specimens above, it was evident that there were a small number of serologically negative specimens that could be used to determine the specificity of the assays. In addition, many specimens had indeterminate results by serology (a gold standard) and therefore could not be used in the analysis. To avoid these problems, the panel 2 specimens were assembled and distributed to the participating laboratories under code. This panel consisted of 43 serologically negative specimens and 93 serologically positive specimens that were also PCR positive by the Labciotti method. The Lanciotti method was the standard method of PCR in the reference laboratory at the time of the study previously shown to be specific (data not shown). Screening specimens with the Lanciotti PCR method allowed the study to focus on dengue virus positive sera. In addition, typing results by the Lanciotti PCR allowed us to select an adequate number of dengue type specific sera to evaluate each PCR method against each virus type. Results for testing of panel 2 specimens are shown table 1.

Sensitivity of detection by dengue virus type

Numbers of dengue virus types identified by virus isolation and serotyping and by each PCR method are presented in Table 3. To compare the sensitivity of each dengue PCR method in detecting each of the 4 dengue virus type, virus isolation using live mosquitoes was used as a criterion standard. Results are summarized in Table 3. The data suggested that some methods were less sensitive for certain dengue virus types than

other methods. For panel 1 specimens, the lowest sensitivity seen by the Henchal, Morita, Lanciotti, and Yenchitsomanus PCR methods were on dengue 4 (33%), dengue 3 (50%), dengue 1 (70%), and dengue 1 (60%), respectively. A similar rank of sensitivity was also seen for panel 2 specimens.

Typing discrepancy

Kappa statistic analysis on typing results of panel 1 and 2 specimens (rating: dengue 1, 2, 3, 4, or negative) revealed a 0.63 to 0.77 range of agreement (70% to 82% concordance). Six specimens yielded discrepancy in types of dengue virus identified therefore repeat testings of these specimens were performed (table 4). Results either remained the same or became negative upon repeat for specimen 01125/94, 01199/94, and 01327/95. Specimen 00938/94 yielded 2 PCR product bands (dengue 1 and 2) on the second run by the Yenchitsomanus PCR while only dengue 1 virus was isolated on the second attempt. Repeat testing of specimen 01517/94 and 30191/95 was not done due to unavailability of the specimens.

Sensitivity of virus detection by days of illness

Specimens from the 69 confirmed dengue cases (panel 1 specimens) were grouped by days after the onset that were generally the days fever started. Percentage of specimens positive for dengue by each method of virus detection is shown graphically in figure 1A. During the first 4 days of illness, the sensitivity of virus detection by

mosquito inoculation and by the Henchal PCR was above 50%. After that, the sensitivity dropped to 50% or below. In contrast, sensitivity of detection by the Morita, Lanciotti, and Yenchitsomanus PCR remained above 50% though declining with time.

Effect of antibody on the sensitivity of detection

Dengue specific IgG titers of the 69 panel 1 specimens were stratified into 3 increasing levels: 0-18, 19-80, 81-285 EIA units (23 specimens per group). The virus detection rates by mosquito inoculation were 65%-74% in the presence of dengue IgG titers of 80 units or less and dropped instantly to 26% with dengue IgG titer of greater than 80 units (Figure 1B). Similarly, virus detection rates by the Henchal PCR were 65%-70% for the first 2 groups of specimens (titer ≤ 80) and dropped to 17% for with dengue IgG titer more than 80. In contrast, virus detection rates by the Morita, Lanciotti, and Yenchitsomanus PCR remained relatively high (65%-96%) for all 3 groups of specimens.